

# **ELECTRIC POWER MARKET AGENT DESIGN**

A Dissertation

Presented to the Faculty of the Graduate School

of Cornell University

In Partial Fulfillment of the Requirements for the Degree of

Doctor of Philosophy

by

HyungSeon Oh

May 2005

© 2005 HyungSeon Oh  
ALL RIGHTS RESERVED

# **ELECTRIC POWER MARKET AGENT DESIGN**

A Dissertation

Presented to the Faculty of the Graduate School

of Cornell University

In Partial Fulfillment of the Requirements for the Degree of

Doctor of Philosophy

by

HyungSeon Oh

May 2005

# **ELECTRIC POWER MARKET AGENT DESIGN**

HyungSeon Oh, Ph. D.

Cornell University 2005

The electric power industry in many countries has been restructured in the hope of a more economically efficient system. In the restructured system, traditional operating and planning tools based on true marginal cost do not perform well since information required is strictly confidential. For developing a new tool, it is necessary to understand offer behavior. The main objective of this study is to create a new tool for power system planning. For the purpose, this dissertation develops models for a market and market participants.

A new model is developed in this work for explaining a supply-side offer curve, and several variables are introduced to characterize the curve. Demand is estimated using a neural network, and a numerical optimization process is used to determine the values of the variables that maximize the profit of the agent. The amount of data required for the optimization is chosen with the aid of nonlinear dynamics. To suggest an optimal demand-side bidding function, two optimization problems are constructed and solved for maximizing consumer satisfaction based on the properties of two different types of demands: price-based demand and must-be-served demand. Several different simulations are performed to test how an agent reacts in various situations. The offer behavior depends on locational benefit as well as the offer strategies of competitors.

## **BIOGRAPHICAL SKETCH**

HyungSeon Oh was born on December 25, 1968 in Seoul, the capital city of Republic of Korea. After completing high school, he enrolled in the Department of Ceramic Engineering at Yonsei University in Seoul, and graduated in 1992. He then joined in a master's program with a concentration on solid state chemistry at Seoul National University and received an MS degree at 1994. After three-year mandatory military service, he enrolled in an MS/Ph. D. program in the Department of Materials Science and Engineering at Cornell University in Ithaca, New York, in January 1998 and received an MS degree at 2002. After then he transferred into the Department of Electrical and Computer Engineering.

**TO MY FAMILY**

## ACKNOWLEDGEMENTS

I received a degree of Master of Science a while ago, and now I am about to receive a degree of Doctor of Philosophy. Ever since I thought about getting into a Ph. D. program, I have has a question to myself: Does it make sense? Before getting a Ph. D., a person was a master of science, i.e., science is a slave. Then Ph. D. turns the person only into a lover to the former slave. I would have liked to remain a master rather than a lover. After seven and half years in a Ph. D. program, I realize that a lover is much more powerful than a master. A slave is willing to work harder for a lover rather than a master. Now I hope that the name can bring what it means. I want to live with science and seek something good for both my lover and myself.

I would like to appreciate those who contributed to this finding. Fist of all, I want to thank my advisor, Professor Robert J. Thomas, for his patience, encouragement and guidance during this work. I would like to express my appreciation for Professor James S. Thorp and Professor Thomas F. Coleman for serving my special committee. I also thank Cornell University for giving me a chance to find the very best committee members.

I am grateful to all the colleagues for friendship. Jie was a good friend as well as an excellent teacher. Without help from Ray, this work could not even begin. I also thank Ms. Sally Bird for wonderful help during entire of my stay. My gratitude is due to Dr. Franklin Baez and Jassim Alseddiqui for correcting some of my English writing. My sincere appreciation goes to my grandparents and parents for continuous support and encouragement in pursuing my graduate study in the United States. An advice from my grandfather brought me here, and I hope he enjoys what his grandson

achieves: I admire you. When I decided to leave materials science, my sister was really helpful to get into this program: Thank you very much.

Finally, but not least, I would like to thank my wife and daughter, Youjin Wang and Sooyoun Oh. I know that living more than seven years as a spouse and a daughter of a student is very hard time. They have been pretending it is not: Thank you. I know my English is poor, but I realize that my Korean is not rich either: I cannot find a proper word to deliver my feeling to you in either language – Thank you again.



# TABLE OF CONTENTS

BIOGRAPHICAL SKETCH.....	iii
ACKNOWLEDGEMENTS.....	v
TABLE OF CONTENTS.....	vii
LIST OF TABLES.....	x
LIST OF FIGURES.....	xi
CHAPTER ONE: INTRODUCTION.....	1
CHAPTER TWO: MODELING FOR AN OFFER AND A BID.....	5
2.1. Literature Review.....	5
2.2. Model for Supply-side Offer Behaviors.....	9
2.2.1. Flattening factor.....	22
2.2.2. Quantity evaluating the market condition.....	24
2.2.3. Boundary effect.....	26
2.3. Model for Demand-side Bid Behaviors.....	26
CHAPTER THREE: EARNING ESTIMATION.....	46
3.1. Mapping Offers to Earnings.....	46
3.2. Market Modeling.....	47
3.2.1. Classification of offer strategies.....	48
3.2.2. Market modeling.....	49
3.3 Mapping Function for Stationary Markets.....	51

CHAPTER FOUR: MARKET DYNAMICS.....	55
4.1. Current Market Monitoring Tool.....	55
4.2. Chaos and Fractals.....	57
4.3. Nonlinear Time Series Analysis.....	60
 CHAPTER FIVE: SIMULATION RESULTS AND DISCUSSION.....	 71
5.1. Agent Classification Based on Its Performance.....	71
5.1.1. Standardized agents.....	71
5.1.2. Classification of an agent.....	74
5.1.3. An example.....	74
5.1.4. Expected earning.....	77
5.1.5. Simulation results and discussion.....	78
5.2. Evaluation of Dimension by Using Price.....	85
5.3. Results from Simulations with Demand-side Agent and Discussion.....	88
5.4. Simulation Results with Adaptive Supply-side Agents and Discussion.....	92
5.4.1. Description of adaptive supply-side agents.....	94
5.4.2. Simulation detail and results.....	98
5.4.3. Simulation with no change in the strategies of competitors.....	102
5.4.4. Simulation with the change in the strategies of competitors.....	109
5.4.5. Simulation with unknown external flow.....	118
5.4.6. Simulation with an agent representing a firm without locational benefit.....	 123
 CHAPTER SIX: CONCLUSIONS AND FUTURE WORK.....	 129

APPENDIX A:	GENERATION SENSITIVITY MATRIX FROM A NETWORK TOPOLOGY.....	134
APPENDIX B:	ERROR MINIMIZATION WITH 2-NORM.....	143
APPENDIX C:	TRUST REGION METHOD.....	146
APPENDIX D:	CHAOS AND NONLINEAR DYNAMICS.....	157
APPENDIX E:	STOCK MARKET AND CHAOS.....	167
REFERNCES.....		169

## LIST OF TABLES

Table 5. 1. Block-by-block offer structure for standardized agents; The table shows the offer strategies of standardized agents when the fairshare block is the $j^{\text{th}}$ block out of $n$ available blocks. MCO, S and W stand for a marginal cost offer, speculate on price and withhold the block, respectively.....	73
---	----

## LIST OF FIGURES

Figure 2. 1. Two commonly observed offer curves. Connecting lines are for visual guidance. These specific offer curves were found in the PJM market where D8 and Y6 are the company code known only to PJM.....	10
Figure 2. 2. Schematic diagram modeling marginal cost offer as well as speculating offer. D denotes the flattening factor of the block representing how easily the price get flat as market condition changes, and q and p refer offer quantity and price, respectively.....	12
Figure 2. 3. Schematic diagram showing movement of expectation of earning ....	13
Figure 2. 4. Fitting results of two offer curves in a same day to equation (19). Two blocks are visible only in b), but the same $p^{\max}$ was used for both fittings.....	21
Figure 2. 5. An offer curve submitted by B5 in July 26 <sup>th</sup> and fitting with equations (13) – (16) and (19). The curve shows a boundary effect at 2200 MW.....	27
Figure 2. 6. An optimal bidding curve for a) price-based demands and b) must-be-served demand.....	43
Figure 2. 7. Change in bidding after one period subject to the occurrence of an energy PRL.....	45

Figure 4. 1. Nodal prices of various generators – data obtained from NYISO web site on <a href="http://mis.nyiso.com/public/P-24Blist.htm">http://mis.nyiso.com/public/P-24Blist.htm</a> during summer 2003 .....	58
Figure 4.2. Electricity market as a signal processing where input and output signal are offer and dispatch result and demand forecast, respectively.....	59
Figure 4.3. Schematic diagram showing how to calculate $C(\varepsilon)$ for a flow. Some neighboring points lying on dynamically uncorrelated parts of the data exist for point A, but point B has only direct images and pre-images of B resulting in dimension of 1. To avoid the incorrect calculation of $C(\varepsilon)$ for estimating dimension, all neighbors over time where $ i - j $ is less than $n_{\min}$ need to be ignored.....	64
Figure 4. 4. A schematic diagram showing evolution of two trajectories of a system with a positive Liapunov exponent. At the beginning, both trajectories were close with each other, but after some time their trajectories are far apart.....	66
Figure 4. 5. A schematic diagram show how to calculate Liapunov exponent; a) at $t = 0$ , several points, $s_{n_0}$ , $s_{n_1}$ and $s_{n_2}$ were selected and trajectories starting from the points were tracked as the system evolves, b) many points inside $\varepsilon$ -ellipsoid ( $u_{s_0}$ , $u_{s_1}$ and $u_{s_2}$ ) were selected and similar to the procedure described in a) was performed (picture taken from Ref [34]).....	68
Figure 4. 6. Estimation of the Liapunov exponent of the NMR laser data in embedded dimension of 2 (upper plot) and 3 ~ 5 (lower plot). The linear parts of the curves are well described by an exponential with $\lambda = 0.3$ . [37].....	70

Figure 5. 1.	Earnings of the standardized agents and the agent of interest.....	76
Figure 5. 2.	Example of a performance of the software agents: in the plot, red square, green and blue circle stand for the earning in a period of MC, WS and SS, respectively.....	80
Figure 5. 3.	Example of a performance of the human agents: red square, green and blue circle stand for the earning in a period of MC, WS and SS, respectively.....	82
Figure 5. 4.	Actual earning vs. Expected earnings calculated from simulation...	84
Figure 5. 5.	Correlation integral for the market clearing price data obtained from the simulation with 500 periods.....	86
Figure 5. 6.	Correlation dimension for various price data obtained from n-period simulation.....	87
Figure 5. 7	The change in systems which agents, York-Warbesse and Cornell, faced during June 2003. While system of Cornell did not change significantly, that of York-Warbasse evolved.....	89
Figure 5. 8.	Modified IEEE 30 bus system with six suppliers. Capacities of lines connecting Area 1–Area 2 and Area 3–Area 2 are lower than those of other lines.....	90

Figure 5. 9. Two typical simulation results with inelastic demand without demand-side participation (red line) and with elastic demand with demand-side participation (blue line). Case a) shows the results in a more competitive market than that for Case b).....93

Figure 5. 10 Simulated historical data for nodal prices at the Bus 23 (Firm 5) in the case that 4 marginal cost offer agents in Area 1 and 3 exist while Firm 6 is a) a marginal cost offer agent or b) speculator with different predetermined the degree of speculation.....99

Figure 5. 11 Simulated historical data for nodal prices at the Bus 23 (Firm 5) in the same cases in Fig. 8. 1., but nearest competitor (Firm 6) changes its strategy completely a) from MC to speculator and b) speculator to MC.....100

Figure 5. 12. Simulated historical data for nodal prices at the Bus 1 (Firm 1) when there is injection at Bus 28 and withdrawal at Bus 16 from the period of 253.....101

Figure 5. 13. Simulated historical data for nodal prices at the Bus 23 (Firm 5) which has no locational benefit; a competitor in Area 2 (Firm 6) changes its strategy in a more speculative way completely at the period of 253.....103

Figure 5. 14. Daily dimension checks for the historical nodal price data obtained from the simulation described in Figure 5. 10 a) and b), respectively.....105



Figure 5. 15	The results of Liapunov exponent calculation performed with the historical nodal price data obtained from the simulations described in Fig. 5. 10 a) and b), respectively.....	107
Figure 5. 16	Simulated historical data for the actual and expected earning of Firm 5 from the cases described in Fig. 5. 10 in blue and red line, respectively.....	108
Figure 5. 17.	Daily dimension check for the historical nodal price data obtained from the simulation described in Figure 5. 11.....	110
Figure 5. 18	The results of Liapunov exponent calculation performed with the historical nodal price data obtained from the simulations described in Fig. 5. 11 a) and b), respectively.....	111
Figure 5. 19	Simulated historical data for the actual and expected earning of Firm 5 from the cases described in Fig. 5. 11 in blue and red lines, respectively.....	114
Figure 5. 20	The degree of speculation and the maximum offer price changes over periods obtained from the simulation described in Fig. 5. 11 a) and b), respectively; black lines indicate the mean values of the variables within the period shown in the horizontal axis.....	116
Figure 5. 21.	The ratio of the maximum offer price to the degree of speculation over the periods shown in the horizontal axis; the corresponding values of both variables were shown in Fig. 5. 20.....	117

Figure 5. 22. Daily check for a) dimension and b) Liapunov exponent calculated with the simulated historical nodal price data obtained from the simulations described in Fig. 5. 12.....119

Figure 5. 23. The main variables and the ratio between the variables over periods obtained from the simulation described in Fig. 5. 12; the black lines in a) represents the mean values of the variables during the period.....121

Figure 5. 24 Simulated historical data for the actual and expected earning of Firm 5 from the cases described in Fig. 5. 12 in blue and red lines, respectively .....122

Figure 5. 25. Daily check for a) dimension and b) Liapunov exponent calculated with the simulated historical nodal price data plotted in Fig. 5. 13.....124

Figure 5. 26. The main variables and the ratio between the variables over periods obtained from the simulation described in Fig. 5. 13; the black lines in a) represents the mean values of the variables during the period.....126

Figure 5. 27 Simulated historical data for the actual and expected earning of Firm 1 from the cases described in Fig. 5. 13 in blue and red lines, respectively .....128

Figure A-1. A schematic diagram for explaining how to determine a weight factor distribution,  $x$ , a) by using traditional LU-factorization and b) by using LU-factorization where  $b' = L^{-1}(P^T b)$ . The thick arrows show where zeros could be assigned in the vector  $x$ , and eliminating  $R$  rows from  $U$  and the assigned elements from  $x$  yields  $U'$  and  $x'$ , respectively .....145

Figure A-2. Solution of the Lorenz equation (in color) and  $xy$ ,  $yz$  and  $zx$  two-dimensional projections which show artifact crosses.....158

Figure A-3 Start with the closed interval  $S_0$ ,  $[0, 1]$ , and remove the open middle third resulting in closed interval  $S_1$ . The same procedure is kept performed to produce  $S_2$ ,  $S_3$  and so on. The limiting set  $S_\infty$  is the Cantor Set.....159

Figure A-4 Start with a line segment  $S_0$ ,  $[0, 1]$ , and delete the middle third and replace with the other two sides of an equilateral triangle,  $S_1$ . Then repeat the same step to generate  $S_2$ ,  $S_3$  and so on. The limiting set  $S_\infty$  is the von Koch curve.....161

Figure A-5 a) The coast of the southern part of Norway. The square grid indicated has a spacing of  $\delta \sim 50$  km (taken from the Figure 2. 1 of [J. Feder, “Fractals”, Plenum Press, New York and London (1998)]) and b) The measured length of the as a function of the size  $\delta$  of the  $\delta \times \delta$  squares used to cover the coastline on the map. The straight line in this log-log plot corresponds to the relation  $L(\delta) = a\delta^{1-D}$  ;  $L$ ,  $\delta$  and  $D$  correspond to  $N$ ,  $\varepsilon$  and  $d$  in equation (A.67).....163

Figure A-6 Log-log plot to estimate the correlation dimension of a fractal. Typically, the plot shows two bends both at lower values of  $\varepsilon$  and at higher values of  $\varepsilon$ .....166

# CHAPTER ONE

## INTRODUCTION

The traditional vertically integrated electricity power system has been defined as a natural monopoly. Under several constraints such as spinning reserve, thermal unit constraints and hydro constraints etc., operation and planning of the system was performed toward declining long-term costs, high threshold investment, and technological conditions that limit the number of potential entrants. In the vertically integrated environment, therefore, a utility would determine generation setpoints based on real costs of operation. Unified control of generation, transmission, and distribution was considered to be the most efficient way of providing service, and as a result, most people were served by a vertically integrated utility. However, as the electric utility industry has evolved, there has been a growing belief that the historic classification of electric utilities as natural monopolies has been overtaken. It has been believed that market forces might replace some of the traditional economic regulatory structure. For example, vertical integration has not been necessary for providing efficient electric service if utilities that do not own all of their generating facilities exist. Moreover, recent changes in electric utility regulation and improved technologies have allowed additional generating capacity to be provided by independent firms rather than utilities.

Over several decades, there has been a major change in direction concerning generation. Improved technologies have reduced the cost of generating electricity as well as the size of generating facilities. Prior preference for large-scale generators has been supplanted by a preference for small-scale ones that can be brought online more quickly and cheaply with fewer regulatory impediments. Consequently, the entry

barrier to electricity generation has been lowered to permit non-utility entities to build profitable facilities. Recent changes in electric utility regulation and improved technologies have allowed additional generating capacity to be provided by independent firms rather than utilities. Therefore, it was hoped that the transition to the restructured markets would make the efficiency of the system increase. With the hope for a more efficient system, the electric power industry has been restructuring in many countries.

In all restructured markets, auctions play a major role in determining both the price of electricity and the quantity of electricity dispatched by individual generating units. In the new regime, generation setpoints are determined by market forces rather than by engineering design. Consequently, it is necessary to create new tools for planning and operating that take account the nature of the market environment. In a traditional system setting, a generator's setpoint is determined by current demand and its marginal cost<sup>1</sup> to produce the next megawatt under several constraints listed above. In the case, all participating agents selected by a unit commitment process are guaranteed to get dispatched. However, it is unlikely that true operating costs will be revealed because of the hedging needed to accommodate uncertainty and opportunities offered by the interconnecting network for exercising market power. A generators' setpoint can be found from the result of an optimization process minimizing total system cost. In the new market setting, each agent representing a generating firm submits price and quantity offer at which it is willing to sell its electric power. For an independent system operator (ISO) who does not have access to the true cost of each generator in the setting, the offer replaces each unit's true marginal cost in the process of

---

<sup>1</sup> marginal cost is the cost of the additional inputs needed to produce that output, i.e., the cost of producing one more MW

determining a setpoint. Because participating generators can change their offers in each period, the tools used for operation and planning in the traditional markets are no longer useful for the new markets. Therefore, it is important to understand the offer behavior of human agents if we are to be successful in designing new tools.

The objective of each generator in the market is to maximize its own profit. An agent can find its optimal offer if actual demand is given and if the competitors' offer strategies are known. When there is a change in the offer strategies of competitors, the optimal offer of the agent will change. Therefore, it is possible to find an optimal offer with proper information, and to figure out when to change the behavior of the agent if needed. However, the information listed above is strictly confidential to an agent.

The main goal of this study is to develop a theory and examples for new agent-based components as an approach to creating new tools for power system planning and operation. Specifically, we seek to develop a planning tool that relies on software agents as a replacement for the human agents that exist in the real world to submit offer energy price and quantity into a market. Well-designed software agents can be used to emulate the offer behavior of human agents provided that it can be shown that, in some sense, their behavior is roughly identical. At a given market environment, there are several types of offer/bid strategies of a human agent. A software agent needs to show a similar behavior at the identical environment. When the environment changes such as the change in the offer/bid strategies of the competitors, a software agent should react to optimize the profit.

In this dissertation, there are six chapters including the introduction. Chapter 2 describes modeling for offer/bid behaviors. Chapter 3 deals with constructing a

mapping function from offer to earning. In the chapter, a theoretical model for an electricity power market in a steady state is developed. Chapter 4 describes tools i) to detect if there is any change in the market due to various reasons such as strategies of the competitors and/or network, and ii) to find whether the change results in another steady state or a chaotic state. Chapter 5 shows several results from different simulations performed with the agents developed in this study. Conclusions and future works are presented in Chapter 6. Several related topics are described in Appendix 1 to 5. Appendix 1 deals with constructing a generation sensitivity matrix by using network parameters. In Appendix 2, a method for an error minimization is described. Trust region method for a numerical function is presented in Appendix 3. In Appendix 4, a method to evaluate dimension and Liapunov exponent presented. Appendix 5 describes a nonlinear time series analysis performed for stock markets.

## CHAPTER TWO

### MODELING FOR AN OFFER AND A BID

#### 2.1. Literature Review

A human agent will update his/her offer behavior based on experience and available information. If competitors do not change their strategies, the auction is similar to a repeated game in game theory. For such a game, the competitors' strategies can be revealed from the result and his/her strategy used during previous play. In the case, a player can update the strategy based on the result of previous play. If competitors do not change their strategies, and all other conditions such as demand do not change, then an agent can find an optimal strategy for the circumstance. However, since the strategies of competitors and other conditions are subject to change in a real market, it is important to have an agent find out hidden information quickly from publicly available data such as the history of the market clearing result. It is easier in studying dynamics to simulate markets with known types of competitors. However, an agent only explores relatively restricted area defined by the types in the market in such a case.

Usually human agents update offer strategies to determine price and quantity according to some process they believe to be profit maximizing. To mimic the ability, several different learning algorithms have been studied. Reinforcement algorithms [1-3] and genetic algorithms [4-6] are most widely studied. Hill climbing is one of the most commonly used reinforcement algorithms. In it, one moves along the direction to which the value of an objective function increases in the previous step. They are



relatively easy to implement since they require small computational cost in terms of computation time and data storage. In any reinforcement algorithm, trial-error experience will contribute differently to any future strategy based on the previous results. A genetic algorithm has a similar property, but it is a little more complicated due to the choice of fitness function and selection mechanism [7]. It is difficult to assess which parameters are most sensitive to the performance index. In other words, mapping prices and quantities of multiple blocks to earning is difficult. For example, consider a non-discriminatory auction which is the most commonly used pricing rule in electricity power markets. In such markets, only marginal blocks set the price. Consequently, the offer prices of other blocks are not relevant to profits.

By its nature, demand is stochastic and any demand forecast will be in error. Typically, load is forecasted by using weather data on an hourly basis as an input such as temperature, humidity, cloud cover and wind. The uncertain and stochastic nature of the demand brings another difficulty in an agent design for electricity markets. In the method discussed above, the nature of the demand is not considered.

Sheble et al [4-6] designed an agent using a genetic algorithm that operates in a significantly simplified market and with zero demand forecast error. In the market, each agent, including suppliers and consumers, can submit price and quantity for only one block of energy. Independent system operator (ISO) clears the market, then, and the agents are paid according to the rules of a discriminatory auction<sup>2</sup>. In such a setup, one can construct a relationship between the offer price to and the price to be paid.

---

<sup>2</sup> All the units dispatched are paid according to their offer price; therefore, they might be paid differently. Unlike discriminatory auction, in a uniform auction, they are paid at a same price

From the procedure, it is possible to connect the offer to the profit, which allows the agent to update the offer in a future period. However, the assumptions of one block offers, no forecast error and discriminative auction are not valid in any real markets in operation today.

An “autonomous” agent designed by Bunn et al [8-10] has been applied in a market which is a little closer to a real one. Like in the work of Sheble et al, a lossless network, no line constraints, no error in demand forecast and discriminatory auction were used, but the agent can offer several blocks. Two points on an offer space comprised of offer price and quantity define a linear offer curve. It is possible to evaluate prices and quantities of multiple blocks if quantity of each block is identical. By using a simple reinforcement algorithm, the agent updates the end points based on the result of market clearing. The market is assumed to be a Markov chain, i.e., current state contains all the relevant information so that the future state can be estimated by using the current state and relevant forecast. Consequently, the reinforcement algorithm is used to create the parameters that determine offer price and quantity of the blocks. Once all the offers are submitted, ISO clears the market. The simple nature of reinforcement algorithm allows the agent to work in a non-discriminatory auction. However, an agent characterized by a linear offer curve may not emulate the real market successfully since widely observed shape of an offer is a hockey-stick. Another problem in the study is that the period of Markov chain is arbitrarily assigned to one day with no reason.

There is another agent developed by Oh [11] which works well in a relatively more realistic market. Like other agents discussed above, a lossless network with no line constraints is used, but it can operate in a market with non-negligible forecast error

and stochastic demand containing. It submits an optimal offer based on initial guess on the strategies of its competitors. Then, as periods go on, it updates the guess and correspondingly its offer strategy based on previous market clearing results. The process minimizes the difference between the estimated and actual earning, i.e., the performance of the agent has an initial value dependence. The difference depends on the arbitrarily assigned initial value for a certain period. Furthermore, it is difficult to assign which parts of data are relevant for estimating a future state if competitors change their strategies during simulation. Due to this difficulty, inappropriate part of data can be used, which results in a high computational cost and inaccuracies of future estimates.

It is rather difficult to update price and quantity of multiple blocks independently. If there is a good fitting curve and the curve contains fitting parameters, then it might be easier to update price and quantity accordingly. Like studies performed by Bunn et al, a linear curve is most widely used due to its simplicity. However, a hockey-stick type is a commonly observed shape for the supply-side offer curve, which is significantly different from a linear curve. Recently, Oh [11] proposed a continuously differentiable equation relating offers with the physical quantity such as total capacity of a generator. The equation fits relatively well with offer curves observed in the Pennsylvania-New Jersey-Massachusetts (PJM) market. A continuously differentiable equation predicts a smooth curve on entire offer space. However, due to a kink observed in real offer curves at the boundary between high-priced and low-priced offer, discontinuous offer curves are observed. Furthermore, the equation predicts that an offer price divulges at a very large quantity offered, but actual offer curves get flat. Therefore, it is important to find a better equation for implementing learning mechanism.

Most current markets have supply-side participation only, and a hockey-stick type offer is generally observed in those markets. In such a situation, price spikes have been observed frequently. Generally speaking, 10%<sup>3</sup> reduced demand might prevent the appearance of most price spikes. Unless the 10% reduction cause bigger drop in profit, a demand-side agent has motivation to reduce its demand since the reduction may increase its profit by purchasing electricity at a lower price.

## 2.2. Model for Supply-side Offer Behaviors

Figure 2.1 shows different offer behaviors, i.e., one with low-priced offer only (D8) and the other with high-priced offer as well (Y6). It is difficult to classify the type of agents since the load forecast data is not provided. If the fairshare<sup>4</sup> [12] of D8 were less than 1,500 MW and that of Y6 were larger than 6,100 MW, D8 and Y6 would be classified as a marginal cost offer agent and a speculator, respectively.

As is shown in Figure 2. 1, there exist at least two different types of agents in a real market. There are two different blocks in the offer curve of Y6: one block with low priced offers with a flat curve and the other with high priced offers with a steep curve in offer price. In the offer curve of D8, only the first block showed up. To model these different types of agents consistently, one should consider the objects of two blocks. The first block is submitted at a low price in order to be dispatched while the second is done to attempt to raise the dispatched price. Due to these objectives, the very beginning of the first block (Block 1) is set to the minimum offer price, and the end of

---

<sup>3</sup> private talk from Prof. T. Mount

<sup>4</sup> the faireshare of an agent is the market share of the agent if all the participating agents offer all the quantities at the same price

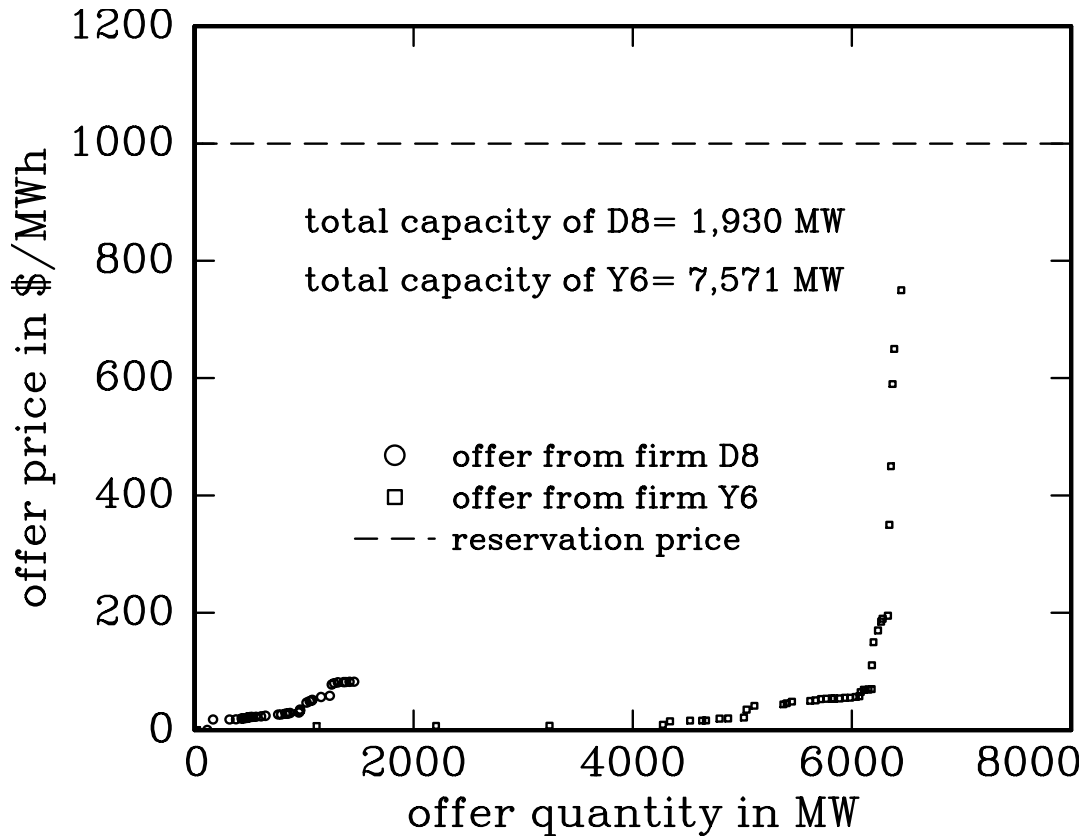


Figure 2. 1. Two commonly observed offer curves. Connecting lines are for visual guidance. These specific offer curves were found in the PJM market where D8 and Y6 are the company code known only to PJM.

the second (Block 2) is done to the maximum price of which an agent might think.

In comparing the two blocks, the second block is more sensitive to a change in market condition defined by the competitiveness of the market. Suppose there is no limitation such as maximum generator capacity and reservation price, i.e., all agents are allowed to submit any offer. In the situation, there would appear two blocks in an offer curve. However, an agent cannot submit an offer price higher than a reservation price, and quantity larger than its maximum capacity. With the limitation, an agent decides where to locate a window on an offer curve to maximize its profit. Furthermore, it can also partially close the window by withholding its capacity. Figure 2. 2 shows the procedure locating and partially closing window based on an optimization process of each agent.

As the market condition changes, it is reasonable to assume that a change in an offer price depends on the first derivative of offer price with respect to the offer quantity. Note that there is no reason two blocks should be paid differently. Therefore, there exists tendency to flatten expected earning<sup>5</sup>, i.e., an agent expects the same earning from both blocks. By adding one small block with an infinitesimally small size  $dq$ , expected earnings increase by  $pdq$  where the block is offered at a price of  $p$ . The expected earning at  $q$  might be calculated from the prices of  $q - dq$  and  $q + dq$ . By the same argument, driving forces<sup>6</sup> acting on expected earning at  $q + \frac{1}{2} dq$  exist.

Figure 2. 3 illustrates the change in an expected earning across a line  $S$ . The offer prices at the two ends of the block are  $p_1$  and  $p_2$ . Note that  $p_2$  is greater than  $p_1$ .

---

<sup>5</sup> earning from the block of interest if the block is dispatched

<sup>6</sup> the tendency to make two different expected earning at nearby blocks equal

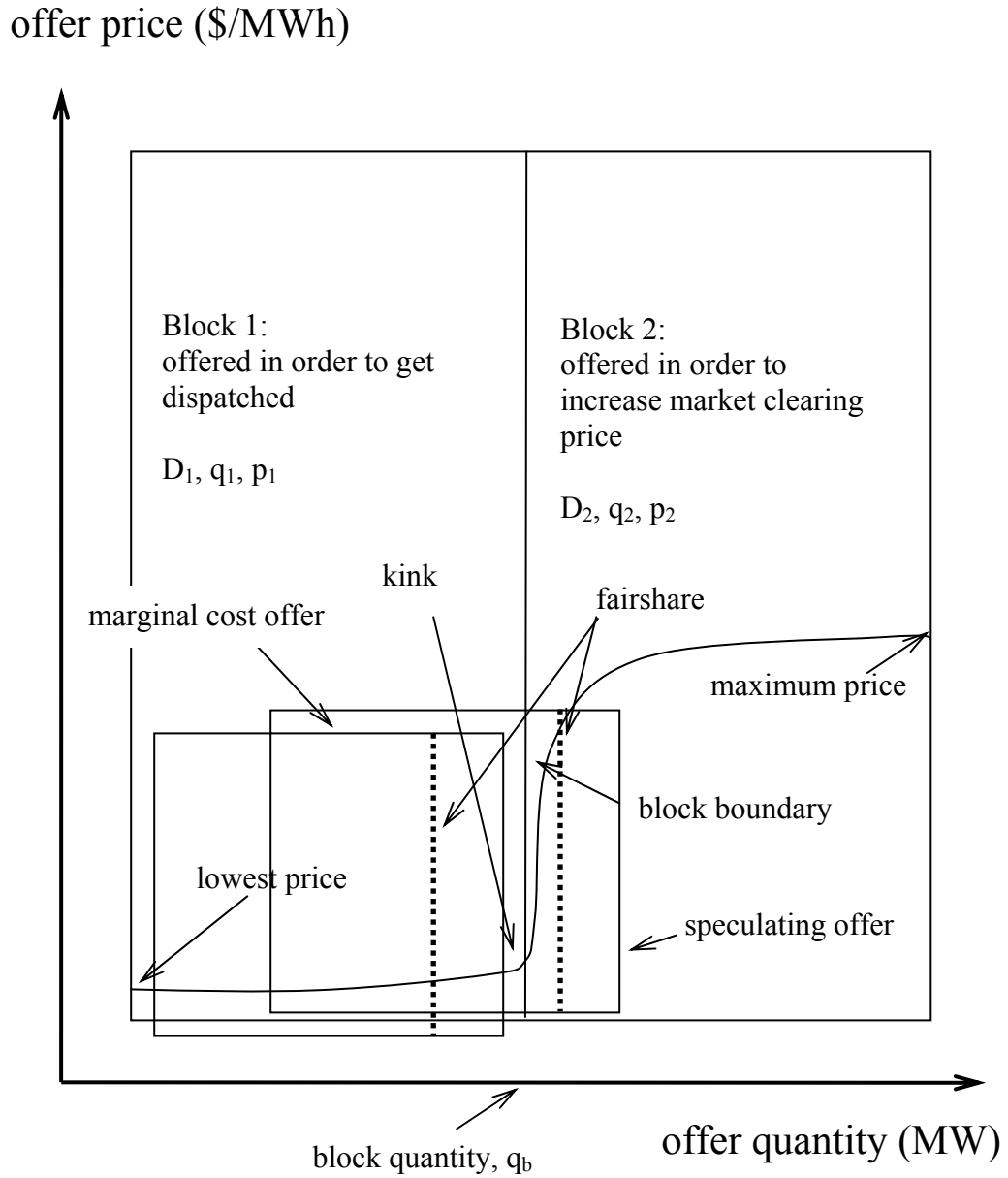


Figure 2. 2. Schematic diagram modeling marginal cost offer as well as speculating offer.  $D$  denotes the flattening factor of the block representing how easily the price get flat as market condition changes, and  $q$  and  $p$  refer offer quantity and price, respectively.

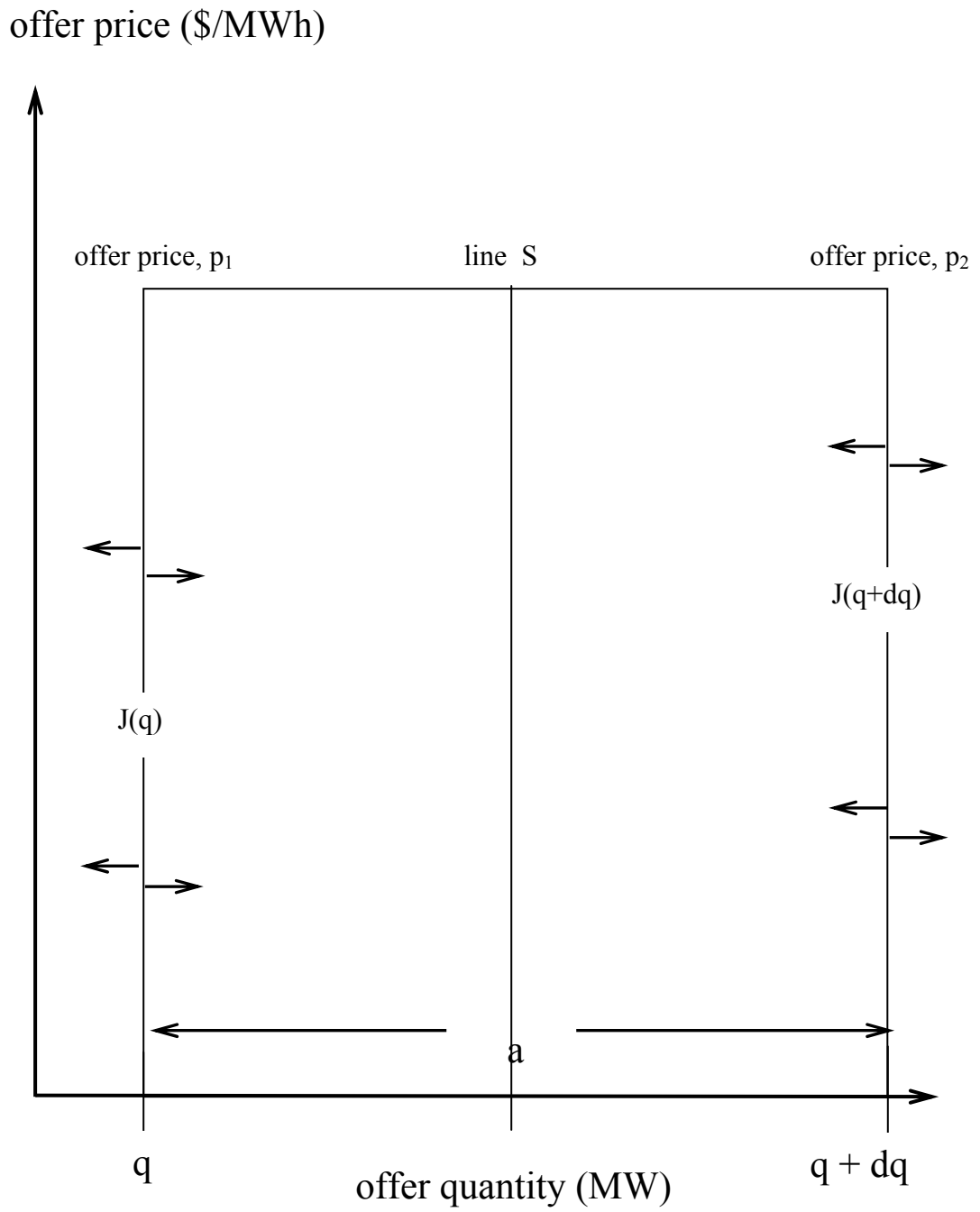


Figure 2. 3. Schematic diagram showing movement of expectation of earning



Driving forces at  $q$  and  $q + dq$  affect the expected earnings at both left and right neighbor. However, the effect from the right side is more than that from the left side since the expected earning is higher at the right one. Consequently, there is a net change to the left, i.e., down the offer price gradient.

For a more competitive market, price tends not to increase abruptly since the probability not to get dispatched increases significantly for a high-priced offer. Therefore, the affection rate to the left is given quantitatively by

$$J[\$/hmc] = \frac{1}{2}n_2\nu - \frac{1}{2}n_1\nu \quad (1)$$

where  $\nu$  is a constant evaluating the effect from a unit of driving force in  $[mc^{-1}]$  and  $mc$  is the unit of evaluating the market condition.

The two terms on the right hand side give the affection rate starting from  $p_1$  end and  $p_2$  end to the middle block, respectively. Note that  $\frac{1}{2}$  came from the fact that the flattening effect from one ends to line S takes only half of the change from one end to the other end. The quantity  $n_1$  and  $n_2$  in  $[\$/h]$  refer to the expected earning from the blocks offered at  $p_1$  and  $p_2$ , respectively. Therefore,

$$J = \frac{1}{2}n_2\nu - \frac{1}{2}n_1\nu = \frac{1}{2}\nu a(p_2 - p_1) \quad (2)$$

If the offer price does not vary rapidly inside the  $dq$  block, the term in the parenthesis can be approximated by Taylor's approximation:

$$p_2 - p_1 \approx -a \frac{\partial p}{\partial q} \quad (3)$$

When equations (2) and (3) are combined, one can find following equation:

$$J = \frac{1}{2}n_2v - \frac{1}{2}n_1v = \frac{1}{2}va(p_2 - p_1) = -\frac{1}{2}va^2 \frac{\partial p}{\partial q} = -D \frac{\partial p}{\partial q} \quad (4)$$

where D in  $[MW^2 / mc]$  is the flattening factor of the block representing how easily the price gets flat as market condition changes.

For the dual blocks, the offer price obeys the following equations:

$$\begin{aligned} J_{p_1} &= -D_1 \frac{\partial p_1}{\partial q} \\ J_{p_2} &= -D_2 \frac{\partial p_2}{\partial q} \end{aligned} \quad (5)$$

where J represents an affection rate, and subscript 1 and 2 stand for the 1<sup>st</sup> and the 2<sup>nd</sup> block as shown in Figure 2. 2.

Consider that there is a block with quantity coordinates q and q + dq as shown in Figure 2. 3. Let there be a change in the market condition with magnitude of dy, and let the affection rates from right to left be J(q + dq) and J(q) at q + dq and q, respectively. The total change in expected earning on plane S over the change in the market condition dy is:

$$[-J(q + dq) + J(q)]dy = -\frac{\partial J}{\partial q} dqdy \quad (6)$$

Note that J(q) is the flow leaving the plane at q, i.e., the gain in the S plane from p plane is -J(p).

The effect in the expected earning by offering S block under a change in market condition  $dy$  is then obtained by applying the formula for a differential:

$$[p(y + dy) - p(y)]dq = \left[ \frac{\partial p}{\partial y} dy \right] dq \quad (7)$$

This quantity must equal the change of the integrated offer in the block such that setting the two expressions equal gives

$$\frac{\partial J}{\partial q} = -\frac{\partial p}{\partial y} \quad (8)$$

Since the flattening factor,  $D$ , depends only on the property of the block, the value of  $D$  does not change with market condition and block size. Combining equations (4) and (8) gives:

$$\frac{\partial p}{\partial y} = -\left( \frac{\partial J}{\partial q} \right) = -\left[ \frac{\partial}{\partial q} \left( -D \frac{\partial p}{\partial q} \right) \right] = D \frac{\partial^2 p}{\partial q^2} \quad (9)$$

Equation (9) applies to the dual blocks:

$$\begin{aligned} \frac{\partial p_1}{\partial y} &= D_1 \frac{\partial^2 p_1}{\partial q^2} \\ \frac{\partial p_2}{\partial y} &= D_2 \frac{\partial^2 p_2}{\partial q^2} \end{aligned} \quad (10)$$

The first block is offered in order to get dispatched. The price can be determined by various parameters related to generators such as operating cost. The second block is offered in the attempt to increase the market clearing price. Since there is no limit in the quantity offered, the maximum price of the block approaches the maximum possible price. Therefore, the offers for the second block are related to the market situation more closely rather than parameters of a generator. The situation is similar to the following case in diffusion. Consider a cylindrical solid with an inner and outer layer exposed to a specific atmospheric condition for a long time. At some time, the outside atmosphere is abruptly changed to a different one, and maintained during some time. The state inside the cylinder is fixed in equilibrium with the initial atmosphere while the state outside is adjusted to the new one. The state from inside to outside smoothly changes from one equilibrium state to the other. By analogy, the situation for an agent is the following: a generator which has two blocks played a role in the traditional market, and then moves into a new market. Consequently, the price of the lowest offer by the generator should be same as a true marginal cost in the traditional market, and that of the highest offer should be the maximum possible offer. Therefore, the boundary conditions for equation (10) can be described by:

$$\begin{aligned} p(q = q_{\min}, y) &= p_{\min} [\$/MWh] \\ p(q = q_{\max}, y) &= p_{\max} [\$/MWh] \end{aligned} \quad (11)$$

where  $y$  evaluates market condition.

At the boundary between low-price and high-priced offers, offer price and affection rate must be continuous since adding an indefinitely small sized quantity does not change both abruptly. The situation defines a condition at the boundary;

$$\begin{aligned}
p(q = q_b^-, y) &= p(q = q_b^+, y) \\
D_1 \frac{\partial p_1}{\partial q} \Big|_{q=q_b^-} &= D_2 \frac{\partial p_2}{\partial q} \Big|_{q=q_b^+}
\end{aligned} \tag{12}$$

With the given conditions, solving equation (10) gives an expression for offer price as a function of market condition,  $y$ , and quantity,  $q$ , for two blocks. Note that for the 1<sup>st</sup> block,  $q$  is less than  $q_b$  where  $q_b$  is the boundary quantity between two blocks) [13]

$$p_1(y, q) = \frac{P_{\max} - P_{\min}}{1 + \sqrt{D_1 / D_2}} \left[ \operatorname{erfc} \left( \frac{q_b - q}{2\sqrt{D_1 y}} \right) - p_1^b \right] \tag{13}$$

where

$$p_1^b(y, q) = \exp \left[ h_1 (q_b - q) + h_1^2 D_1 y \right] \operatorname{erfc} \left( \frac{q_b - q}{2\sqrt{D_1 y}} + h_1 \sqrt{D_1 y} \right) \tag{14}$$

and

$$h_1 = \frac{k}{D_1} \left( 1 + \sqrt{\frac{D_1}{D_2}} \right)$$

and for the 2<sup>nd</sup> block where  $q$  is greater than  $q_b$

$$p_2(y, q) = \frac{P_{\max} - P_{\min}}{1 + \sqrt{D_1 / D_2}} \left\{ 1 + \sqrt{\frac{D_2}{D_1}} \left[ \operatorname{erf} \left( \frac{q - q_b}{2\sqrt{D_2 y}} \right) + p_2^b \right] \right\} \tag{15}$$

where

$$p_2^b(y, q) = \exp[h_2(q - q_b) + h_2^2 D_2 y] \operatorname{erfc}\left(\frac{q - q_b}{2\sqrt{D_2 y}} + h_2 \sqrt{D_2 y}\right)$$

and

(16)

$$h_2 = \frac{k}{D_2} \left(1 + \sqrt{\frac{D_2}{D_1}}\right)$$

where the superscript b represents boundary effect, which comes from the different characteristics of two different blocks, and k stands for the boundary constant quantifying the boundary effect<sup>7</sup>.

If a generator (or a firm) has only one decision maker submitting its offer, there should be no boundary effect, i.e.,  $k \rightarrow \infty$ . In such a case, both  $p_1^b$  and  $p_2^b$  approach zero, and the expressions for offer prices are

$$p_1(y, q) = \frac{p_{\max} - p_{\min}}{1 + \sqrt{D_1 / D_2}} \left[1 - \operatorname{erf}\left(\frac{q_b - q}{2\sqrt{D_1 y}}\right)\right]$$
(17)

$$p_2(y, q) = \frac{p_{\max} - p_{\min}}{1 + \sqrt{D_1 / D_2}} \left[1 + \sqrt{\frac{D_2}{D_1}} \operatorname{erf}\left(\frac{q - q_b}{2\sqrt{D_2 y}}\right)\right]$$
(18)

Offer curves could be fitted to the following equation:

$$p(y, q) = u(q_b - q)p_1(y, q) + u(q - q_b)p_2(y, q)$$
(19)

where u is the unit step function;

---

<sup>7</sup> if two blocks have different properties, boundary effects might be present, i.e., the offer curve might not be continuous

$$u(x) = \begin{cases} 0 & \text{if } x < 0 \\ 1 & \text{otherwise} \end{cases} \quad (20)$$

The data shown in Figure 2. 1 was used to fit equation (19), and the results are shown in Fig. 2. 4. The cutoff quantity,  $q_c$ , can be defined as an agent's maximum offer quantity. The cutoff quantities for D8 and Y6 were about 1,500 and 6,200 MW, respectively. The  $q_c$  of D8 was larger than the quantity at the boundary,  $q_b$ , while that of Y6 was smaller than  $q_c$ . In order to characterize the behavior of an agent, it is useful to define the deviation quantity,  $q_d \equiv \min\{q_c, q_b\}$ . Then, the distance from the fareshare to the deviation quantity is a measure of the degree of speculation (DOS). DOS is an important factor to classify offer behavior. For example, even if an offer curve of an agent contains a high-priced offer as well as a low-priced one, the agent might make the market more competitive if the block containing fairshare is offered at a lower price. DOS is defined as the relative location of boundary from the fareshare:

$$\text{DOS} = \begin{cases} 50 \times \frac{\text{capacity} - q_b}{\text{capacity} - \text{fairshare}} & \text{if } q_b \geq \text{fairshare} \\ 50 \times \frac{2 \times \text{fairshare} - q_b}{\text{fairshare}} & \text{if } q_b < \text{fairshare} \end{cases} \quad (21)$$

To define DOS, it is crucial to calculate fairshare based on demand forecast. For a lossless system with no network, this is easy since fairshare can be the simply capacity ratio of an agent. For a real system, the simple ratio of capacity does not work since real systems always have loss, line constraints and distributed load. However, an agent could calculate fairshare by running an AC optimal power flow (OPF) with identical offer curves for all the participating generators once network is known to the agent.

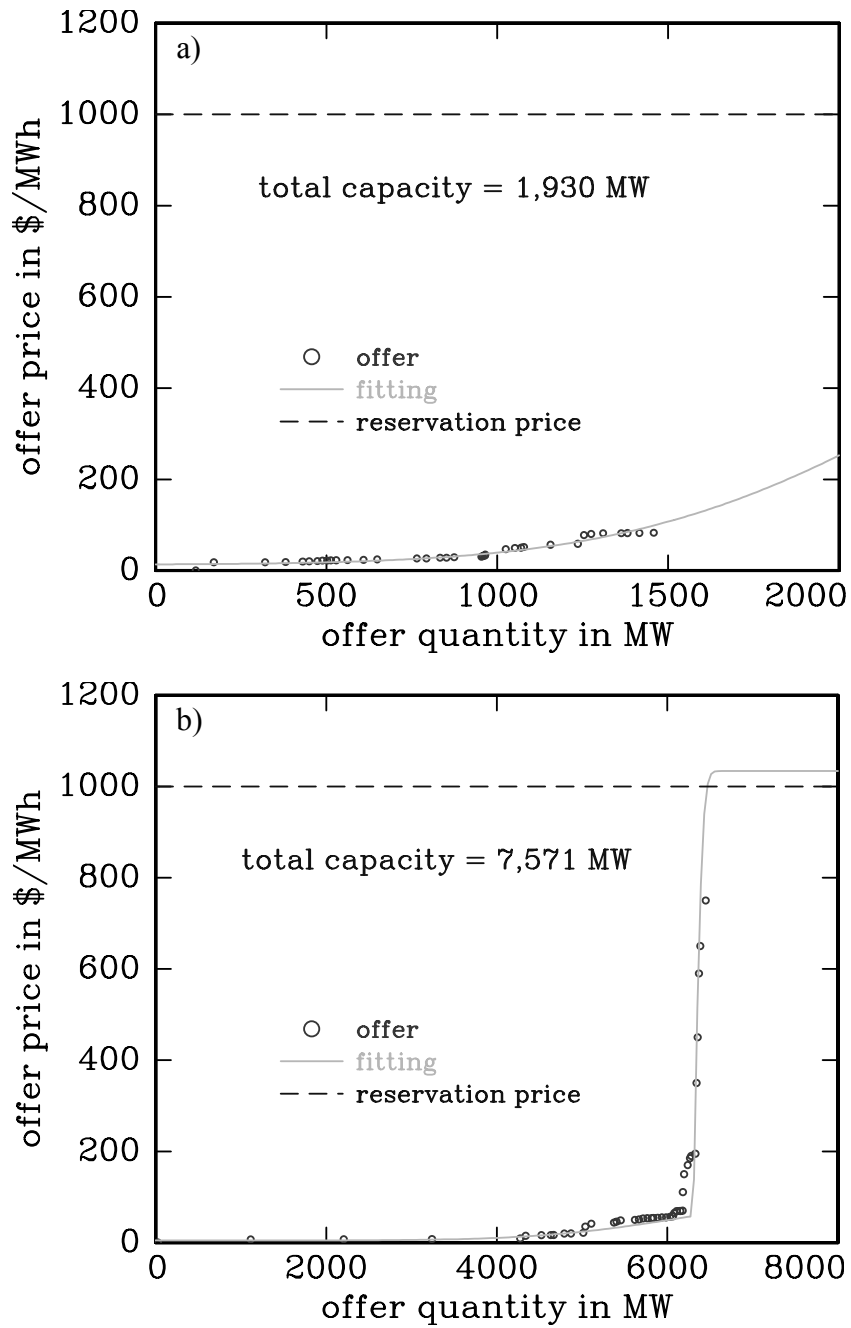


Figure 2. 4. Fitting results of two offer curves in a same day to equation (19). Two blocks are visible only in b), but the same  $p^{\max}$  was used for both fittings



The dispatched quantity from OPF gives approximate for the fairshare at given load forecast

With this model, it is possible to submit a price according to a quantity. There are several factors that make use of the model quantitatively in designing an agent such as the flattening factor (D) and market condition (y).

### 2.2.1. Flattening factor

Flattening factor (D) dictates the slope of the offer curve. D in an offer curve describes how fast a quantity offered at a same price changes as a market condition changes. Therefore, an agent with a higher D quickly responds to change in the market condition since it is easy for such an agent to change price for all the quantity in an offer space.

There are several factors determining the magnitude of the tendency. The flattening is an activated process, which means that there are two competing forces to govern the tendency: a flattening force and an ordering force. More flat curves will be obtained as a flattening force increases and/or an ordering force decreases.

Similar to solid state physics, for an activated process as was mentioned before, there exists an Arrhenius type equation to describe the process;

$$D(T) = D_0 \exp\left(-\frac{E}{kT}\right) \quad (22)$$

where  $D_0$ ,  $E$  and  $kT$  are the flattening factor with infinitely high disordering force, ordering and disordering forces, respectively.  $D_0$  may depend on the generator itself due to its operating cost since an operating cost itself has a slope.

In this modeling, ordering force is a quantification of regulations, and disordering force is that of the tendency toward risk<sup>8</sup>. Regulations in existing markets apply to all the market participants equally, and make participants difficult to speculate, which results in a flat curve in offer space. For a given agent, the introduction can be implemented by adding  $E^{new}$ :

$$\begin{aligned} D^{new} &= D_0 \exp\left[-\frac{(E + E^{new})}{kT}\right] = \left[D_0 \exp\left(-\frac{E}{kT}\right)\right] \exp\left(-\frac{E^{new}}{kT}\right) \\ &= D^{old} \exp\left(-\frac{E^{new}}{kT}\right) \end{aligned} \quad (23)$$

Therefore, in real markets, regulation is additive by nature.

The tendency toward risk differs for each individual supplier statistically. The tendency might be changed in case of a change in ownership and/or in mind of a decision maker. A change in tendency toward risk alters offer curves completely, i.e., a new flattening factor must be re-evaluated. There are three categories in tendency to consider: risk-averse, risk-neutral and risk-seeking. To model these different tendencies, utility functions are introduced by Bernoulli [14]. Grayson found a good fit between Bernoulli's logarithmic function and the actual utility function [15]. An agent having a utility function with concave shape like logarithmic function is referred

---

<sup>8</sup> Each agent has different tendency toward risk; risk-averse, risk-neutral and risk-seeking. The tendency can be evaluated based on its utility function which maps benefit that the earning brought from earning

as risk-averse since its evaluation on uncertain earning is less than that on the same amount of actual earning. Other tendencies such as risk-neutral and risk-seeking have linear and convex curve for utility functions. The value of  $T$  in equation (22) increases as tendency changes from risk-averse to risk-seeking since a risk-seeking agent is willing to increase an offer price of a lower block, which results in a flat offer curve.

### **2.2.2. Quantity evaluating the market condition**

Flattening phenomena considered here is a process connecting two different equilibrium states. For a given market condition  $y_0$ , system stays in one state, and the state changes toward a new equilibrium state as the condition changes to different condition,  $y_1$ . Suppose there is a sufficiently small change in a market condition. With the small change, the resulting price-quantity profile depends on a flattening factor of a block considered ( $D$ ) and a market condition  $y$ . The profile built contains all the equilibria between two states. For example, if the price at one equilibrium state is 0 and that at the other is 100, then the profile at the change in a market condition  $y$  contains all the values of price from 0 to 100.

Market condition  $y$  is a term quantifying degree allowed for a price of a block to change from one state to another. As mentioned before, a block that was in one equilibrium state becomes another in a different state. For example, offer in a traditional market was a true marginal cost, but that in a totally deregulated market with no regulation should be different from marginal cost such as a speculative one. Market condition may allow an agent to exploit the market. For example, once an

agent finds its competitors are speculators, then it will submit a more flat offer in order to take advantage of the less competitive market environment.

Publicly available information such as historical data of nodal price is chosen to determine the value of a market condition since price is considered most unbiased and relevant information. However, the price might be different according to the location of an agent. But, the change in  $y$  should be in common among all agents since all prices are correlated with each other<sup>9</sup>. If the agent of interest is the only agent which speculates in the market,  $y$  should not be high since the environment that the agent faces actually competitive in spite of high prices. To compensate this effect, dispatched quantity is also added to estimate  $y$  in this study:

$$y = \frac{\text{share}}{\text{fair share}} \frac{\overline{p_{recent}}}{\overline{p}} \quad (24)$$

where  $\text{share}$ ,  $\overline{p_{recent}}$  and  $\overline{p}$  stand for the quantity dispatched, mean of recent nodal prices and mean of nodal prices in the same state, respectively. In this study,  $\overline{p_{recent}}$  is chosen as the mean price over most recent one week. It is noteworthy that an actual value for  $\overline{p_{recent}}$  does not change significantly with the choice of the period.

If the system evolves, all state properties including market condition cannot be invariant. Therefore, it is worthwhile to mention that both  $\overline{p_{recent}}$  and  $\overline{p}$  must contain data only in the same state.

---

<sup>9</sup> Relationship among price can be driven during the derivation of the generation sensitivity matrix with respect to price; for a detailed derivation, see Appendix A

### 2.2.3. Boundary effect

Typical offer behaviors without boundary effect have been discussed. Note that  $k$  in such case approaches infinity in equations (14) and (16). However, it is possible for an offer to show such an effect. In the PJM market, Fig. 2. 5 shows a discontinuous offer curve found on July 26<sup>th</sup> by B5 after a first price spike observed on June 7<sup>th</sup>. Before the first price spike, the firm had submitted low-price offer only. The discontinuity can be modeled as a boundary effect which is resulted in by no perfect communication between two blocks. The fitting is performed by using equations (13), (15) and (19).

### 2.3. Model for Demand-side Bid Behaviors

As was described earlier, a boundary quantity is defined as non-differential points of an offer curve, i.e., the point where offer curve departs from a lower price. When fairshare is located higher than the boundary quantity, the agent is classified as a speculator. Approximately 10% reduced demand results in shifting fairshare far down to the boundary quantity at the given offer curve. Therefore, demand-side participation is suggested for potential efficiency improvement of a market. For practical reasons, a new method for demand-side participation might includes following features; 1) end consumers do not need to evaluate electricity all the times like 24 times in a day, 2) small discrepancy between dispatch and actual demand does not matter much for a consumer, 3) some consumers are willing to sacrifice reliability to reduce an electric bill to some degree, 4) some don't mind paying a high price for a reliability such as hospital or synchrotron, etc. such demands are termed must-be-served demands while others are defined as price-based demands.

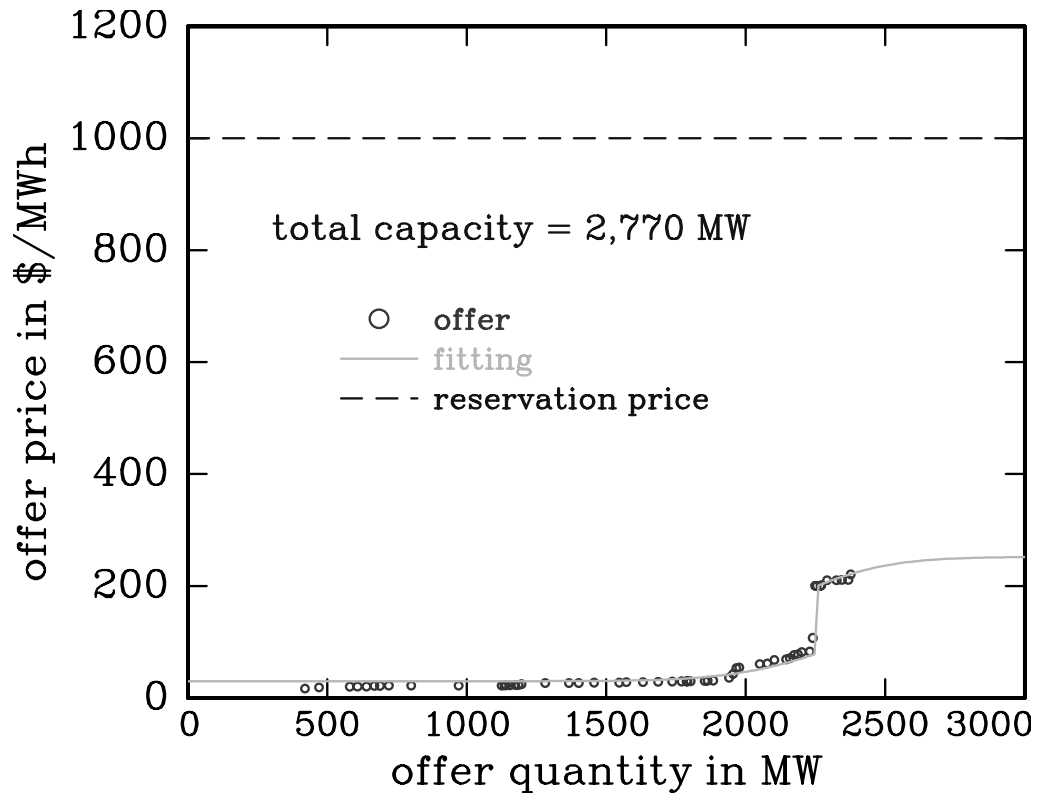


Figure 2. 5. An offer curve submitted by B5 in July 26<sup>th</sup> and fitting with equations (13) – (16) and (19). The curve shows a boundary effect at 2200 MW.

To develop a demand-side model, one must bear in mind that consumers sacrifice reliability marginally (e.g., 10 %) to reduce an electric bill, but too frequent serious price-response-load (PRL) must be avoided. As was mentioned in feature 1), the method reducing demand should be easily performed or another agent should take over the job for consumers. For a given market structure, a distributor (e.g., NYSEG) may submit bids for consumers, and buy electric power from generators, and then distribute electric power based on priorities to fulfill elementary demands. After each period, the distributor checks the discrepancy between dispatch and actual demand. If the discrepancy does not exceed predetermined value, it can assume all the demand were successfully fulfilled. Otherwise, it declares a PRL. A predetermined value for PRL needs to be defined in a contract made between the distributor and end consumers. Every given period, it signs a new contract with consumers. For example, every year it makes a contract that fulfilling 90% of demand is acceptable, but fulfilling less than that is claimed as a PRL. Suppose no more than 10 times of PRL in a month is allowed. For 10 times, an agent does not need to satisfy all the demands. Consequently, the agent has freedom not to satisfy all demands proportional to the remaining allowed number of PRL. The freedom is inversely proportional to the number of remaining periods before current contract period ends since there is a non-negligible possibility of a PRL for more remaining periods. For a simple summary, an agent would have a contract with end consumers in the category of price-based demand containing following terms; 1) it can have  $n_{PRL}$ -times allowed PRL's in a given period like a month, 2) where the term PRL is defined the case that only less than a predetermined percentage of forecast and/or actual demand is served, 3) after  $n_{PRL}$ -times of PRL in the given period, the bid should be same as an inelastic demand curve, and finally 4) big penalty should be given if the agent does not serve electricity

properly more than  $n_{PRL}$ -times while it can. An agent might offer several options for different values of  $n_{PRL}$  to accommodate various needs of end consumers.

If an end consumer does not want to sacrifice reliability, then it is also possible to have another type of contract such that a distributor always serve such a customer before serving any other demands if price is below a certain price,  $p_c$ . Demands associated with such contracts are called must-be-served demands. Since the demand forecast is not always accurate and must-be-served demand prefers being served even in the situation of underestimated forecast, the contract should include another price for insurance. Note that the price for insurance is less than  $p_c$ . For example, a contract defines  $\xi$  and  $p_m$  in a way that the consumer agreed to pay for electricity to fulfill actual demand up to  $(1+\xi)$  times of forecasted demand if price is less than or equal to  $p_m$ .

Before developing a demand model, one needs to consider the characteristics of electricity as well as demand. There is a minimum quantity of energy to satisfy an individual demand. Consequently, elementary individual demand can be quantized and ranked in terms of priority which is evaluated in terms of bidding price. For example, one wants to turn on an electric bulb and a fan which need 150 Watts each. If only 150 Watts is available, only one demand between turning on the bulb and on the fan can be fulfilled, not both. Since elementary demand has such a repelling property there exists an exclusion principle in case that available quantity is limited. When all the elementary needs are augmented according to their priorities, one can construct a bidding function, i.e., demand curve which represents a willingness to pay for electricity. Note that there is no limit in available quantity for must-be-served demands. Consequently, an exclusion principle does not apply to such demands.



In general, prices are increasing with respect to quantity offered. With a given supply curve, quantities to fulfill demands occupy different state according to their prices offered. The state is called quantity state. For constructing problem, consider a system of demands with allowed quantity state  $q_i$  to satisfy individual demand  $n_i$ . Note that higher state corresponds to higher price. Let  $g_i$  be the number of allowed demand at quantity state  $q_i$ , and  $n_i$  be the actual number of demand fulfilled. Note that the values of  $q_i$  and  $g_i$  are fixed, and the value of  $n_i$  is random according to the particular demand arrangement. In this problem, both the number of all individual demands and that of total quantity state are fixed. From thermodynamic theory, a system is most stable when its entropy is maximized. Without external forces, configuration entropy is the largest portion of the total entropy. Configuration entropy is evaluated in terms of the number of possible configurations in a following way [16].

$$S = k \log W \quad (25)$$

where  $S$ ,  $k$  and  $W$  stand for system entropy, Boltzmann constant and the number of possible configurations, respectively.

For a demand-side agent, most stable configuration is to distribute fulfilled demand that maximizes profit of demand-side. Therefore, the distribution is optimal. The bidding function describes the distribution. The optimal distribution must satisfy two constraints: total fulfilled demand should be no more than the total demand, and total quantity state for fulfilling demand should be no more than the quantity state defined by offered quantity. With given setup, one wants to optimize the distribution of fulfilled demand based on the preference:

$$\begin{aligned}
& \max_{n_i} \text{klog}W(n_i) \\
& \text{subject to } \sum_i n_i \leq N_{tot} \\
& \quad \sum_i n_i q_i \leq Q_{tot}
\end{aligned} \tag{26}$$

where  $N_{tot}$  and  $Q_{tot}$  denote the number of all individual demand and total quantity state.

As was mentioned earlier, on the distributors' point of view individual demand is equal entity. Each individual demand cannot share elementary quantity and not distinguishable either. Therefore, for a demand fulfilling state  $\bar{n} = (n_1, n_2, n_3, \dots)$ <sup>10</sup>, the conditional probability that a state at a given quantity  $q_i$  to be fulfilled is  $f(q_i | \bar{n}) = n_i / g_i$ , and the distribution  $f(q_i)$  is following;

$$f(q_i) = \sum_{\bar{n}} f(q_i | \bar{n}) p(\bar{n}) = \sum_{\bar{n}} f(q_i | \bar{n}) \frac{W(\bar{n})}{W_{tot}} = \frac{1}{W_{tot}} \sum_{\bar{n}} f(q_i | \bar{n}) W(\bar{n}) \tag{27}$$

where  $W(\bar{n})$  and  $W_{tot}$  denote the number of such fulfillment and that of total possible fulfillment, respectively.

To calculate the distribution for fulfillment  $W(\bar{n})$ , count the number of combination to place  $n_i$  fulfilled demand into  $g_i$  offered quantity state when  $g_i > n_i$ . Note that the number of total offered quantity state is total capacity to accommodate demand. Since the number of fulfilled demands at  $i^{\text{th}}$  quantity state cannot exceed the capacity, there should be occupied and unoccupied demands at  $i^{\text{th}}$  quantity state. The number of possible combinations to arrange those occupied and unoccupied sites is:

$$w(n_i) = \binom{g_i}{n_i} = \frac{g_i!}{(g_i - n_i)! n_i!} \tag{28}$$

---

<sup>10</sup> the demands in the parenthesis are fulfilled

Since each combination for  $n_i$  in the distribution  $\bar{n}$  is independent with each other, the overall distribution to have  $\bar{n}$  state,  $W(\bar{n})$  is

$$W(\bar{n}) = \prod_i w(n_i) = \prod_i \frac{g_i!}{(g_i - n_i)! n_i!} \quad (29)$$

One can evaluate equation (29) by using Stirling approximation for a sufficiently large  $N$ :

$$N! \cong (2\pi N)^{1/2} N^N \exp\left(-N + \frac{1}{12N} + \dots\right) \quad (30)$$

Taking logarithm on both sides of equation (30) gives:

$$\log N! \cong \frac{1}{2} \log(2\pi) + \left(N + \frac{1}{2}\right) \log N - N + \frac{1}{12N} \quad (31)$$

For a large value of  $N$ , a further approximation can be done for simplification in a following way

$$\log N! \cong N \log N - N \quad (32)$$

For simplicity, the Boltzmann constant in the original optimization problem shown in equation (26) can be dropped since it is a positive constant:

$$\begin{aligned} & \max_{n_i} \log W(n_i) \\ & \text{subject to } \sum_i n_i \leq N_{tot} \\ & \sum_i n_i q_i \leq Q_{tot} \end{aligned} \quad (33)$$

Lagrange method is a well known procedure to solve an optimization process like equation (33). A Lagrangian with undetermined multipliers can be formed;

$$\begin{aligned}
L(\bar{n}) &= \log W(\bar{n}) + \mu_1 \left( N_{tot} - \sum_i n_i \right) + \mu_2 \left( Q_{tot} - \sum_i n_i q_i \right) \\
&= \log \left[ \prod_i \frac{g_i!}{(g_i - n_i)! n_i!} \right] + \mu_1 \left( N_{tot} - \sum_i n_i \right) + \mu_2 \left( Q_{tot} - \sum_i n_i q_i \right) \\
&= \sum_i \{ \log(g_i!) - \log[(g_i - n_i)!] - \log(n_i!) \} \\
&\quad + \mu_1 \left( N_{tot} - \sum_i n_i \right) + \mu_2 \left( Q_{tot} - \sum_i n_i q_i \right)
\end{aligned} \tag{34}$$

By using equation (32), the Lagrangian can be approximated by:

$$\begin{aligned}
L(\bar{n}) &= \sum_i [g_i \log g_i - (g_i - n_i) \log(g_i - n_i) - n_i \log n_i] \\
&\quad + \mu_1 \left( N_{tot} - \sum_i n_i \right) + \mu_2 \left( Q_{tot} - \sum_i n_i q_i \right)
\end{aligned} \tag{35}$$

From maximization, one finds Kuhn-Tucker multipliers ( $\mu_1$  and  $\mu_2$ ) as well as critical points for individual demand. Kuhn-Tucker condition<sup>11</sup> [17] gives

---

<sup>11</sup> Assume that  $f(x)$ ,  $g_i(x)$  are differentiable functions satisfying certain regularity condition<sup>2</sup>. Then  $x^*$  can be an optimal solution for the nonlinear programming problem only if there exist  $m$  numbers  $u_1, u_2, \dots, u_m$  such that all the following conditions are satisfied:

1.  $\left. \frac{\partial f}{\partial x_j} - \sum_{i=1}^m \mu_i \left( \frac{\partial g_i}{\partial x_j} \right) \leq 0 \right\}$
2.  $\left. x_j^* \left[ \frac{\partial f}{\partial x_j} - \sum_{i=1}^m \mu_i \left( \frac{\partial g_i}{\partial x_j} \right) \right] = 0 \right\}$  at  $x = x^*$  for  $j = 1, 2, \dots, n$
3.  $\left. g_i(x^*) - b_i \leq 0 \right\}$
4.  $\left. u_i [g_i(x^*) - b_i] = 0 \right\}$  for  $i = 1, 2, \dots, m$
5.  $x_j^* \geq 0$  and  $u_i \geq 0$

$$\begin{aligned}
n_i \left[ \frac{\partial L(\vec{n})}{\partial n_i} \right] &= n_i \left[ \log \left( \frac{g_i - n_i}{n_i} \right) - \mu_1 - \mu_2 q_i \right] = 0 \\
\mu_1 \left( N_{tot} - \sum_i n_i \right) &= 0 \\
\mu_2 \left( Q_{tot} - \sum_i n_i q_i \right) &= 0
\end{aligned} \tag{36}$$

Since fulfilled demand  $n_i$  is nonzero by definition, the first part in equation (36) allows

$$\frac{n_i}{g_i} \equiv f(q_i) = \frac{1}{1 + \exp(\mu_1 + \mu_2 q_i)} \tag{37}$$

The distribution described in equation (37) optimizes the profile of fulfilled demand.

From the knowledge of optimization, the Kuhn-Tucker multipliers are shadow prices of corresponding constraints. Fulfilling one additional demand increases demand-side profit while requiring more electricity might increase market clearing price. In other word, addition of one more demand increases Lagrangian by  $\mu_1$  if the constraint is binding, but increase in demand reduces profit of demand-side by requiring more electricity. Consequently,  $\mu_1$  takes a negative value. On the other hand, adding one additional quantity to the system increases profit of demand-side by  $\mu_2$ . This addition results in different satisfaction to individual demand since  $i^{\text{th}}$  demand needs  $q_i$  quantity to fulfill. In demand-side perspective, market clearing prices tend to be low when more electricity is available, which results in increasing demand-side profit.

When a demand must be served such as in hospital, synchrotron etc., any quantity state can accommodate many demands. In such a case, there is no limit to the occupation number at each level, i.e., no exclusion principle exists. For finding

optimal fulfilling distribution for such demands, one calculates the number of ways to assign  $n_i$  fulfilled demands in  $q_i$  quantity states. Note that all the demands are indistinguishable to a demand-side agent. Since price is not important to fulfill such demands, all the quantity states are identical if the prices for the states are acceptable. Then all available state can be fulfilled regardless  $q_i$ . After fulfilling, one can find the fulfillment configuration by finding which state is occupied. Therefore the problem is distributing identical demands on various sites where there is no limit. The situation is identical to putting  $n_i$  identical balls into  $g_i$  sites or to arranging  $n_i$  identical balls and  $(g_i - 1)$  identical barriers. For getting an analogy to the case described in the last sentence, suppose that there are  $(g_i - 1)$  partitioned sites in a same quantity state and assign  $n_i$  identical demands. This is identical to the number of combinations that there are  $(n_i + g_i - 1)$  white balls sitting on each site and one picks up  $n_i$  balls and paints them with red color. Finally, there are  $(g_i - 1)$  white balls remaining. In the case, the number of possible configurations to arrange red and white balls is:

$$w(n_i) = \binom{n_i + g_i - 1}{n_i} = \frac{(n_i + g_i - 1)!}{n_i!(g_i - 1)!} \quad (38)$$

Then one can construct an optimization problem with the same constraints used in the previous case. Thus, the Lagrange method for the problem gives:

$$\begin{aligned} L(\bar{n}) &= \log W(\bar{n}) + \mu_1 \left( N_{tot} - \sum_i n_i \right) + \mu_2 \left( Q_{tot} - \sum_i n_i q_i \right) \\ &= \log \left[ \prod_i \frac{(n_i + g_i - 1)!}{n_i!(g_i - 1)!} \right] + \mu_1 \left( N_{tot} - \sum_i n_i \right) + \mu_2 \left( Q_{tot} - \sum_i n_i q_i \right) \\ &= \sum_i \{ \log[(n_i + g_i - 1)!] - \log(n_i!) - \log[(g_i - 1)!] \} \\ &\quad + \mu_1 \left( N_{tot} - \sum_i n_i \right) + \mu_2 \left( Q_{tot} - \sum_i n_i q_i \right) \end{aligned} \quad (39)$$

Since  $n_i$  and  $g_i$  are sufficiently large, 1 in equation (39) can be ignored and applying equation (32) allows the Lagrangian approximated:

$$L(\vec{n}) = \sum_i [(n_i + g_i) \log(n_i + g_i) - n_i \log n_i - g_i \log g_i] + \mu_1 \left( N_{tot} - \sum_i n_i \right) + \mu_2 \left( Q_{tot} - \sum_i n_i q_i \right) \quad (40)$$

For maximization, one needs to find optimality conditions for individual demand as well as Lagrange multipliers:

$$\begin{aligned} n_i \left[ \frac{\partial L(\vec{n})}{\partial n_i} \right] &= n_i \left[ \log \left( \frac{n_i + g_i}{n_i} \right) - \mu_1 - \mu_2 q_i \right] = 0 \\ \mu_1 \left( N_{tot} - \sum_i n_i \right) &= 0 \\ \mu_2 \left( Q_{tot} - \sum_i n_i q_i \right) &= 0 \end{aligned} \quad (41)$$

As was mentioned earlier,  $n_i$  cannot be zero. Then, the first part in equation (41) allows

$$\frac{n_i}{g_i} \equiv f(q_i) = \frac{1}{\exp(\mu_1 + \mu_2 q_i) - 1} \quad (42)$$

Note that the Lagrange multipliers are associated with the same constraints as before.

One can find an analogy in statistical physics similar to these distribution functions. The distribution, equation (37), for price-based demand has a similar form as Fermi-Dirac distribution<sup>12</sup> that a particle obeys following exclusion principle [18]:

---

<sup>12</sup> a distribution that indistinguishable particles following Pauli's exclusion principle obey

$$f(E) = \frac{1}{1 + \exp\left(\frac{E - E_F}{kT}\right)} \quad (43)$$

where  $(E - E_F)/k$  and  $T$  are ordering and randomizing forces, respectively.

In equation (43),  $E_F$  is a reference energy state, called Fermi Energy. Loosely speaking, Fermi energy represents the energy state that a particle can occupy the state with probability of  $1/2$  for a given randomizing force. Since  $f(E)$  is the distribution function of a particle,  $f(E)dE$  stands for the probability that a particle can be found in an energy state between  $[E, E + dE]$ . The probability is proportional to how many particles to accommodate by adding  $dE$  more energy state. One can derive following equation of differential accommodation

$$f(E)dE = \frac{1}{1 + \exp\left(\frac{E - E_F}{kT}\right)} dE = kT d \left\{ \ln \left[ \frac{\exp\left(\frac{E - E_F}{kT}\right)}{1 + \exp\left(\frac{E - E_F}{kT}\right)} \right] \right\} \quad (44)$$

The change in accommodation decreases with increasing  $E$ , i.e., system wants to prevent higher energy state.

One can define a priority function or a willingness to pay function,  $B(q)$ , representing true evaluation to the electricity of individual needs. Then  $B(q)dq$  represents the amount of demands can be accommodated by dispatching more quantity by  $dq$ .



$$B(q)dq = fr \, d \left\{ \ln \left[ \frac{\exp\left(\frac{q - q_F}{fr}\right)}{1 + \exp\left(\frac{q - q_F}{fr}\right)} \right] \right\} = \frac{dq}{1 + \exp\left(\frac{q - q_F}{fr}\right)} \quad (45)$$

From this analogy, a bidding function can be defined as a similar way in the Fermi-Dirac distribution:

$$B(q) = \frac{1}{1 + \exp\left(\frac{q - q_F}{fr}\right)} \quad (46)$$

where  $fr$  stands for freedom of an agent for the period.

One can find the similarity between equations (43) and (46). The bidding function is the distribution function that optimizes demand-side satisfaction. By comparison, Kuhn-Tucker multipliers are identified in a following way;

$$\begin{aligned} \mu_1 &= -\frac{q_F}{fr} \\ \mu_2 &= \frac{1}{fr} \end{aligned} \quad (47)$$

As was described earlier, the value of  $\mu_1$  is negative with the magnitude of weighted reference quantity which individual demand has on average.  $\mu_2$  is positive with a value of inverse of freedom that demand-side agent has. When a demand-side agent has more freedom, it does not add one more quantity, i.e., less value for  $\mu_2$ .

For an agent, priority of an individual demand is important only because it reflects true evaluation in terms of bidding price, i.e.,  $B = p/p_{\max}$  where  $B$ ,  $p$  and  $p_{\max}$  represent

a priority of each demand, bidding price and the maximum possible bidding price for a current period, respectively. A distributor needs to get electric power to meet demand. For example, suppose NYSEG has five more remaining periods before contract expires, but it has six more allowed PRL's. In such a case, NYSEG may not need to satisfy all the demands. Then freedom,  $fr$ , can be defined

$$fr = \begin{cases} m \frac{n}{N} & \text{if } n < N \\ \infty & \text{if } n \geq N \end{cases} \quad (48)$$

where  $m$  is a positive constant, and  $n$  and  $N$  stands for the number of allowed PRL remained and remaining periods for next bid, respectively.

One unaddressed subject is the reference quantity,  $q_f$ . Every period, an agent is informed a demand forecast from ISO. By using a forecast  $q_f$ , a bidding function can be written;

$$p(q) = \frac{P_{\max}}{1 + r \exp\left(\frac{q - q_f}{fr}\right)} \quad (49)$$

$$\text{where } r \equiv \exp\left(\frac{q_f - q_F}{fr}\right).$$

To evaluate  $r$ , consider two following extreme cases; 1) an agent has no freedom, i.e., the agent exhausted all allowed PRL's before current contract expires, and 2) an agent has infinite freedom i.e., the number of unused PRL's is greater than that of remaining periods. For the first case,  $fr = m(n/N)|_{n=0} = 0$  which leads the following

equation, which explains the reason an agent must accept any price because it cannot afford any more PRL's:

$$p(q) = \frac{P_{\max}}{1 + r \exp\left(\frac{q - q_f}{fr}\right)} \Bigg|_{fr \rightarrow 0} = \begin{cases} P_{\max} & \text{if } q \leq q_f \\ 0 & \text{otherwise} \end{cases} \quad (50)$$

For the second case, an agent offers a reasonable price,  $p_r$ , for all the quantities, i.e.:

$$p(q) = \frac{P_{\max}}{1 + r \exp\left(\frac{q - q_f}{fr}\right)} \Bigg|_{fr \rightarrow \infty} = \frac{P_{\max}}{1 + r} = p_r \quad (51)$$

which leads  $r = \frac{P_{\max} - p_r}{p_r}$ . Therefore, a bidding function is written

$$p(q) = \frac{P_{\max}}{1 + \frac{P_{\max} - p_r}{p_r} \exp\left(\frac{q - q_f}{m \frac{n}{N}}\right)} \quad (52)$$

For must-be-served demands, there exists a similar form in statistical physics, the Bose-Einstein distribution<sup>13</sup> [18], which is shown in the following equation:

$$f(E) = \frac{1}{\exp\left(\frac{E - E_F}{kT}\right) - 1} \quad (53)$$

---

<sup>13</sup> a distribution when there is no limit to the occupation number at each level of quantum state for indistinguishable particles

By the same analogy as before, a bidding function can be written for a given forecast  $q_f$

$$p(q) = \frac{P_{\max}}{h \exp\left(\frac{q - q_f}{fr}\right) - 1} \quad (54)$$

where  $h \equiv \exp\left(\frac{q_f - q_F}{fr}\right)$ .

To evaluate  $h$ , consider the prices for the quantity at  $q = q_f$  and at  $q = (1+\xi)q_f$ , which was promised to the consumer by contract. For the first case,  $p = p_c$  which leads to the following equation.

$$p(q) = \frac{P_{\max}}{h \exp\left(\frac{q - q_f}{fr}\right) - 1} \Bigg|_{q=q_f} = \frac{P_{\max}}{h - 1} = p_c \quad (55)$$

which leads to

$$h = \frac{P_{\max} + p_c}{p_c} \quad (56)$$

For the second case, the offer price should be  $p_m$  according to the contract, i.e.:

$$p(q) = \frac{P_{\max}}{h \exp\left(\frac{q - q_f}{fr}\right) - 1} \Bigg|_{q=(1+\xi)q_f} = \frac{P_{\max}}{\frac{P_{\max} + p_c}{p_c} \exp\left(\frac{\xi q_f}{fr}\right) - 1} = p_m \quad (57)$$

which leads to

$$fr = \frac{\xi q_f}{\ln \left[ \left( \frac{p_{\max} + p_m}{p_m} \right) \left( \frac{p_c}{p_{\max} + p_c} \right) \right]} = \frac{\xi q_f}{\eta} \quad (58)$$

where

$$\eta = \ln \left[ \left( \frac{p_{\max} + p_m}{p_m} \right) \left( \frac{p_c}{p_{\max} + p_c} \right) \right] \quad (59)$$

Note that  $\eta > 0$  since  $p_c > p_m$ . Consequently, a bidding function can be written as:

$$p(q) = \frac{p_{\max}}{\frac{p_{\max} + p_c}{p_c} \exp \left[ \frac{\eta}{\xi} \left( \frac{q - q_f}{q_f} \right) \right] - 1} \quad (60)$$

The shape of the bidding function, equation (60), is very steep curve similar to an inelastic demand curve. This can be understood since the demand is must-be-served. Fig. 2. 6 illustrates the shapes of two demand bidding curves.

In statistical physics, the particles following equations (43) and (53) are called fermion and boson, respectively. When temperature approaches to zero, Bose-Einstein condensation<sup>14</sup> occurs. A similar condensation occurs in this modeling also as the freedom  $fr$  approaches to zero. The values for bidding prices for both types of demand go to maximum price since the demand-side agent must fulfill all demands including price-based demand.

The value for constant  $m$  can be obtained by fitting observed willingness to pay for an additional 1 MW for an hour. The willingness to pay depends on actual customers.

---

<sup>14</sup> a phenomenon that occurs at low temperatures in systems consisted of large numbers of bosons whose total number is conserved in collisions

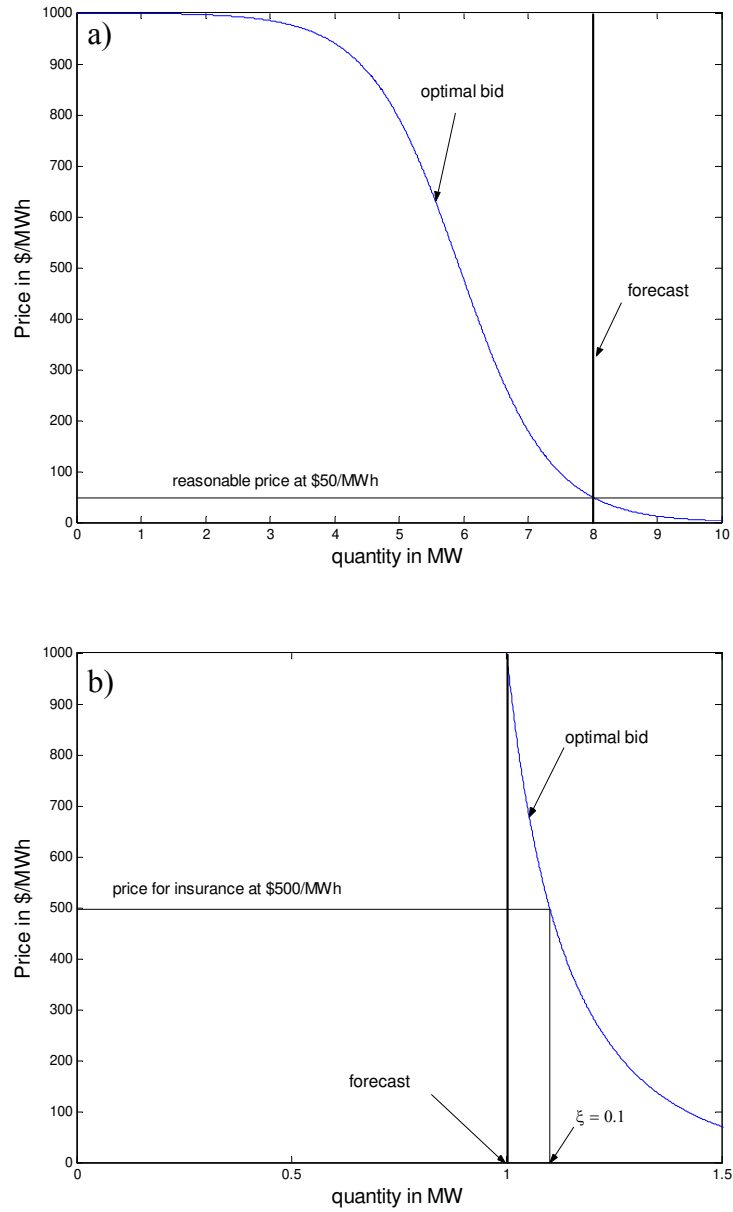


Figure 2.6. An optimal bidding curve for a) price-based demands and b) must-be-served demand

Consequently, the value is different among consumers, and furthermore it may vary with time even for an identical consumer. The basic idea of the algorithm is simply to capture the most important aspects of a real problem facing a learning agent interacting with its environment to maintain reliability in an economic way. Clearly the demand-side agent can sense the market state to some extent and take actions by adjusting its bid. In this study, an agent updates the value for  $m$  according to reinforcement algorithm<sup>15</sup>. The duration of contract and the number of allowed PRL are divided into  $N_1$  segments. After each segment, the number of PRL declared is checked, and then the agent adjusts the value of  $m$  in a following way:

$$m_{k+1} = m_k + \text{sign}\left(n_k - \frac{n_{total}}{N_1}\right)\Delta \quad (61)$$

where  $\Delta$  denotes a step size.

There is no need for an agent to bid for a quantity more than needed. For a security purpose, an agent might bid up to a certain fraction of forecast than needed, and then bid price drops down to zero beyond the fraction. Figure 2. 7 shows different bidding curves for several cases. Blue line stands for the bid curve submitted at  $n^{\text{th}}$  period. If there was no PRL at the period, freedom increases only slightly from  $n/N$  to  $n/(N-1)$ . Consequently, bid price is reduced in a very small amount. On the other hand, an occurrence of PRL significantly reduces the value of freedom, and then bid curve becomes much steeper.

---

<sup>15</sup> reinforcement algorithm is learning how to map situations to actions so as to maximize a numerical reward signal; the agent is not told which actions to take, but instead must discover which actions yield the most reward by trying them

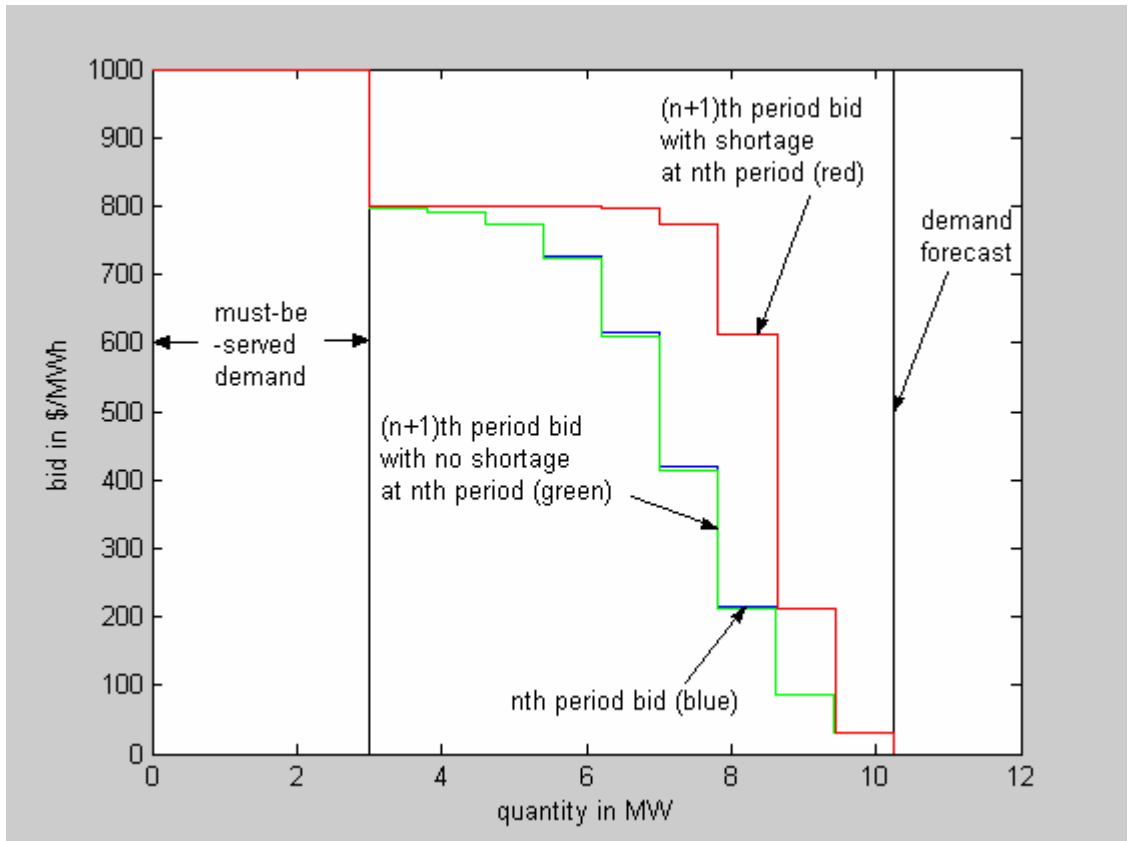


Figure 2. 7. Change in bidding after one period subject to the occurrence of an energy PRL



## CHAPTER THREE

### EARNING ESTIMATION

#### 3.1. Mapping Offers to Earnings

The objective of a supply-side agent is to maximize its earning by submitting an optimal offer. Finding an optimal solution is a maximization problem with several constraints such as generation limits and power balance equations<sup>16</sup>, etc if there is a way to estimate earnings for given offers. There are several algorithms to find an optimal solution for a given objective function and constraints, e.g., the Lagrangian relaxation method. Therefore, it is important to construct a mapping function from control variable to objective function value. As was shown in chapter two, the offer curve is highly nonlinear which leads to a nonlinear objective function. Even though competitors' offers are required to construct an objective function, they are unknown to an agent. Residual demand approach is widely used because of its convenience to deal with unknown strategies of competitors in a firm-level optimization process [19-23]. However, it is difficult to construct the realistic curve since both actual demand and the offers submitted by other firms are not known. In this chapter, it is discussed how to construct a numerical mapping function from offers to earnings, and then how to find an optimal solution.

Another issue to construct a mapping function in a firm level is related to the size of the electric power system. There exist several tens of thousand generators for an ISO. Since the number of competitors is large, the number of possible combinations of their

---

<sup>16</sup> Total generation is sum of total demand and loss

strategies is too enormous to compute the value of mapping function in a real time. A useful concept to deal with such a situation is cluster analysis<sup>17</sup>. A transmission network might be decomposed into sub-regions based on the network topology, and then a group of firms located in the same sub-region can be clustered together.

### **3.2. Market Modeling**

A mapping function from offers to earning can be constructed by analyzing the characteristics of the market in which an agent participates. Market is a combinatory sum of each market participant for a given transmission network and demand profile, etc. Therefore, it is possible to construct a mapping function if offer behaviors of market participants are known for a given network and demand profile. In this study, it was assumed that information related to transmission network is estimated with a good precision. In this section, behavior of market participants will be discussed and modeled in terms of their influence.

---

<sup>17</sup> The term cluster analysis actually encompasses a number of different classification algorithms. A general question facing researchers in many areas of inquiry is how to organize observed data into meaningful structures, that is, to develop taxonomies. For example, biologists have to organize the different species of animals before a meaningful description of the differences between animals is possible. According to the modern system employed in biology, man belongs to the primates, the mammals, the amniotes, the vertebrates, and the animals. Note how in this classification, the higher the level of aggregation the less similar are the members in the respective class. Man has more in common with all other primates than it does with the more distant members of the mammals, etc.

### 3.2.1. Classification of offer strategies

In a regulated electricity market, ISO decides each generator setpoint based on the costs of all participating generators. The marginal cost of different generators plays an important role in determining price. In a restructured market, offers based on marginal cost are often observed especially when the market is competitive.

An agent offering marginal cost without withholding its capacity from the market is called a marginal cost agent (MC). This type of agent might withhold capacity when there is a strong possibility of not being dispatched if offered. When an agent withholds more capacity than necessary in an attempt to increase prices, it is classified as a “Cournot competitor”. Offer behavior of this type is similar to that of an MC in that all submitted offers are low-priced. However, the effect on the market is practically identical to that of a speculator to be discussed [12].

A third type of agent, called a speculator, is one whose offers are mixed between high-priced and low-priced offers. Usually, most of the quantities are offered at a lower price and only small quantities are at a high price. Because of the shape, its offer curve is sometimes called a “hockey-stick”. Speculators are willing to take the risk of not being dispatched in an attempt to raise the market clearing price.

These three types of behavior are the most commonly observed offer behaviors in a real market. There have been several attempts to fit the offer curves. Figure 2. 1 of previous chapter shows a typical offer curve of a speculator (D8) observed in the PJM market. The most striking feature of the curve is the existence of a “kink point” between low-priced and high-priced offer.

### 3.2.2. Market modeling

The three types of agents are commonly observed from all over the uniform price auction market. However, their effects vary with different market, which makes some markets more stable than others. For example, a Cournot-type agent helps a speculator to gain market power. In some scenarios, Oh et al. [12] classified the agent as a speculator according to the withheld quantity with respect to the fairshare. However, in a very competitive market the performance of the identical agent is similar to that of a marginal cost offer agent. Consequently, Oh et al. proposed that an agent must be classified based not on the shape of offer curves but on the performance in the market considered since the same offer strategy has different effect on a market according to the types of the competitors of the agent. The behavior of an unknown agent was classified by comparing the performance with those of standardized agent<sup>18</sup>.

To explain experimental results performed on unknown complex system, one of the most powerful and commonly used techniques is to try and form a basis set that spans the unknown system. When there exists a basis set to span, a unknown system  $|\phi\rangle$  can be spanned in terms of the known set  $|\varphi\rangle$ :

$$|\phi_i\rangle = \sum_j c_{ij} |\varphi_j\rangle \quad (62)$$

where  $c$  is a probability distribution.

It is possible to identify an offer behavior for player  $i$ ,  $|\phi_i\rangle$ , in terms of a basis set. If the basis set is orthonormal, the probability,  $c_{ij}$ , is simply an inner product between  $i^{\text{th}}$

---

<sup>18</sup> an agent offering all the quantity with no withholding at “standardized” price based on the degree of speculation

and  $j^{\text{th}}$  states. However, the form of the basis set is unknown, which means that the form is not necessarily expressed in an offer curve. Suppose there is an offer basis set to express an offer behavior like weak speculator (WS), strong speculator (SS). Then elements in the offer basis set can be spanned in terms of the basis set. If the set is complete to span an offer space, there exists an inverse relation that allows inverse expansion which is projection of the basis set into the offer space:

$$|\phi_j\rangle = \sum_k d_{jk} |\phi_k\rangle \quad (63)$$

Note that the offer basis set is not orthonormal, but it spans in an offer space. Consequently, one can find an expansion of a unknown offer behavior in terms of known offer set by combining equations. (62) and (63):

$$\begin{aligned} |\phi_i\rangle &= \sum_j c_{ij} |\phi_j\rangle = \sum_j c_{ij} \left( \sum_k d_{jk} |\phi_k\rangle \right) = \sum_j \sum_k c_{ij} d_{jk} |\phi_k\rangle \\ &= \sum_k \sum_j d_{jk} c_{ij} |\phi_k\rangle = \sum_k \left( \sum_j d_{jk} c_{ij} \right) |\phi_k\rangle = \sum_k v_{ik} |\phi_k\rangle \end{aligned} \quad (64)$$

where  $V$  is a weight factor distribution which is not a probability distribution any more.

Therefore, it is possible to classify an offer behavior as long as there are enough elements in the offer basis set. An insufficient offer basis set results in proper classification with large error instead of wrong classification. Inconsistent offer behavior will lead an overall offer behavior, but it might be classified properly if different behaviors are properly divided and analyzed.

Similarly, the state of a market is a cumulative sum of the effects of an individual agent in the market. It is easier to model an individual agent than an unknown market especially when network effects are considered. Suppose there is a system  $|\Phi_i\rangle$  with known offer behaviors of its  $m$  market participants. Then, the system can be expressed in terms of the offer basis set in a following way:

$$\begin{aligned} |\Phi_i\rangle &= |\phi_1; \phi_2; \dots; \phi_m\rangle = \left( \sum_k V_{1k} |\phi_k\rangle \right) \left( \sum_k V_{2k} |\phi_k\rangle \right) \dots \left( \sum_k V_{mk} |\phi_k\rangle \right) \\ &= \sum_{k_1} \sum_{k_2} \dots \sum_{k_m} K_1 K_2 \dots K_M |\phi_{k_1}; \phi_{k_2}; \dots; \phi_{k_m}\rangle = \sum_i W_i |\psi_i\rangle \end{aligned} \quad (65)$$

where  $|\psi_i\rangle$  is a cumulative offer behavior of competitors in the offer basis set, which is a scenario set.

### 3.3. Mapping Function for Stationary Markets

A system with unknown offer behavior can be spanned in terms of known offer behavior as follows:

$$|\Psi\rangle = \sum_{i=1}^N p_i |\psi_i\rangle \quad (66)$$

where  $|\Psi\rangle$  represents an unknown system expressed in terms of  $|\psi_i\rangle$  which is  $i^{\text{th}}$  elements in the scenario set, and  $p_i$  stands for the probability that the unknown system is in the  $i^{\text{th}}$  scenario. Then the experimental observations can be interpreted as:

$$\langle \phi_j | H | \Psi \rangle = \sum_{i=1}^N p_i \langle \phi_j | H | \psi_i \rangle \quad (67)$$

where  $\langle \phi_j |$  offer of the  $j^{\text{th}}$  agent and a Hamiltonian  $H$  represents observation from participating in the unknown market.

Suppose an interaction drove the system along the direction of the eigenvector of the system. Such an interaction is called an eigenvalue measurement. Then the interaction does not change the state of a system due to the interaction. For an eigenvalue measurement of the Hamiltonian  $H$ , consecutive experiments do not alter the system. The eigenvector can be calculated from the measurements with given sets. In general, orthonormal basis sets are commonly selected due to convenient calculation since the interaction between two bases set does not exist. For an unknown system with unknown basis sets, it is not possible to derive the eigenvector experimentally. Note that when a system is spanned in terms of an arbitrarily chosen set, equations (66) and (67) need modification, i.e., instead of probability, weight factor  $w_i$  must be used since a scenario set,  $|\psi_i\rangle$ , is not a complete basis set any more. One can write an expression to describe the experiments performed on a market measurement,  $H$  for measuring the earning of an agent:

$$\begin{bmatrix} \langle \phi_1 | H | \psi_1 \rangle & \langle \phi_1 | H | \psi_2 \rangle & \cdots & \langle \phi_1 | H | \psi_N \rangle \\ \langle \phi_2 | H | \psi_1 \rangle & \langle \phi_2 | H | \psi_2 \rangle & \cdots & \langle \phi_2 | H | \psi_N \rangle \\ \vdots & \vdots & \ddots & \vdots \\ \langle \phi_m | H | \psi_1 \rangle & \langle \phi_m | H | \psi_2 \rangle & \cdots & \langle \phi_m | H | \psi_N \rangle \end{bmatrix} \begin{pmatrix} w_1 \\ \vdots \\ w_N \end{pmatrix} = \begin{pmatrix} \langle \phi_1 | H | \Psi \rangle \\ \langle \phi_2 | H | \Psi \rangle \\ \vdots \\ \langle \phi_m | H | \Psi \rangle \end{pmatrix} \quad (68)$$

where the elements in the square bracket in the left hand side,  $\langle \phi_x | H | \psi_y \rangle$ , represent the earning of an agent when it submits an offer  $\langle \phi_x |$  to the market under a specific scenario  $|\psi_y\rangle$ , i.e., a simulated earning from the known scenario, and those in the right hand side  $\langle \phi_x | H | \Psi \rangle$  are an actual earning for the same offer submitted into actual unknown market  $|\Psi\rangle$ . A well defined weight factor distribution minimizes the

difference between the inner product in the left hand side and the vector in the right hand side. This question is widely known as a linear least square (LLS) problem. The method used to minimize the error for this study is described in Appendix B.

By using equation (67) with estimated weight factor distribution obtained from error minimization process instead of probability distribution, an agent can construct a mapping function from offers to earnings if the competitors do not change their strategies. The offer function shown in equations (13), (15) and (19) has three types of variables; main ( $p_{\min}$  and  $q_b$ ), short-term ( $y$ , market condition) and long-term ( $D$ , flattening factor) variables. Short- and long-term variables are determined not from optimization process. For maximizing its profit, an agent needs to find an optimal value for the main variables. For sake of simplicity, call the main variables  $x$  and  $y$ , and let the mapping function be  $F(x, y)$ . Then the following optimization problem can be set up:

$$\begin{aligned} & \max_{(x,y)} F(x, y) \\ & \text{subject to } x \leq x_{\max} \\ & \quad \quad \quad y \leq y_{\max} \end{aligned} \tag{69}$$

where  $F(x, y) = \sum_i w_i f_i(x, y)$ .

In equation (69),  $f_i$  and  $w$  stand for mapping function for  $i^{\text{th}}$  scenario set and corresponding weight factor, respectively. One can solve the optimization problem in an analytic way. At the optimal point  $(x^*, y^*)$ , the first-order necessary condition should be met;



$$\begin{aligned} \left[ \frac{\partial F(x, y)}{\partial x} \right]_y &= \sum_i \left\{ w_i \left[ \frac{\partial f(x, y)}{\partial x} \right]_y \right\} = 0 \\ \left[ \frac{\partial F(x, y)}{\partial y} \right]_x &= \sum_i \left\{ w_i \left[ \frac{\partial f(x, y)}{\partial y} \right]_x \right\} = 0 \end{aligned} \quad (70)$$

From equation (70), two unknown variables  $x$  and  $y$  can be found from an optimal solution. For this purpose, one needs to evaluate the first derivative from scenario shown inside cusp brackets. To evaluate them, one needs to run AC OPF for multiple times for each  $i$ . It might be computationally expensive to evaluate all individual derivatives. Therefore, if there is other ways for finding optimum solution with less computational effort, computational cost would be saved significantly. It is reasonable to assume that the numerical function is continuously differentiable since it is unlikely for earning to change abruptly due to a small change in offer. In this study, it is not guaranteed to get a global optimizer. Instead, the goal is to find a local optimizer since many applied problems are well-solved by locating a local optimizer. However, it is possible to tell whether the optimizer found is global or not. Among many numerical optimization algorithms, a trust region method is used in this study since it does not need many function evaluations. Appendix C presents a detail description for the method. For a better estimate of earning with respect to a given offer, more precise prediction for demand profile is required. To achieve a better precision of the demand forecast, a neural network is used [24-26].

## CHAPTER FOUR

### MARKET DYNAMICS

In the previous chapter, a mapping function was constructed for a stationary market in which competitors do not change their strategies. However, the strategies are subject to change due to a fluctuation in demand or various reasons such as ownership changes of competing generators. In a current market, there are several market monitoring systems based on a snap-shot approach<sup>19</sup>. However, inconsistent change in offer strategies or stochastically driven change might get caught by the approach while they do not affect the earning of an agent on average. On the other hand, small and slow but consistent change affects the earning significantly, but the monitoring systems do not capture such a change. Furthermore, sudden and consistent change in the strategies of other competitors might not affect the earning of an agent if the change is not effective to alter the market state. Therefore, it is desirable to construct a toolbox to capture only consistent and effective changes, which affects the earning of the agent of interest.

#### **4.1. Current Market Monitoring Tool**

California ISO provides a web site<sup>20</sup> explaining its market monitoring system. The easy-to-calculate snap-shot approach gives a quick check on the market. When

---

<sup>19</sup> an approach to analyze a system at a fixed time

<sup>20</sup> California Independent System Operator, “ISO Market Monitoring & Information Protocol”, on <http://www.caiso.com/docs/2002/02/12/2002021215391318952.pdf> (2002)

anomalous market behavior<sup>21</sup> is observed, it will take further action. According to the web site "... The evidence of such behavior may be derived from a number of circumstances, including; withholding of Generation capacity under circumstances in which it would normally be offered in a competitive market; unexplained or unusual re-declarations of availability by generators; unusual trades or transactions; pricing and bidding patterns that are inconsistent with prevailing supply and demand conditions; unusual activity or circumstances relating to imports from or exports to other markets or exchanges...". This means that to analyze market properly ISO should have correct and up-to-date knowledge about other economic situation such as gas price. Proper knowledge is also important when ISO takes a further action since market participants may claim the information that ISO has is not correct. Even with proper information, there are other problems associated with the snap shot approach. Suppose there is a market operating at the situation when a little more withholding results in a price spike. Suppose an agent in the market slowly changes its strategy from a marginal cost offer to Cournot-type offer. At a certain point, the market has price spikes, but ISO cannot figure out what causes the price spikes with a snap-shot approach. This might be a shortcoming in the usage of the tool since a current tool requires for ISO to identify causes responsible for the occurrence of price spikes. Another problem is a false alarm, i.e., even if some price spikes are inevitable due to load profile and network constraints, the current market monitoring possibly requires a further investigation. To monitor a change in the market state, a proper tool must be sensitive enough only for a consistent and successful change.

---

<sup>21</sup> according to its web site [27], behavior that departs significantly from the normal behavior in competitive markets that do not require continuing regulation or behavior leading to unusual or unexplained market outcomes

## II. Chaos and Fractals

As was mentioned in chapter two, market clearing price is a good measure to analyze a change in the market state. Figure 4. 1. shows several nodal prices observed in the NY ISO over a month during summer in 2003. During the summer, demands for electricity increase due to hot weather, which gives more chance for an agent to get a higher price. Consequently, speculators change their strategies early in summer to take the chance.

Nodal price is greatly dependent on the offers from the generators located at the bus. Therefore, a nodal price is an indicator to check if there is any change in strategies of the agents located at the bus. Visual inspection of Fig. 4. 1 gives that there were about 25 times of price spikes for both generators. Background prices also increased about two times in comparison to those at early in June. One can claim that there are changes in both systems during the time period.

Figure 4. 2 illustrates how an agent interacts through price signal. The top graph shows data flow in an electricity market. Agents get information from ISO on demand forecast and historical market clearing data, and submit offers into ISO. Then, ISO collects the offers to clear the market and declares the results. The bottom graph illustrates the translation of the market operation into a signal processing point of view. An observer sends an input signal to the system and receives an output signal, i.e., an agent submits offers and then receives market clearing results.

Game theory has dealt with an auction and bidding strategies, which are closely related to the deregulated electricity market. In game theory, the most commonly

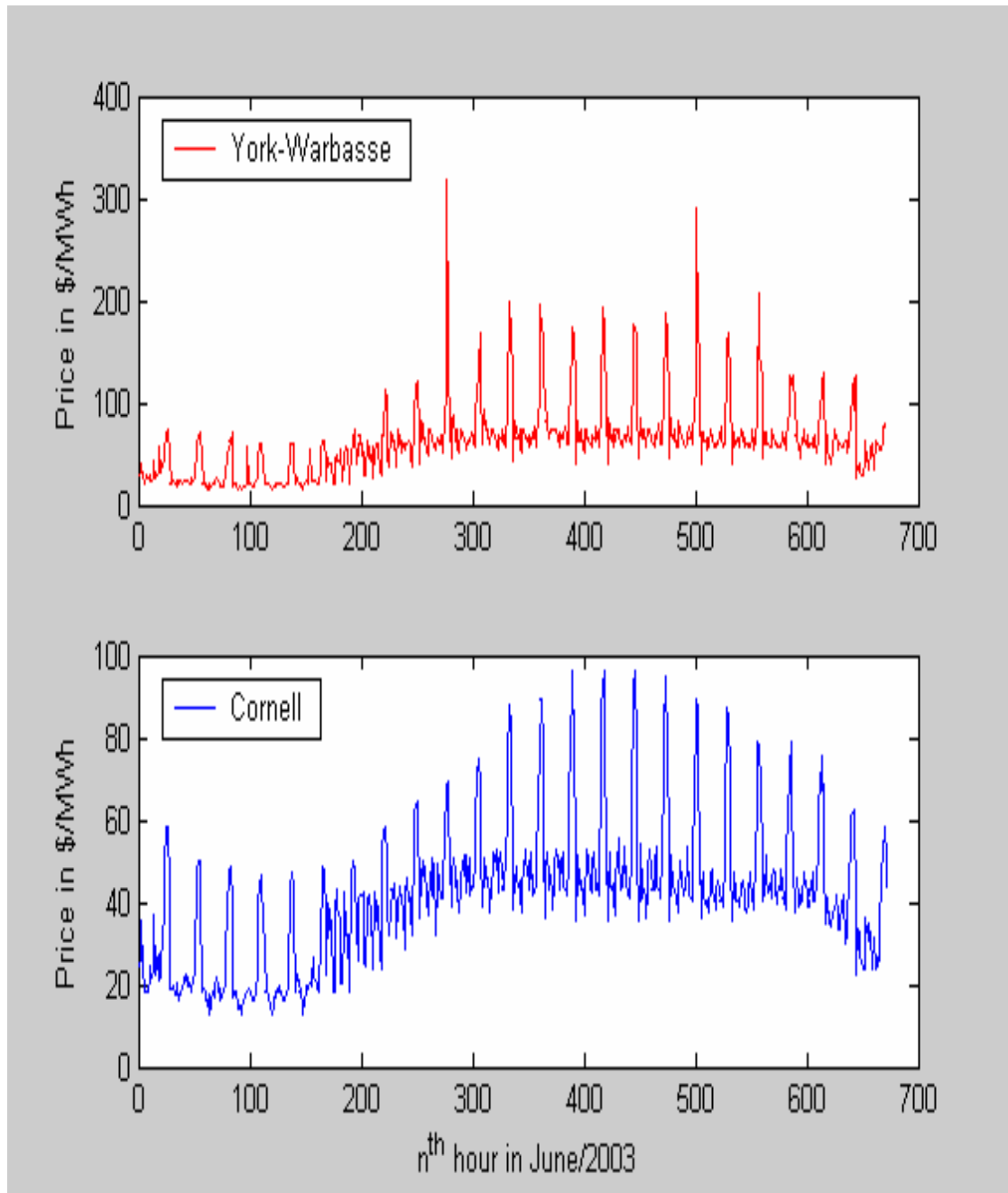
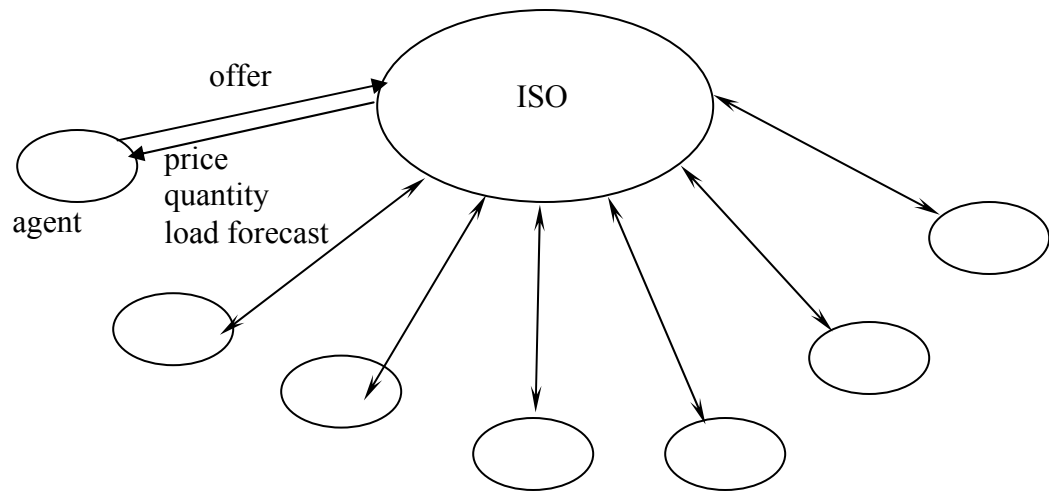


Figure 4. 1. Nodal prices of various generators – data obtained from NYISO web site on <http://mis.nyiso.com/public/P-24Blist.htm> during summer 2003



Schematic diagram showing electricity market

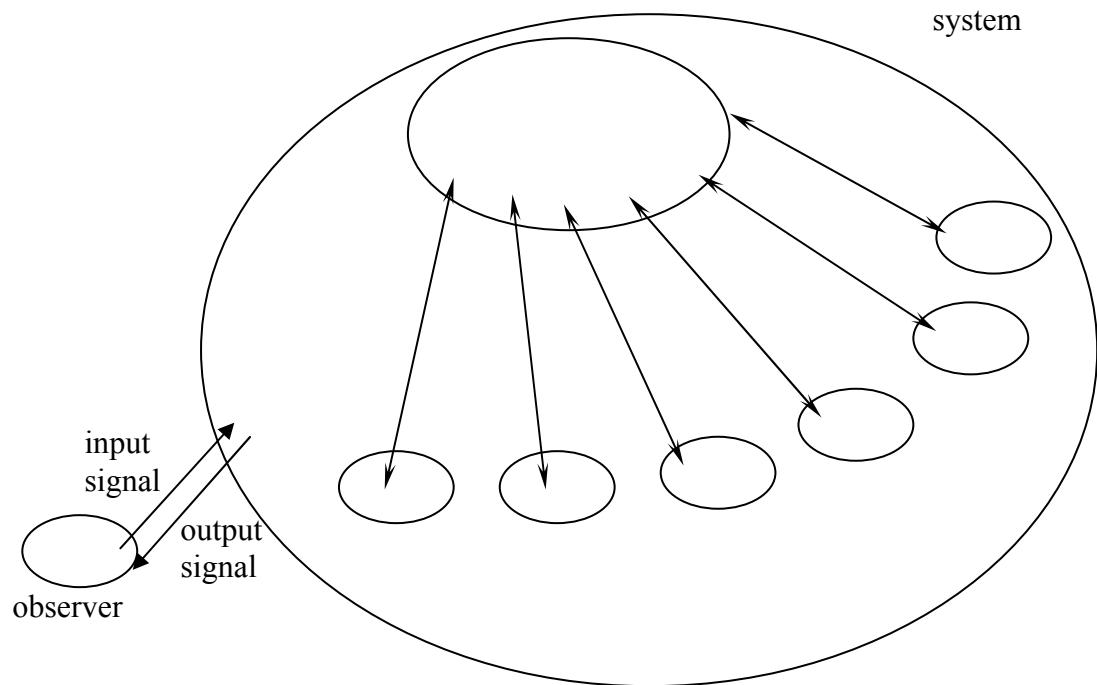


Figure 4.2. Electricity market as a signal processing where input and output signal are offer and dispatch result and demand forecast, respectively

discussed type of equilibrium for this market is Nash equilibrium<sup>22</sup> [28-29] for a very simplified situation. Game theory is not practical for a very complicated system like a deregulated electricity market due to the multi-dimensional strategic space and the uncertainty associated with a market. For a real market, it is not even clear if the system moves toward any equilibrium state. It seems that the system exhibits aperiodic behavior that depends on the initial condition sensitively. Consequently, it is impossible to perform a long-term prediction. This type of behavior of a system is called chaos [30-31], which is a term describing aperiodic long-term behavior<sup>23</sup> in a deterministic<sup>24</sup> system that exhibits sensitive dependence on initial conditions<sup>25</sup>. It would be better to monitor; i) any change in the market state, ii) forecasting a future state, e.g., a new equilibrium or a chaos if there is any change and iii) assigning how recent data are relevant for estimating a future state.

### 4.3. Nonlinear Time Series Analysis

Self-similarity is one of characteristics in describing a chaotic behavior, so called fractal. Dimension is defined the minimum number of independent variables to describe fractal. Two different fractals may have a same value of dimension, but two fractals with different values of dimension are guaranteed to be different. Consequently, the value of dimension is a signature of a change in the system state.

---

<sup>22</sup> Nash equilibrium is a term used in the game theory – a state after playing a game for a long time when all the players in a game follow the way described below; each player looks at the behavior of opponents, and determines the best response to the behaviors of the opponents’.

<sup>23</sup> there are trajectories which does not settle down to fixed points, periodic orbits or quasi-periodic orbits as time diverges

<sup>24</sup> the system has no random or noisy inputs or parameters

<sup>25</sup> nearby trajectories separates exponentially – positive Liapunov exponent

Therefore, monitoring the value of dimension would give an answer for i). ii) and iii) can be assigned by monitoring time response after a change. There is a quantity to measure for a fractal such a time response, so called the Liapunov exponent<sup>26</sup>.

It has been shown that dimension can be defined in several ways for describing fractals as is described in Appendix D. However, it is not clear where the definitions are useful for analyzing experimental data. Most frequently used technique for analyzing consecutive data set is a linear time series analysis due to its simplicity. The basic assumption underlying linear methods is linear correlations, i.e., the intrinsic dynamics of the system are governed by the linear paradigm that small causes lead to small effects. Furthermore, only exponential change or periodic oscillation can be obtained from linear equations, and then all aperiodic behavior needs to be assigned to the results of an external force. Some idea of the system or failure on using linear model have brought people consider nonlinear dynamics which is greatly related to chaos. Deterministic chaos provides a striking explanation for irregular behavior and anomalies in systems which do not seem to be inherently stochastic.

Similar to a stock market [32] discussed in Appendix E, the electricity market also shows nonlinear behavior since there exists highly nonlinear relationship between offers submitted by suppliers and the market clearing price. However, in comparison to Hurst exponent [33] used for a stock market, the quantities like Liapunov exponent and the dimension of a fractal are much less affected by error due to the ordered structure of electricity markets. Therefore, it is possible to evaluate values of the parameters reflecting the state of the market without the “filter process” as described in Appendix E, and to characterize market based on the values of the parameters.

---

<sup>26</sup> an index showing how fast neighboring trajectories separate exponentially



In practical applications where the geometric object has to be reconstructed from a finite sample of data points with errors, correlation dimension is most widely used. As a system evolves for a long time, one can obtain a set of many points  $\{x_i, i = 1, \dots, n\}$  on a phase space. The dimension of experimentally measured data can be evaluated with the knowledge of nonlinear dynamics by using equations (A.69) and (A.70) in Appendix D. However, the measured quantity is not a phase space object but a time series that is a sequence of scalar measurements of some quantity depending on the current state of the system. In this study, a measurable scalar quantity such as market clearing price is chosen. Therefore, it is necessary to convert the observations into state vectors by reconstructing a phase space. It is important that components in one vector must be independent with each other. One way to solve this problem is the method of delay. Suppose, there is a sequence of measurements  $s_n$ ;  $s_n = s[x(n\Delta t)] + \delta_n$  where  $s_n$  is  $n^{\text{th}}$  observation with noise of  $\delta_n$  measured at every  $\Delta t$ . Forming an  $m$ -dimensional vector  $r$  by using  $s$  allows a delay reconstruction;  $r_n = (s_{n-(m-1)\nu}, s_{n-(m-2)\nu}, \dots, s_{n-\nu}, s_n)$  where  $\nu$  stands for number of samples in a reconstructed space. The term of delay time,  $\tau$ , refers the time difference in number of sample between adjacent components of the delayed vectors. In general, the attractor formed by the vector  $r_n$ 's is equivalent to the attractor in the unknown space which the original system is on if the embedded dimension,  $m$ , is sufficiently large enough for components in one vector to be independent with each other. The equivalency is guaranteed when  $m$  is larger than twice the number of actual degrees of freedom,  $d_{em} > 2d$  where  $d_{em}$  stands for an embedded dimension. Therefore, embedded dimensionality is not a problem as long as the vectors are reconstructed in a dimension higher than twice of the "true" attractor. Wolf et al. [34] suggested a relationship to estimate delay time and embedding dimension in a following way:

$$m \times \tau = Q \quad (71)$$

where Q stands for mean orbital period<sup>27</sup>.

A reasonable rule of thumb to choose Q is the time where the autocorrelation function decays to 1/e. [35] In this study, correlation dimension of a fractal can be evaluated by using the following equation:

$$C(\varepsilon) \equiv \frac{2}{N(N-1)} \sum_{i=1}^N \sum_{j=i+n_{\min}}^N H(\varepsilon - \|x_i - x_j\|) \propto \varepsilon^d \quad (72)$$

where  $n_{\min}$  is the minimum number of measurement satisfying  $n_{\min} = t_{\min} / \Delta t$ ;  $t_{\min}$  and  $\Delta t$  represent autocorrelation time<sup>28</sup> and time delay of measurement, respectively.

Another important term for analyzing a fractal and estimating for future events is the Liapunov exponent. The Liapunov exponent shows how far two initially adjacent trajectories stay near. Consequently, two trajectories starting very close with each other are somewhat near within the Liapunov exponent. When a current state is properly analyzed, an estimate to near future within Liapunov exponent is valid since real and estimated state are close. Suppose there is a trajectory on an attractor, and  $x(t)$  is a point on the attractor and  $x(t) + \delta(t)$  is located close to  $x(t)$  with an initial separation length  $\|\delta_0\|$ . For the Lorenz attractor, one finds that:

$$\|\delta(t)\| \propto \|\delta_0\| \exp(\lambda t) \quad (73)$$

---

<sup>27</sup> Suppose the situation that the pairs entering the sum are not statistically independent. For time series data with nonzero autocorrelations, independence cannot be assumed; embedding vectors at successive times are often close in phase space – see Figure 4. 3

<sup>28</sup> the time where the autocorrelation function decays to 1/e

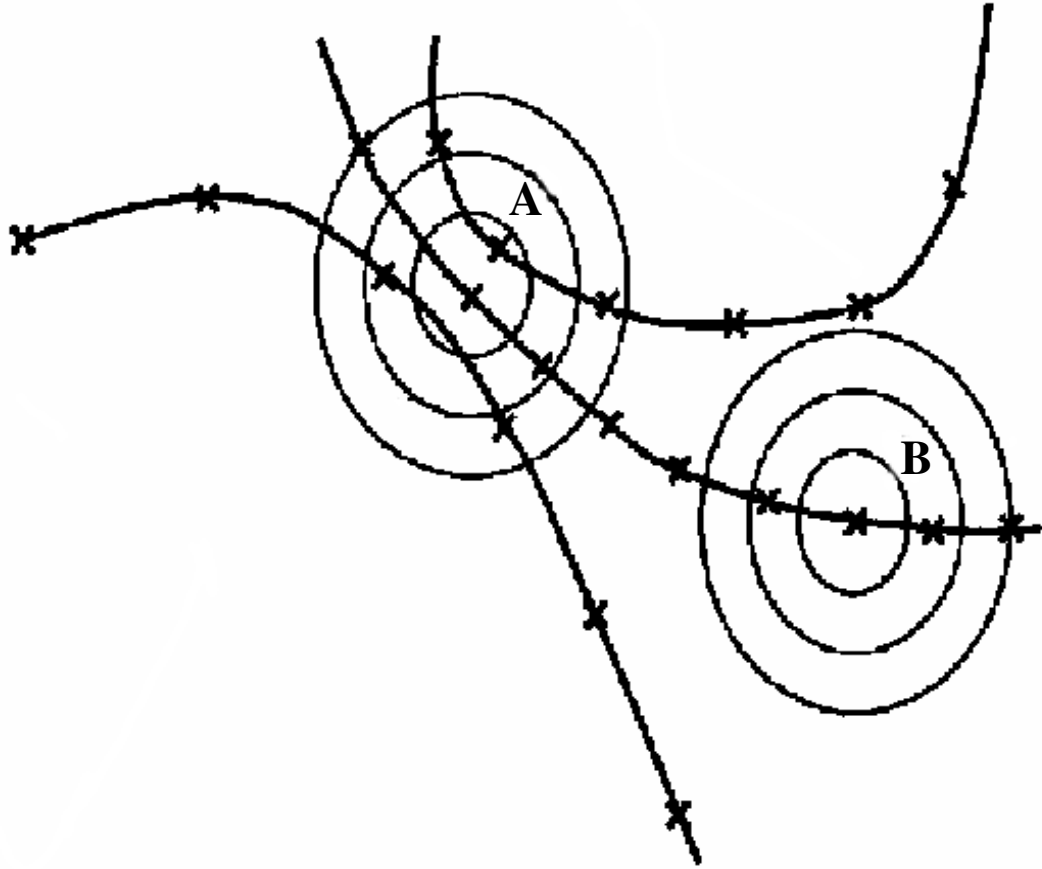


Figure 4.3. Schematic diagram showing how to calculate  $C(\epsilon)$  for a flow. Some neighboring points lying on dynamically uncorrelated parts of the data exist for point A, but point B has only direct images and pre-images of B resulting in dimension of 1. To avoid the incorrect calculation of  $C(\epsilon)$  for estimating dimension, all neighbors over time where  $|i - j|$  is less than  $n_{\min}$  need to be ignored.

where  $\lambda$  represents inverse time constant, so-called Liapunov exponent. Note that the value of  $\lambda$  can be positive or negative.

The Liapunov exponent carries the unit of an inverse time, and takes a positive value for the divergence or a negative value for convergence of neighboring trajectories. Since the Liapunov exponent is invariant under any transformation, one can rescale and/or shift the measurements. For a negative Liapunov exponent, all the data in the same state are relevant for future estimate since all the trajectories converge together. For a computational reason, only several recent data can be used without loss of precision in expectation. For a positive Liapunov exponent, trajectories diverge as is shown in Figure 4. 4.

Since there exist  $[d]^{29} + 1$  independent variables, there are  $[d] + 1$  independent variables needed to describe all the points on the trajectories. They have different evolution characteristics in general for the variables are independent with each other. Consequently, there are  $[d] + 1$  Liapunov exponents associated with a fractal. Consider the evolution of an infinitesimal sphere of perturbed initial conditions. Initial system analysis contains an error, which results in a small sphere whose radius is the magnitude of system estimate error, then actual system must exist within the sphere. In evolution, the sphere becomes distorted into an ellipsoid according to Liapunov exponents associated with  $[d] + 1$  axis. Let  $\lambda_k$  denote the Liapunov exponent along  $k^{\text{th}}$  principal axis of the ellipsoid, and then the length of the ellipsoid along the axis,  $\delta k(t)$  after time  $t$  is  $\delta k(t)$  which is  $\delta k(0) \exp(\lambda_k t)$ . After a sufficiently long time, the most positive  $\lambda$  controls the diameter of the ellipsoid. Therefore the largest one

---

<sup>29</sup>  $[x]$  is a Gauss function – largest integer that is less than or equal to  $x$ , i.e.,  $[x] = n$  where  $n \leq x < n + 1$  for an integer  $n$

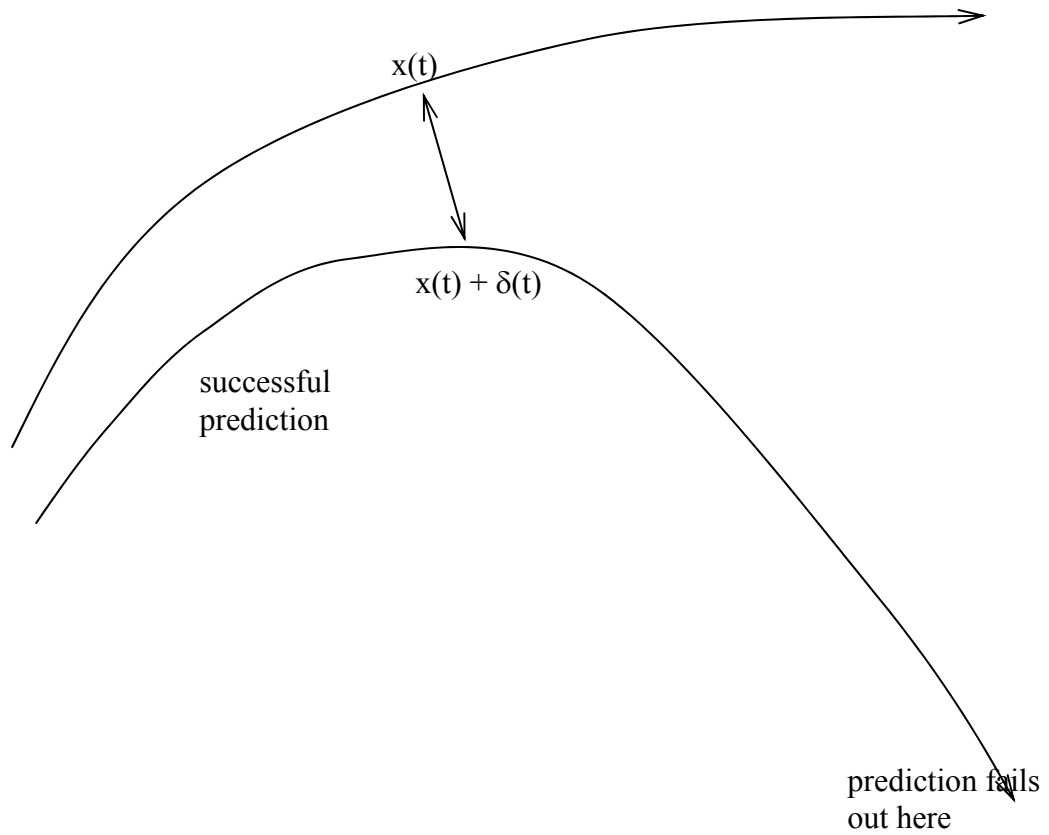


Figure 4. 4. A schematic diagram showing evolution of two trajectories of a system with a positive Liapunov exponent. At the beginning, both trajectories were close with each other, but after some time their trajectories are far apart.

among Liapunov exponents is most important to estimate a state in near future. As was shown in Fig. 4. 4, prediction breaks down after inverse largest Liapunov exponent.

As was mentioned earlier, an attractor does not shrink/diverge at the same rate everywhere. The Liapunov exponent is an average of the local divergence rates over the whole data. Generally speaking, experimental data contain noise of which effect can be minimized by an appropriate averaging statistics. From experiments, only one trajectory can be obtained from the time series measurement from one initial point.

However, a vector close to the point can be considered as a new initial point which shows different trajectory since the trajectory is equally valid if it started from the new initial point. Figure 4. 5 illustrates the evolution and replacement procedure used to estimate Liapunov exponent from experimental data. Let  $s_{n_0}$  be a point of the time series in the embedding space. Reference embedding vector after embedded dimension is determined by using equation (72). One can calculate the average distance of all neighbors to the reference part of the trajectory as a function of the relative time. The logarithm of the average distance at time  $t$  is effective expansion rate over the time span containing all the deterministic fluctuations due to projection and dynamics. Repeat this calculation for many values of  $n_0$ , and then the fluctuation of the expansion rates will be average out. The Liapunov exponent  $\lambda$  can be obtained in the following equation [36-37]:

$$S(t) = \frac{1}{N} \sum_{n_0=1}^N \log \left[ \frac{1}{|u(s_{n_0})|} \sum_{s_n \in u(s_{n_0})} |s_{n_0}(t) - s_n(t)| \right] \propto \exp(\lambda t) \quad (74)$$

where  $u(s_{n_0})$  stands for the neighborhood of  $s_{n_0}$  within  $\varepsilon$ , and  $s_{n_0}(t)$  and  $s_n(t)$

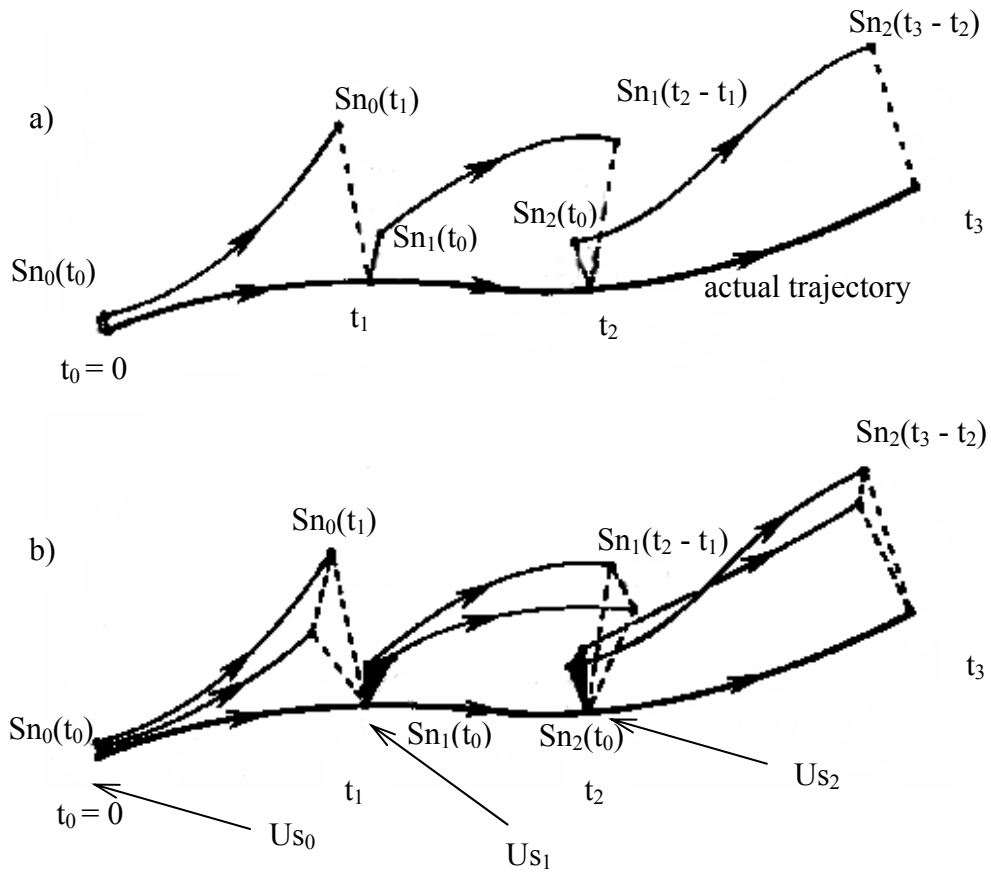


Figure 4. 5. A schematic diagram show how to calculate Liapunov exponent; a) at  $t = 0$ , several points,  $s_{n_0}$ ,  $s_{n_1}$  and  $s_{n_2}$  were selected and trajectories starting from the points were tracked as the system evolves, b) many points inside  $\epsilon$ -ellipsoid ( $u_{s_0}$ ,  $u_{s_1}$  and  $u_{s_2}$ ) were selected and similar to the procedure described in a) was performed (picture taken from Ref [34])

represent embedded vector after time  $t$  evolved from  $s_{n_0}$  and  $s_n$ , respectively.

The size of neighborhood,  $\varepsilon$ , should be as small as possible, but large enough to contain enough points to calculate its neighborhood. Figure 4. 6 shows an example for estimation of the maximal Liapunov exponent from a data set.

After calculating correlation dimension and largest Liapunov exponent, an agent decides how recent data are relevant for estimating a future state. For a negative Liapunov exponent, all the data obtained from the same state are useful, and then an agent is free to choose the amount of data for computation. For a positive Liapunov exponent, a system evolves with time, and then initial system analysis is valid within the exponent inverse. Consequently, an agent has a guideline how recent data need to be added.



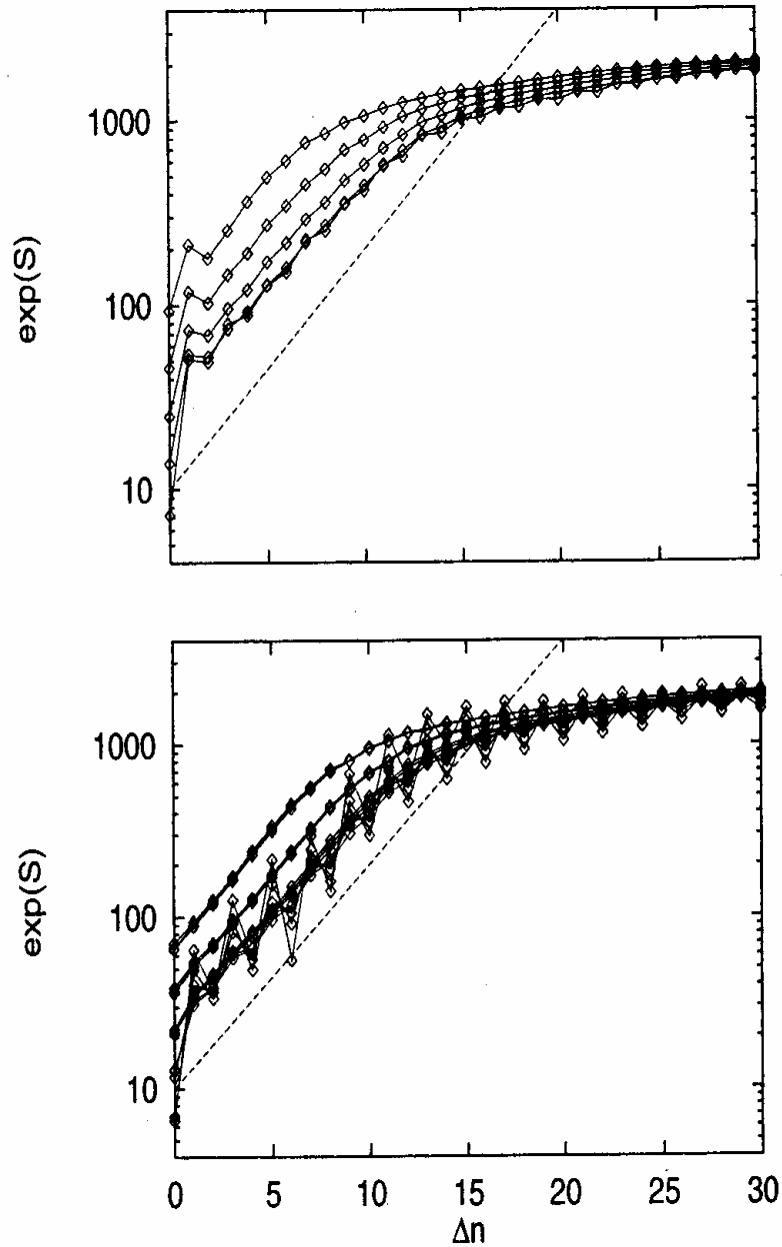


Figure 4. 6. Estimation of the Liapunov exponent of the NMR laser data in embedded dimension of 2 (upper plot) and 3 ~ 5 (lower plot). The linear parts of the curves are well described by an exponential with  $\lambda = 0.3$ . [37].

## CHAPTER FIVE

### SIMULATION RESULTS AND DISCUSSION

#### **5.1. Agent Classification Based on Its Performance**

To find proper number of elements in offer basis set, several different types of agents were simulated with known types of agent. For a large enough number of elements, the agents can be classified properly in terms of its performance. If a classification is properly performed, the agents classified in the same group must show similar performance, i.e., the actual earning of the agents must be highly correlated with expected earning based on the classification.

##### **5.1.1. Standardized agents**

To develop a simulation environment, five standardized agents are implemented consisting of one marginal cost offer agent and four speculators. That is, human or software agent with unknown behavior can be classified based on its play against known agent types. Marginal cost offer agent is an agent that offers all of its blocks at marginal cost without withholding any of them. The speculator agents exhibit different degrees of price and quantity speculation. In order to be classified as a speculator, at least one block must be consistently offered at a high price. It is crucial that a speculator be able to consistently determine which block or blocks are to be offered at a high price and which blocks are to be withheld. Speculators are classified based on the amount of risk they are willing to take. For simplicity, any offer submitted at a

high price is made at the same price regardless of the type of speculation. A fairshare of the market is calculated based on a load forecast. The block in which the fairshare quantity falls is termed the “fairshare block”. If this were the last block chosen for the unit by the auction, then it would be the units’ marginal block. Thus, the fairshare calculation is just a means for trying to predict a unit’s marginal block a period ahead and any calculation to accomplish that prediction is suitable for the purpose we have in mind.

The strategies for offers of the standardized agents are shown in Table 5. 1. The standardized agent with the weakest degree of speculation, called a weak speculator (WS), was designed to speculate with the block that is adjacent to and more expensive than its fairshare block. If the load forecast had no significant error, the behavior of a WS agent was found to be similar to that of an MC agent with some withholding capacity. Since no speculator could speculate less than a WS, the agent is called weak speculator. The agent with a stronger DOS than a WS, termed a strong speculator (SS), offers a high price for its fairshare block. This agent is willing to take the risk of not being dispatched for the chance of a higher market clearing price. Two stronger speculators (SS2, SS3) were also implemented. SS3 speculates with all the blocks to the fairshare block while SS2 submits (j-1)th block at a high price where j<sup>th</sup> block is a faieshare block.

Table 5. 1. Block-by-block offer structure for standardized agents; The table shows the offer strategies of standardized agents when the fairshare block is the  $j^{\text{th}}$  block out of  $n$  available blocks. MCO, S and W stand for a marginal cost offer, speculate on price and withhold the block, respectively

	$j-k$ block; $2 \leq k \leq j-1$	$(j-1)^{\text{th}}$ block	$j^{\text{th}}$ block	$(j+1)^{\text{th}}$ block	$j+k$ block; $2 \leq k \leq n-j$
MC	MCO	MCO	MCO	MCO	MCO
WS	MCO	MCO	MCO	S	W
SS	MCO	MCO	S	W	W
SS2	MCO	S	W	W	W
SS3	S	S	S	W	W

### 5.1.2. Classification of an agent

Suppose there are  $n$  identical agents normalized for size in a lossless and uncongested network. If all the agents behave identically, presumably they would each receive an equal share of the market. But suppose one behaved differently. Then, average earnings of others would be affected, which should lead to a change in the offers of all agents. A change in offer behavior is reflected in the earning which is typical of a feedback process. In such a case, the earning can be a measure of offer behaviors, i.e., if two agents consistently have the same earnings at various environments, the offer behaviors of the two agents are effectively identical.

### 5.1.3. An example

Consider a market simulation with five offer agents comprised of some mix of standardized agents and one agent of interest. Note that the agent of interest can be either a software or a human agent. A specific combination of the five standardized agents is one scenario for a simulation. If there are  $n$  standardized agents then there are  $M$  unique scenarios<sup>30</sup>. By running all scenarios with the agent of interest, all agent-of-interest behavior should be captured if the set of standardized agent is complete. It is theoretically important to determine the number of elementary bases to expand the market since the number is the dimension of a market. Since the various

---

<sup>30</sup> construct a space in  $n$ -dimension with the boundaries  $0 \leq x_i \leq na$  and  $\sum_i x_i = na$ ,

where  $na$  is the number of agents in the simulation (in this example,  $na$  equals 5), then  $M$  is the number of points inside the space of which coordinates are all integers; note that all the agents are interchangeable since losses and line constraints are all ignored. If network effects are considered, the number of possible scenarios are  $na^n$

set comprised of standardized agents is chosen for convenience rather than theoretic analysis, the expansion might be either redundant or insufficient.

However, a market can be expressed in terms of a scenario set if the set contains all possible offer behaviors. For each scenario, the six agents competed for 200 periods and their earnings plotted as a function the earnings of the agent of interest for each period. Figure 5. 1 illustrates a possible plot of the earnings of the participating agents for one scenario. The six lines show how corresponding agents performed in each period. All lines have different slopes, which characterizes the type of agent. Among the lines, the  $y = x$  represents the earning of the agent of interest. If the  $y = x$  line is “close” to one of lines showing the earnings of a standardized agent, the agent of interest is classified as an agent whose behavior is similar to that of the standardized agent that produced that line. For example, the agent shown in Figure 5. 1 is classified as a strong speculator (SS).

In the scenario that produced this plot, an MC earned the most while an SS3 earned the least. Note that an SS3 is the speculator with the strongest degree of speculation. In simulations with software agents, this feature was found to be true in general. As an agent gets less speculative, the market becomes more competitive and consequently everyone including the agent itself earns less. This might encourage an agent to speculate if it wants to maximize its own profit without concern for the earnings of others.

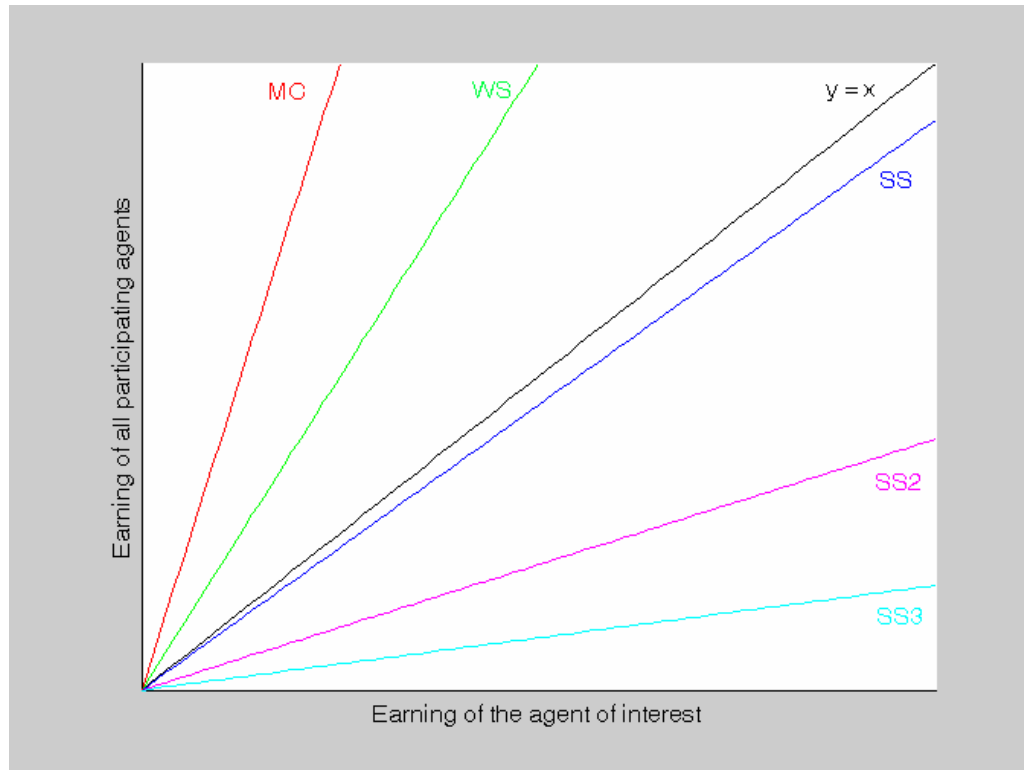


Figure 5. 1. Earnings of the standardized agents and the agent of interest

#### 5.1.4. Expected earning

To calculate the earnings of six different types of agents, an electricity market was simulated only with the standardized agents present. From the simulations, the actual earnings of participating agents were obtained for each scenario. Expected earnings of the software agents were calculated based on the actual distribution of the software agents once they were classified. After classification, one can calculate the earning of each agent from each scenario, and then multiply the earning by a weight factor. The weight factor is calculated based on the probability that the agent might be in the same group in agent competition as the competition where it earned the profit under consideration. For example, suppose that there are 24 agents. Suppose we had classified them as 5 speculators and 19 marginal cost offer agents. Now, suppose we were interested in one of the speculators competing against five other agents from the group of 24. The following enumerate the choices: Number of possible choices when selecting 5 agents without regard to type from the 23 agents left in the pool is:

$${}_{23}C_5 \times {}_1C_1 = \frac{23!}{(23-5)!5!} \times \frac{1!}{(1-1)!} = 33,649 \quad (75)$$

The number of choices that have no speculator in a group is 11,628 ( $= {}_4C_0 \times {}_{19}C_5 \times {}_1C_1$ ). From similar calculations the possible number of choices can be calculated for other mixes of agents. The corresponding probabilities can also be calculated. For example, the probability that the agent of interest participates in a market with no speculator is 0.3456 ( $= 11,628/33,649$ ). The probabilities that the market has one, two, three and four speculators are 0.4608, 0.1728, 0.0203 and  $5.65 \times 10^{-4}$ , respectively. That is, the probability that all marginal agents are competing



with the chosen speculative agent is 0.3456. Note that there are no speculators in the competition other than the chosen speculative agent. If, for example, the agent of interest earns \$100, \$300, \$700, \$1,800 and \$2,500 in each of 5 competitions where each has a different mix of competing agents as listed above, then the weighted earning of agent  $k$ ,  $E^k$ , is about:

$$E^k = \sum_{\substack{i \in \text{possible} \\ \text{group}}} p_i^k \times e_i^k \approx \$332 \quad (76)$$

where  $p_i^k$  is the probability that agent  $k$  is in group  $i$  and  $e_i^k$  is the earnings for agent  $k$  if the agent  $k$  competes against standardized agents in the group  $i$ , respectively. The expected earnings obtained in this way were used for a further comparison of the actual earnings.

### 5.1.5. Simulation results and discussion

In the fall of 2002, fourteen different software agents were submitted by the students taking the class ECE 551/AEM655 (Electricity Markets) at Cornell University. These agents competed in a class competition and were subsequently used as early tests of the classification ideas. From experiments performed in the same class with the students, it was believed that MC, WS and SS were the most common types of agents. Therefore, only those types of standardized agents were used.

After performing simulations in which all possible combinations of three standardized agents were used, the classifications of each agent of interest by certain of those simulations were found to be redundant, i.e., classifications using one

scenario and that using a different one were identical. If the agent of interest behaves consistently, the result from each scenario should indicate identical classification. By noting that human subject might be inconsistent, six scenarios were chosen to produce distinctive classifications: 4 WS + 1 MC, 3 WS + 2 MC, 4 SS + 1 MC, 3 SS + 2 MC, 1 SS + 2 WS + 2 MC and 1 SS + 1 WS + 3 MC. One randomly selected set of forecasted and actual load was assigned for the scenario. Average load was 470 MW, and the maximum error between forecast and actual load was 20 MW.

Each of the fourteen software agents and five standardized agents formed a group for the simulation, and corresponding plots were generated based on the results of the simulations. According to the plots, the fourteen agents were classified into three groups, which are 5 MC, 4 WS and 5 SS. It seemed that most agents tested were speculators to some extent with the degree of speculation somewhere between WS and SS. It is worthwhile noting that from the scenario the earnings of an agent were close to those of the standardized agents classified as the same type as the agent.

Figure 5. 2 shows a plot of the earnings of a randomly selected software agent classified as SS for four scenarios. The classification of the software agents was straight forward since the strategy used was consistent for a given scenario. In other words, no learning algorithms were implemented. For most of the agents, strategies seemed not to change for different scenarios, i.e., different type of competitors. It was also found that no agents developed by the students used learning algorithms which would alter the results significantly. Since the agent code is available, it is possible to check the results.

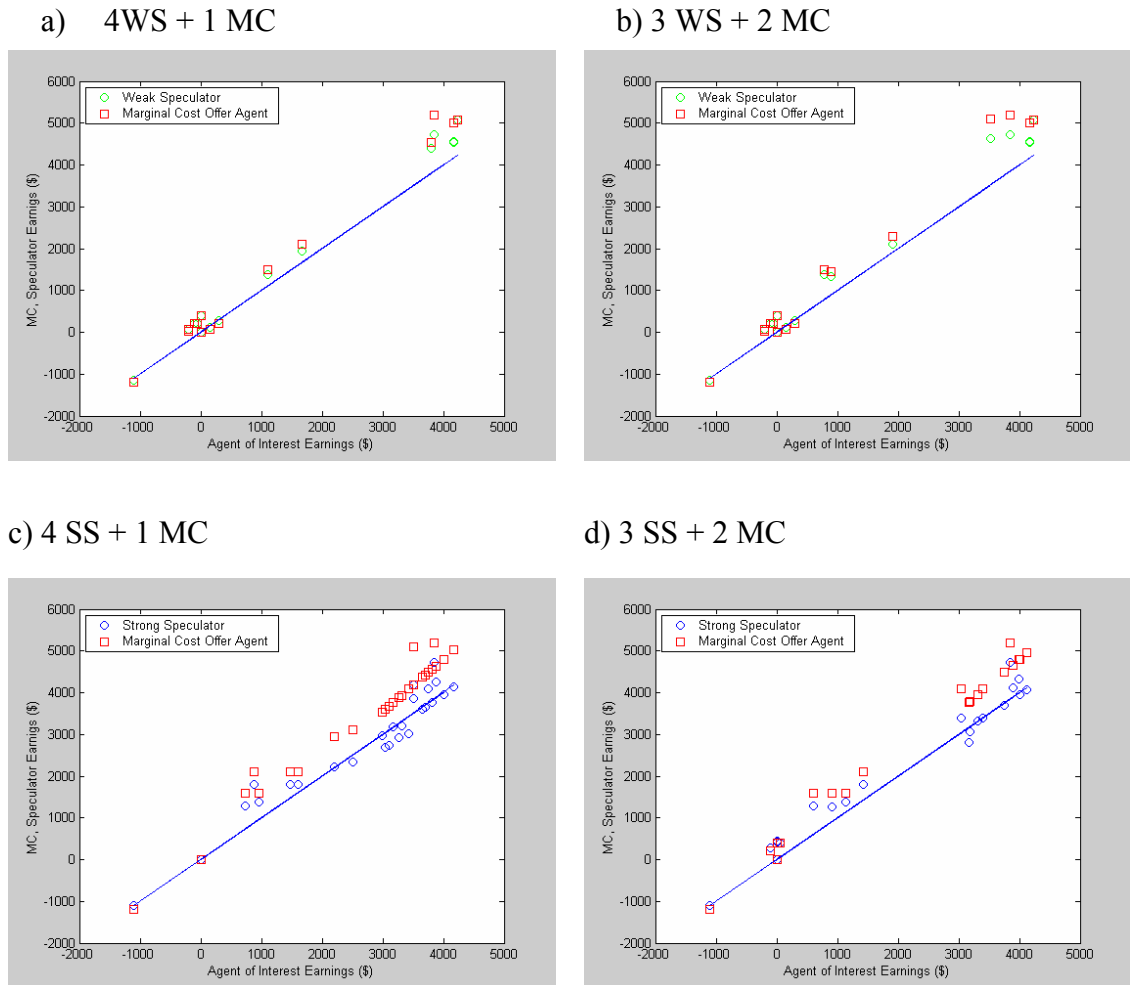


Figure 5. 2. Example of a performance of the software agents: in the plot, red square, green and blue circle stand for the earning in a period of MC, WS and SS, respectively

For a simulation with a human subject, twenty students were recruited from the class ECE 451, electric power systems, at Cornell University. Each of twenty students participated in the simulation with five standardized agents just like the software agents. The purpose of this experiment was to find out if the same technique that was successful for classifying software agents could be used to determine human strategies. The same sets of forecast and actual load were used for the simulation. They learned from experience, and were consistent only in some scenarios. Therefore, the data obtained only after a period of learning was useful for classification of the scenarios. After examining earning data, ten periods were assigned to the learning period. It was also found that the offer behavior of one student was similar to that of an SS in some scenarios while the same student behaves like a WS in other scenarios, i.e. different strategies were used when competing against different types of competitors, which is logical behavior. Strategies other than ones used by the standardized agents were also observed. The conclusion was that the set of standardized agents was not rich enough and that it was possible to classify some of the different strategies by adding the speculating agents SS2 and SS3 to the mix. A typical simulation result is shown in Figure 5. 3.

In the case of a) and b), one was classified as SS2 and SS3 while the same one was classified WS and SS in the case of c) and d), respectively. When SS3, a standardized agent with the strongest degree of speculation, participated in the scenario described above, a common feature was shown in plot b). What SS3 did was effectively withhold its entire capacity from the market unless the market clearing price was high. Therefore the market clearing price was high even in the low demand period, which caused the earnings of all competitors to increase considerably. Even though this type of strategy seemed not to be reasonable, it was often observed, especially when the

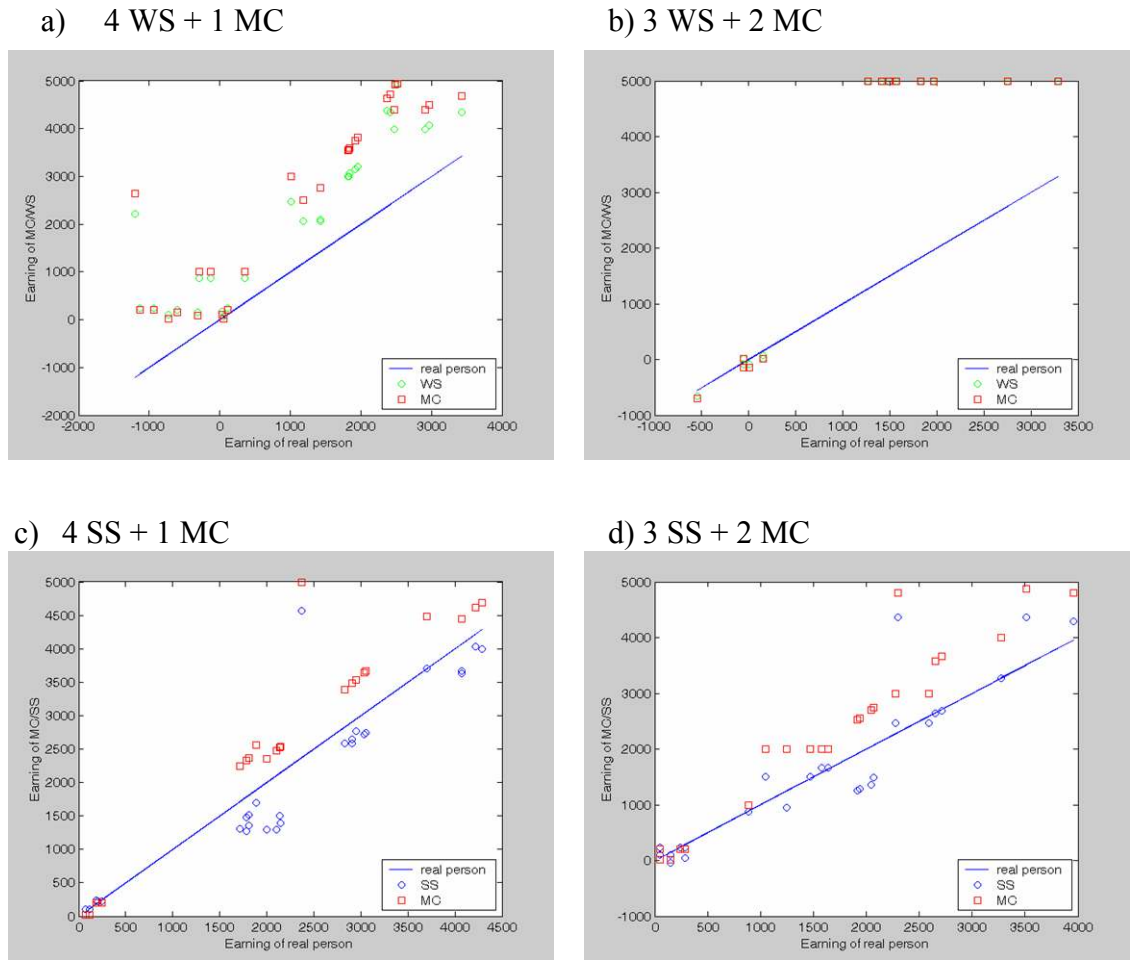


Figure 5. 3. Example of a performance of the human agents: red square, green and blue circle stand for the earning in a period of MC, WS and SS, respectively

market was very competitive, i.e., for markets with an agent mix such as 3 WS + 2 MC that is in aggregate not very speculative. In less competitive mixes, such as 4 WS + 1 MC or 3 SS + 2 MC, the strategy was rarely used.

For the case in which it was possible to classify a human agent, the total earnings of a human agent from the scenario was compared to that of the standardized agent of the same type from the same scenario. The comparison between the two earnings is shown in Figure 5. 4. The line corresponds a perfect correlation, which is  $y = x$ .

The correlation between two earnings was checked for both a software agent and a human agent as long as it was possible to classify the agent of interest. It is critically important to include all the standardized agents with extreme offer behaviors in order to classify an agent of interest. Otherwise, some agent might not be properly classified. For example, the agent of which earning is plotted in Fig. 5. 3. b) is not classified properly since the agent of interest is far more speculative than WS and/or MC. Another difficulty in classification is consistency. If the offer behavior of the agent of interest is not consistent, the classification method described here would be judged not reliable.

There was one interesting software agent worthy of special note. The agent offered some of its capacity into the market at marginal cost, but started to withhold some from its fairshare block. Therefore, its offer function was similar to that of SS except that it withheld capacity from the fairshare block instead of offering it at a high price. This offer behavior is termed a Cournot speculation. This agent was classified as SS as long as at least one speculator exists in the market regardless of type such as WS or SS.

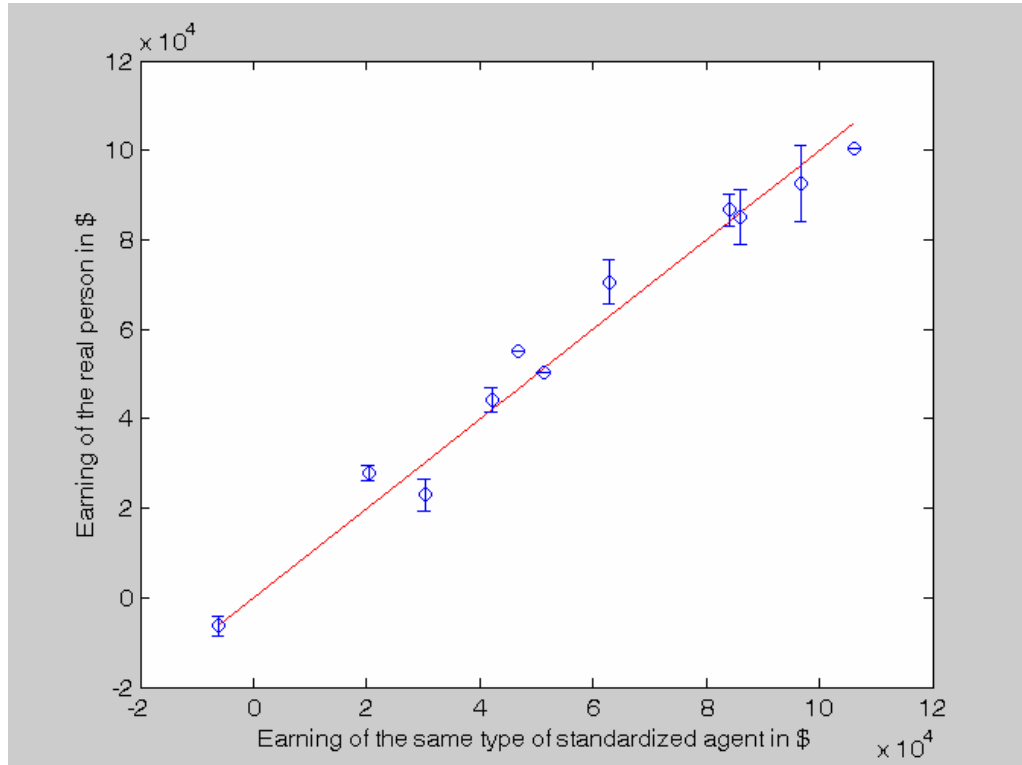


Figure 5. 4. Actual earning vs. Expected earnings calculated from simulation

## 5.2. Evaluation of Dimension by Using Price

Simulation results obtained from Ref. [12] were used for evaluating dimension of the data. Since the price is a measure of the market considered, the dimension evaluated is an estimate of the dimension of the market. The value for the mean of demand was 490, and the error of demand forecast was 50. Price data obtained from simulation of 300 to 1,000 periods were used for the dimension analysis. To estimate  $d$ ,  $C(\varepsilon)$  and  $\varepsilon$  is plotted in log-log scale in the range of  $\varepsilon$  from  $10^{-2}$  to  $10^6$  as is shown in Figure 5. 5, and power law is used. If the relation equation (72) were valid for all  $\varepsilon$ 's, there should be a straight line of slope  $d$ . In this case like other practical cases, the power law holds only over an intermediate range of  $\varepsilon$ . The curve saturates at large  $\varepsilon$  because the balls with radius of  $\varepsilon$  surround the whole attractor and therefore the number of neighborhood within  $\varepsilon$  cannot grow any further. On the other hand, the balls with extremely small radius  $\varepsilon$  contains  $x$  only. Therefore, the power law holds only in the intermediate scaling region. Data only in the intermediate region were chosen for evaluating dimension.

From the analytical process, fractal dimension was obtained as a function of the embedded dimension as is shown in Figure 5. 6. The true dimension was determined about 2. Therefore, an embedded dimension of 5 should indicate a true dimension. Fig. 5. 6 shows that the true dimension at the embedded dimension is about 2 which is properly evaluated. The value for dimension depends on precision of demand forecast as well as the types of market participants. In other word, dimension is a quantity reflecting whole system under consideration. Once there is any change affecting the system, dimension analysis will identify the occurrence of the change even though it cannot tell what causes the change. The value of dimension is most sensitive to the



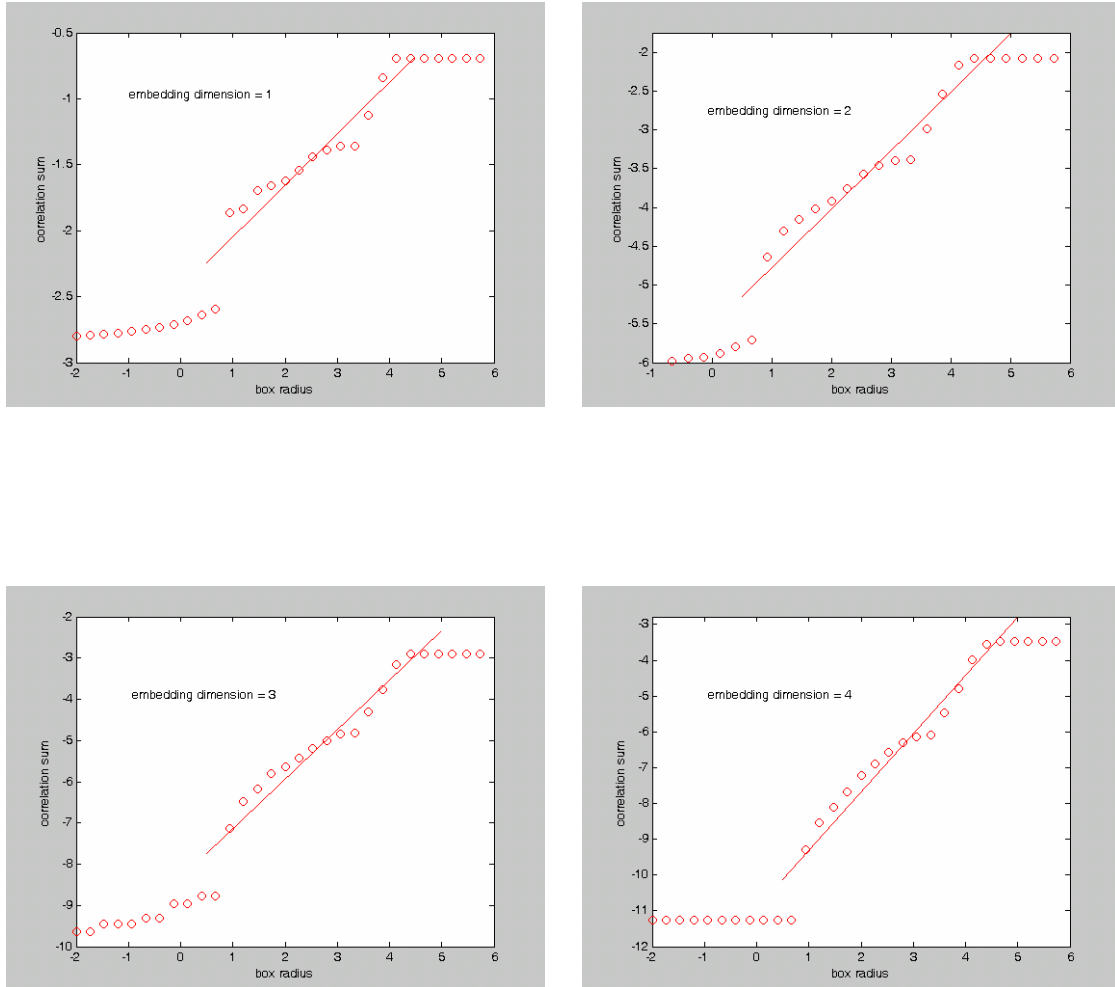


Figure 5. 5. Correlation integral for the market clearing price data obtained from the simulation with 500 periods

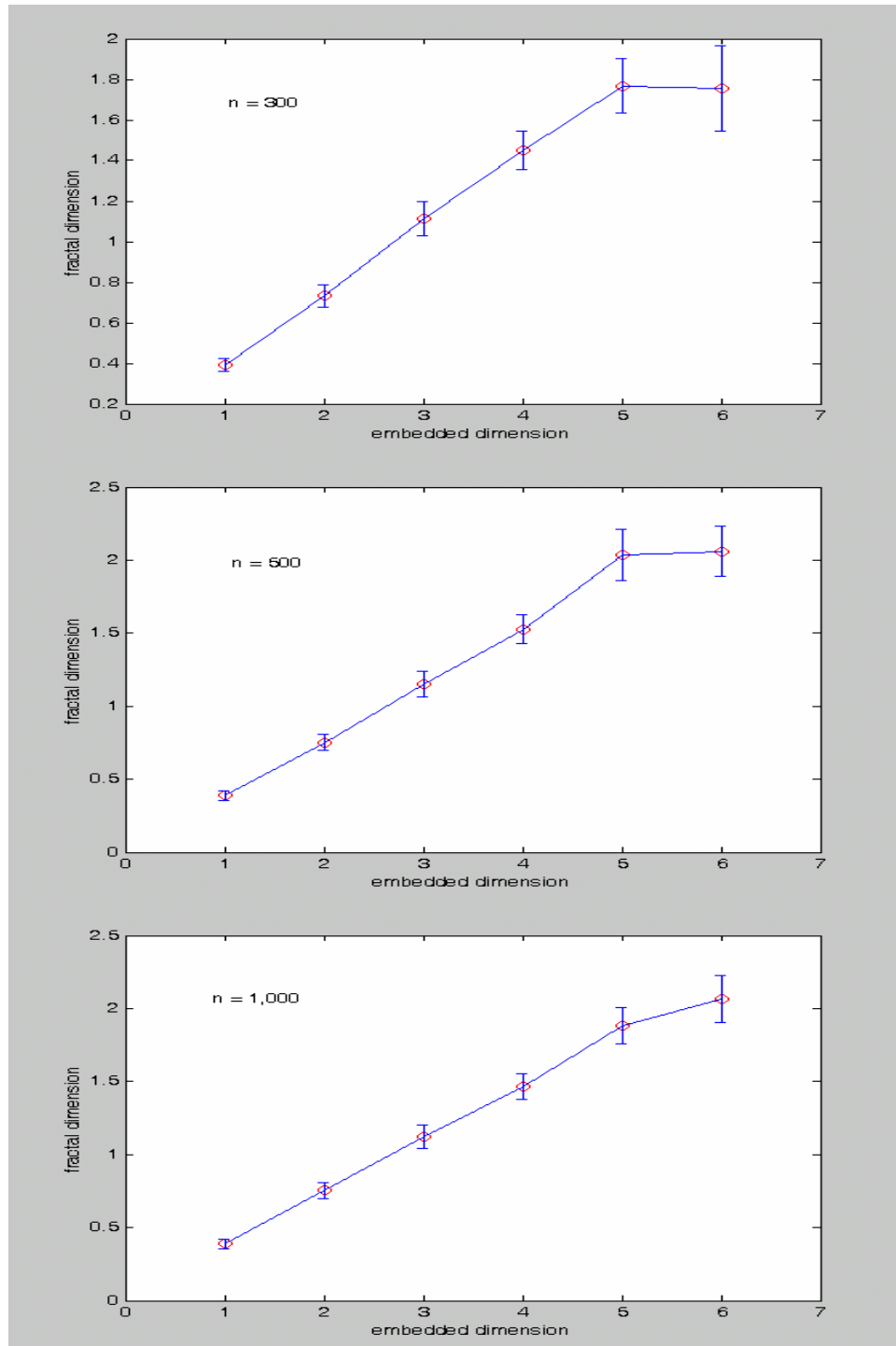


Figure 5. 6. Correlation dimension for various price data obtained from  $n$ -period simulation

type of market participants. Besides, change in the precision of demand forecast or other changes can be captured by other statistical tools too. Therefore, given results of other analysis, it is possible to tell if the strategies of market participants have been changed.

Figure 4. 1 shows several nodal price data obtained from the NY ISO's web site. The data were analyzed to estimate the value of correlation dimension and the Liapunov exponent. When summer came, some agents changed their strategies to increase clearing price. Then system dimension should change accordingly, which results in the change in clearing price. But, the nodal price is more closely related to the strategy of the agents located at the bus. As is shown in Fig. 5. 7, the state of York-Warbase changed during the period while that of Cornell did not. There might be several reasons to change the state beside change in the strategy, i.e., a change in network or offer strategies of other agents. However, only interest here is to check if the system state which an agent must deal with has been changed. During the period, York-Warbase faced a different market from that before the period while Cornell did the same or unnoticeably different market. Both cases, the Liapunov exponent had a negative value which means the markets were settling down to a new equilibrium, consequently all the data were relevant to estimate a future state.

### **5.3. Results from Simulations with Demand-side Agent and Discussion**

A modified IEEE 30 bus system with 6 generators and 20 loads was used for a simulation. Fig. 5. 8 shows the transmission network used in this study. In the system, there are three different areas divided due to line constraints. A closer look to data for

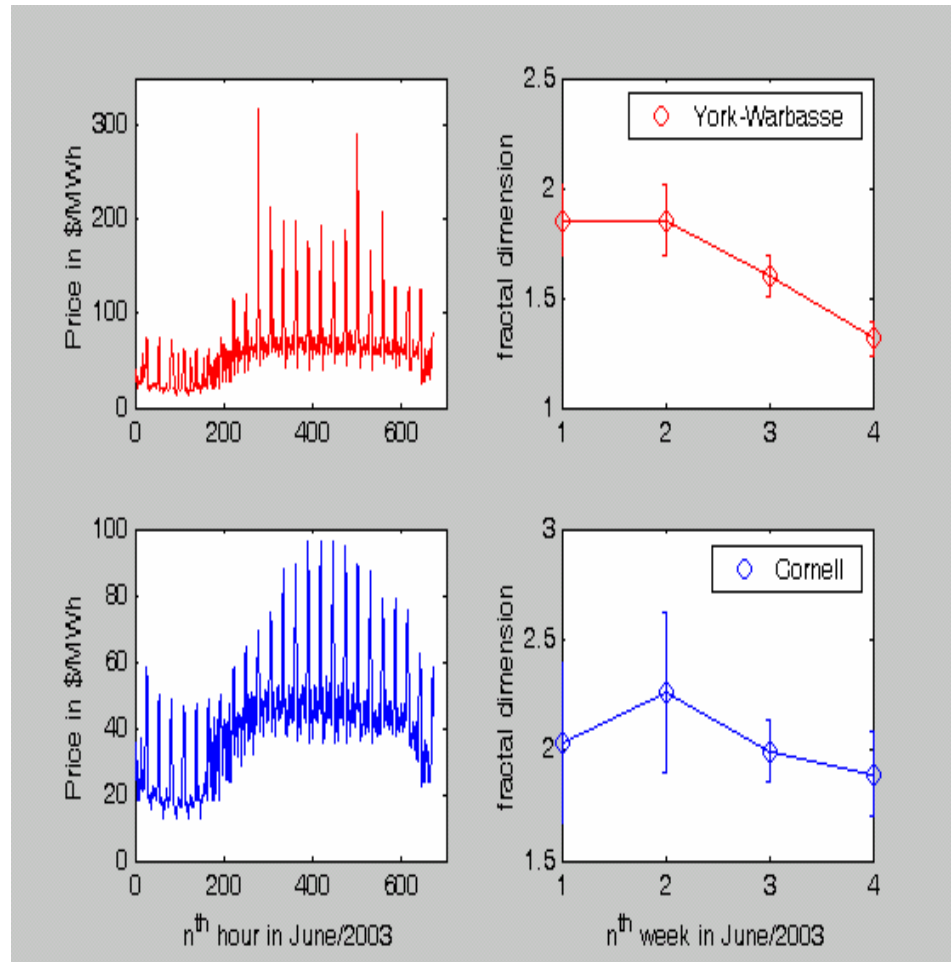


Figure 5.7 The change in systems which agents, York-Warbesse and Cornell, faced during June 2003. While system of Cornell did not change significantly, that of York-Warbesse evolved.

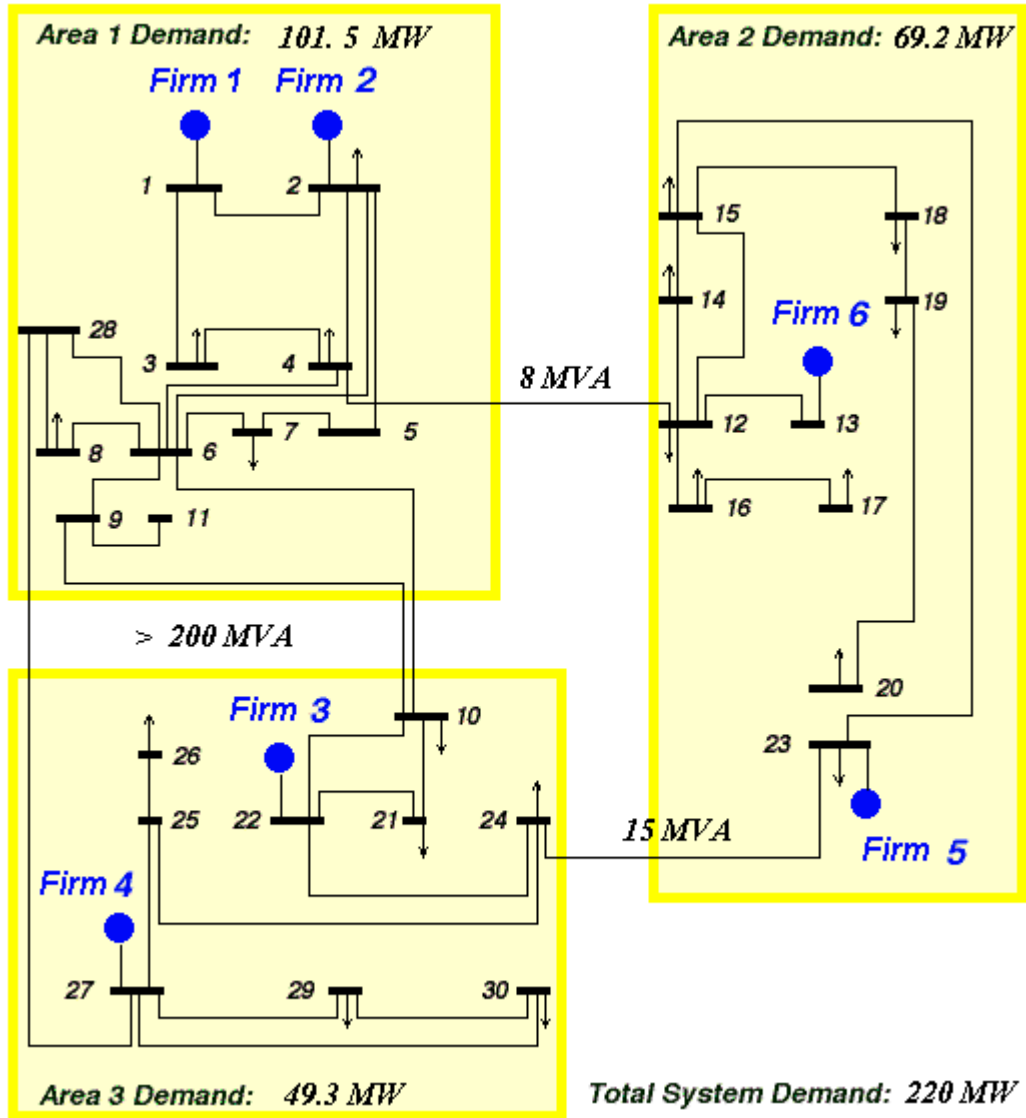


Figure 5. 8. Modified IEEE 30 bus system with six suppliers. Capacities of lines connecting Area 1–Area 2 and Area 3–Area 2 are lower than those of other lines.

line constraints allows clustering between Area 1 and 3 with no significant loss of generosity since line capacities between the two areas are large. Due to strict line constraints between Area 2 and the clustered area, Firm 5 and 6 have a locational benefit in case of heavy load in the Area 2, which implies a potentially duopoly situation. Actual demand seems to have weekly and hourly periodicities. To mimic these periodic behaviors, a convolution between two sine functions added with small values of random number were taken for an actual demand. For the purpose, convolution of two functions  $f(x)$  and  $g(x)$  over a finite range  $[0, t]$  is performed in the following way:

$$f \otimes g \equiv \int_0^t f(\tau)g(t-\tau)d\tau \quad (77)$$

where the symbol  $f \otimes g$  denotes convolution of  $f$  and  $g$ .

To emulate the periodic behaviors of load as well as stochastic behaviors, the functions  $f$  and  $g$  were taken as

$$\begin{aligned} f(t) &= \frac{A_{day}}{2} \left[ \sin\left(\frac{2\pi}{\tau_{day}}t\right) + 1 \right] + B_{day} \delta_{day} \\ g(t) &= \frac{A_{week}}{2} \left[ \sin\left(\frac{2\pi}{\tau_{week}}t\right) + 1 \right] + B_{week} \delta_{week} \end{aligned} \quad (78)$$

where  $A$ ,  $B$  denote fluctuation of load for periodic part and that for stochastic part, respectively, and  $\tau$  and  $\delta$  stand for periodicity and for random value in  $[0, 1]$ , respectively, and subscripts represent time period.

Several simulations with various types of supply-side agents have been performed. There are two extreme cases in the simulations: all suppliers are marginal cost offer

agents or all speculators. For the first case, there is no need to include demand side participation since a market clearing price is already low enough. On the other hand, there is no need for demand side participation for the second case either because demand-side participation can make little improvement on the situation since must-be-served unit needs power regardless price and dispatching only the unit already requires a high market clearing price. To get a more realistic simulation result, two scenarios were selected based on the types of real suppliers observed in PJM market shown in Figure 5. 9. For Case a) which is the more competitive market, while the average market clearing price is about \$ 550/MWh with inelastic demand without demand-side participation, it was less than \$ 100/MWh with a demand-side participation. Case b) is more interesting in that there were many price spikes to meet inelastic demand due to highly volatile market. Demand-side participation lowers the number of price spikes as well as average price in both cases. Some price spikes are eliminated by backing up less than 10 % of load while some are reduced by a significant amount that requires declaring PRL. When significant deduction occurs, the number of allowed PRL is decreased by one which resulted in a decrease in freedom. Consequently, a bid curve approaches the inelastic demand curve. When number of allowed PRL goes to zero, the bid curve of demand-side agent looks identical to that of inelastic demand. Therefore, market clearing price are same. For example, the results with elastic demand after 720 periods is equal to those without.

#### **5.4. Simulation Results with Adaptive Supply-side Agents and Discussion**

In this section, implementation detail for a supply-side agent is presented. Furthermore, several simulation results with the agents designed in this study are

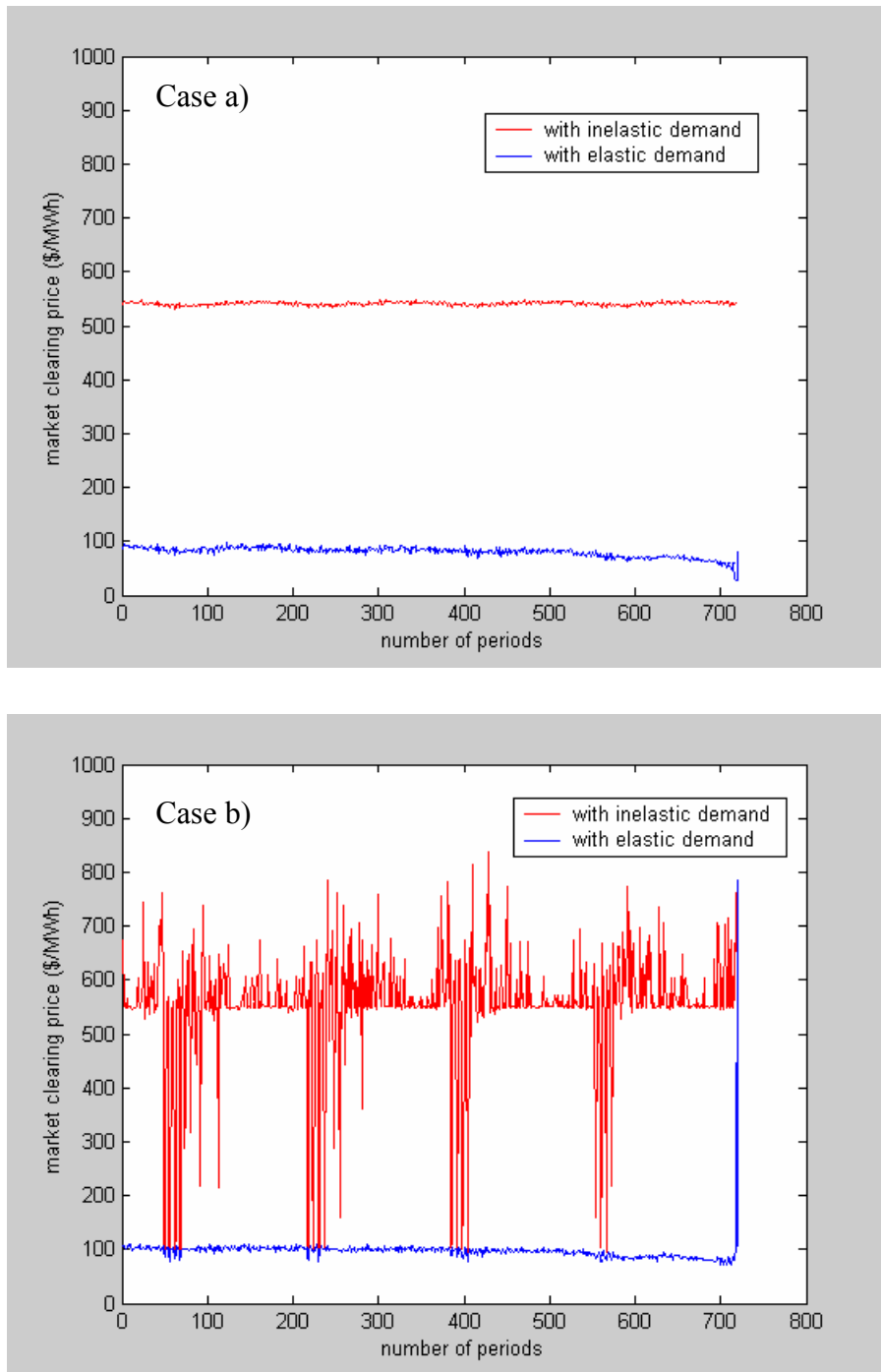


Figure 5. 9. Two typical simulation results with inelastic demand without demand-side participation (red line) and with elastic demand with demand-side participation (blue line). Case a) shows the results in a more competitive market than that for Case b).



presented and discussed.

#### **5.4.1. Description of adaptive supply-side agents**

With no change in behavior of all the participants, the state of a market remains unaltered even under stochastic demands as long as the distribution of demand does not change significantly. However, by the nature of a market, there is always a change in the strategy of market participants. Once there exists such a change in the market, the change acts as a new driving force leading to a change in the market state. Consequently, future state somewhat deviates from an expectation if the expectation was extrapolated from the observation made on the previous state of a system. Therefore, the offers in learning period must be carefully selected in order not to disturb the market. Otherwise, the observation made is not useful for the estimate of future market. Since current market rules do not allow communication amongst market participants, the only way to collect data is participating in the market. Once the agent participates in the market to collect data, the participation inevitably drives a system into a new state, which makes its collection of data irrelevant. The best way to solve this dilemma<sup>31</sup> is minimizing the difference between current and new state. For a dynamic system, it is well known that the degree of the change in system proportionally depends on the magnitude of the driving force. There are two ways to minimize the magnitude of the driving force: minimizing driving forces in each period and minimizing the sum of driving forces. Withholding most capacity from the market for all the periods may introduces a minimal change in the system when the

---

<sup>31</sup> to collect data, an agent needs to participate in the market, but participation may change the system which makes collecting data useless

perturbation due to the introduction of the agent is small enough not to alter market much. However, this should be avoided since such participation results in exploring only limited area of a search space of mapping function. A better way is the second choice: exploring more search space while the offer does not alter the state much. When significantly many random vectors are summed over, the net vector has a very small magnitude since they are canceled out with each other [18]. With given values of short-term and long-term variables, the main variables are randomized in a following way: for  $n$  learning periods, equally distributed vectors  $a$  and  $b$ <sup>32</sup> are chosen from distributed from minimum to maximum values of each variable, and then the elements in two vectors are randomly selected for an offer.

Each period in a learning process, the element in a matrix for simulated earning,  $A$ , is calculated based on initial scenarios. After learning period, the scenario set is evaluated to test its validity. Since the scenario set is not the complete basis set, a wrongly chosen one cannot represent the actual market properly. From an error minimization process with simulated and actual earning  $A$  and  $b$ , the weight factor  $x$  is estimated. When the process does not give a satisfactory result<sup>33</sup>, the scenario set will be altered based on the contribution to expected earning. The actual earnings are more closely related to the competitor(s) located at the same area. Therefore, only the portion of scenarios for the competitors will be modified while the portion of scenarios for “far apart” agents which are located in different area are intact. It is noteworthy to mention that all the extremes must be included in the scenario sets even after the

---

<sup>32</sup>  $a \in [\underline{d}, \bar{d}]$  and  $b \in [\underline{p_{max}}, \overline{p_{max}}]$  where  $d$ ,  $p_{max}$ ,  $\underline{x}$  and  $\bar{x}$  stand for degree of speculation, maximum offer price, minimum and maximum value of the variable  $x$ , respectively

<sup>33</sup>  $\frac{\|Ax - b\|_2}{\|b\|_2} \leq \delta$  where  $x$  is the result of the minimization of  $\|Ax - b\|_2$  and  $\delta$  is the satisfactory limit

modification in order to guarantee that the scenario set represents the actual competitors.

When a learning period ends, an agent finds a proper scenario set minimizing the error of  $\|Ax - b\|_2$ . With the modified scenario set, it finds an optimal offer for each period. For the optimization process, the expected demand for a coming period is obtained by using neural networks. To achieve this, the data obtained during learning process is eliminated for a better estimate since its offer strategy after learning period is not randomly distributed anymore. For this period, the new offer strategy might make the whole market evolve. Therefore, a dimensionality check during learning and this period is not required since the new state is not guaranteed to be relevant to previous ones. The dimensionality check is performed after another  $k$  periods. It is possible that the state after  $k$  periods might be different from that of the state before since the new strategy during  $k$  periods may system evolve. However, the state cannot be far from the last state since the strategy of the agent did not change over  $k$  periods. Consequently, the expectation based on similar state should work well.

After the first dimension check, the agent keeps checking dimension every day to see if there is any change in the market. If it finds no significant change in dimension, it assumes that the current state is not far away from former state, and then keeps using the current data set with more added market clearing results. When there is change in the value of the dimension, there assumed three main possibilities which make system changed: change in the strategy of its own, those of competitors and condition of market such as network change, etc. The first possibility is easiest to detect since the agent already knows even before the check. Note that dimensionality check will give a clue on the effects of the change in its strategy if there is any. The third possibility is

also easily found by assumption that the agent has good knowledge on network by using external information, e.g., Genscape<sup>34</sup>. Once the agent detects the change in dimensionality and also finds the reason is not any of those two above, and then it assumes the change in the strategies of its competitor(s) makes the state of the system evolve. In the case that there is unknown change in network resulting in a change in the system state, it will get a wrong reason about the change. Consequently, the weight factor distribution from the error minimization  $\min_x \|Ax - b\|_2$  might cause a bigger error. However, as far as its earning concerned, the weight factor distribution performs well in the optimization process since the distribution came from the process of the error minimization. Once it detects the change in the state for any reason, scenario sets and matrix A need to be modified for a better system estimate.

When an agent finds any change in the state, there may not be enough data obtained from a new system. In such a case, the number of row in A is less than that of column, i.e., an underdetermined system. In treating a underdetermined system in the matrix computation, the weight factor distribution inevitably contains many zeros which may lead inappropriate representation to a real market. To avoid this problem, the most recent data obtained from the old state are added to the new data under assumption that old state might not be too different from the new one. To have the new data more impact on the weight factor distribution, heavy weight is given to the new data by adding many copies of the new data into the matrix A and the vector b. If difference between the two states is significantly different, the weight factor distribution might results in a bigger error for a mapping function from offer to earning. However, if this is the case, the market is very unstable, and then no agent performs well in the circumstance.

---

<sup>34</sup> <http://www.genscape.com/na/index.shtml>

#### 5.4.2. Simulation detail and results

Several simulations have been performed with the supply-side and demand-side agents described here. All demand-side agents have must-be-served demand about 10 % of their total demands. To see the performance, only one supply-side agent was placed on the Bus 23, and standardized agents represented other firms. To emulate different situations, several markets with different types of competitors have been simulated. Figure 5. 10 shows simulated historical nodal price data both competitive and volatile markets. In these simulations, none of competitors change their strategies, but it is common for each agent to exercise market power by trying other strategies. To test how an agent reacts against a permanent and consistent change, after some periods, a competitor changes its strategy consistently. The results are shown in Figure 5. 11. For the current market, it is allowed for a buyer to purchase electricity from a seller from outside. When there exists such an independent contract, external flow must be injected through network. The external flow might not be known to all the supply-side agents, but it changes power flow to some extent. The change results in a virtual change in the network. If a supply-side agent does not know the existence of the flow, its ability to find a change of the market state needs to be tested. Furthermore, it might be useful to know how the agent reacts against the change if it finds. To check this ability, a simulation with five standardized agents and one supply-side agent from outside has been performed in a following way: no change in the strategies of the standardized agents was made, but after 200 periods external flows about 10 MW from the Bus 28 to the Bus 20 are injected. Figure 5. 12 shows the prices obtained from the simulation. Above three different simulations, the agents of interest always have locational benefit. For testing the performance in case without locational benefit, a simulation was performed with an agent on behalf of Firm 1 in the

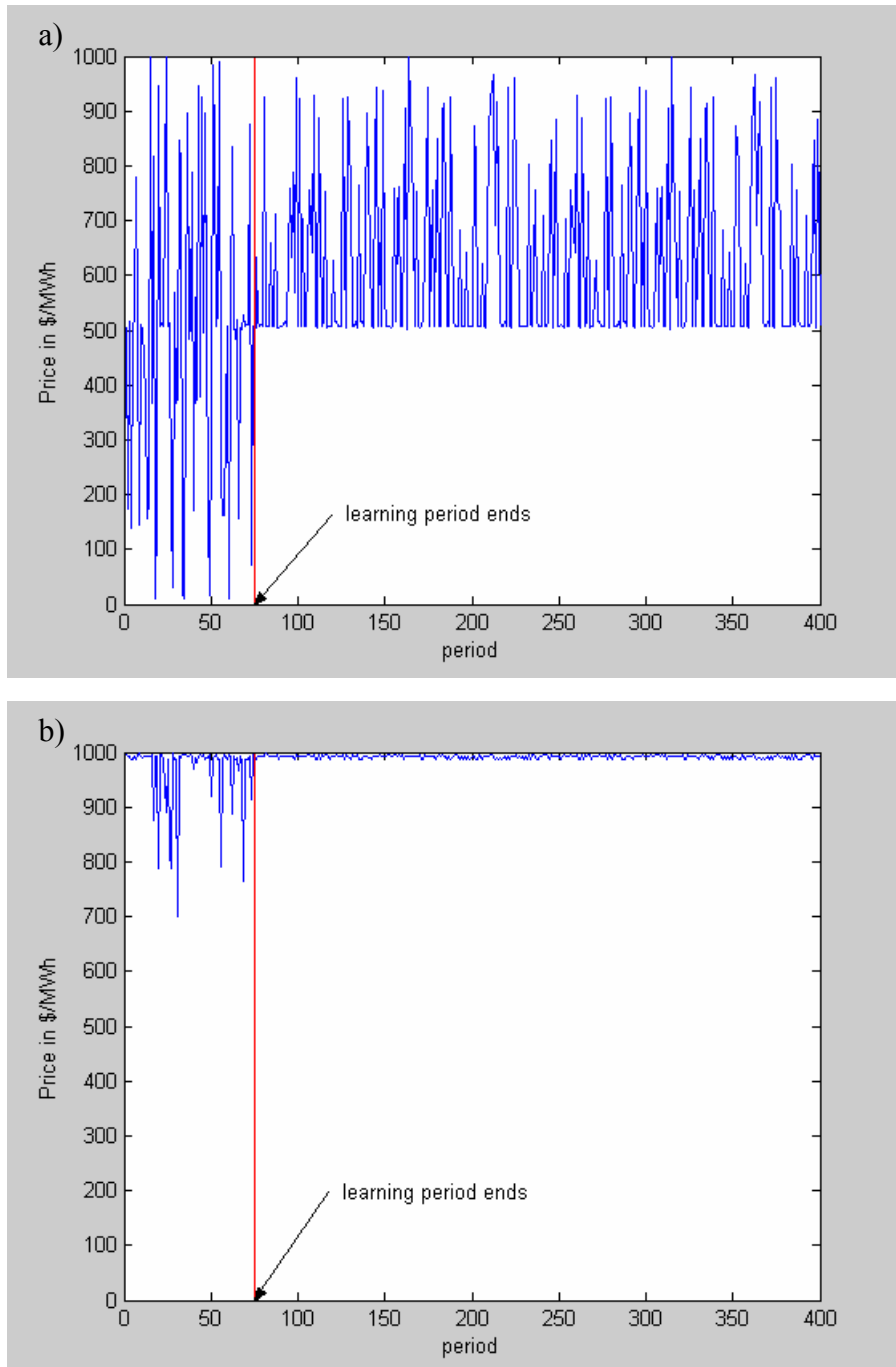


Figure 5.10 Simulated historical data for nodal prices at the Bus 23 (Firm 5) in the case that 4 marginal cost offer agents in Area 1 and 3 exist while Firm 6 is a) a marginal cost offer agent or b) speculator with different predetermined the degree of speculation

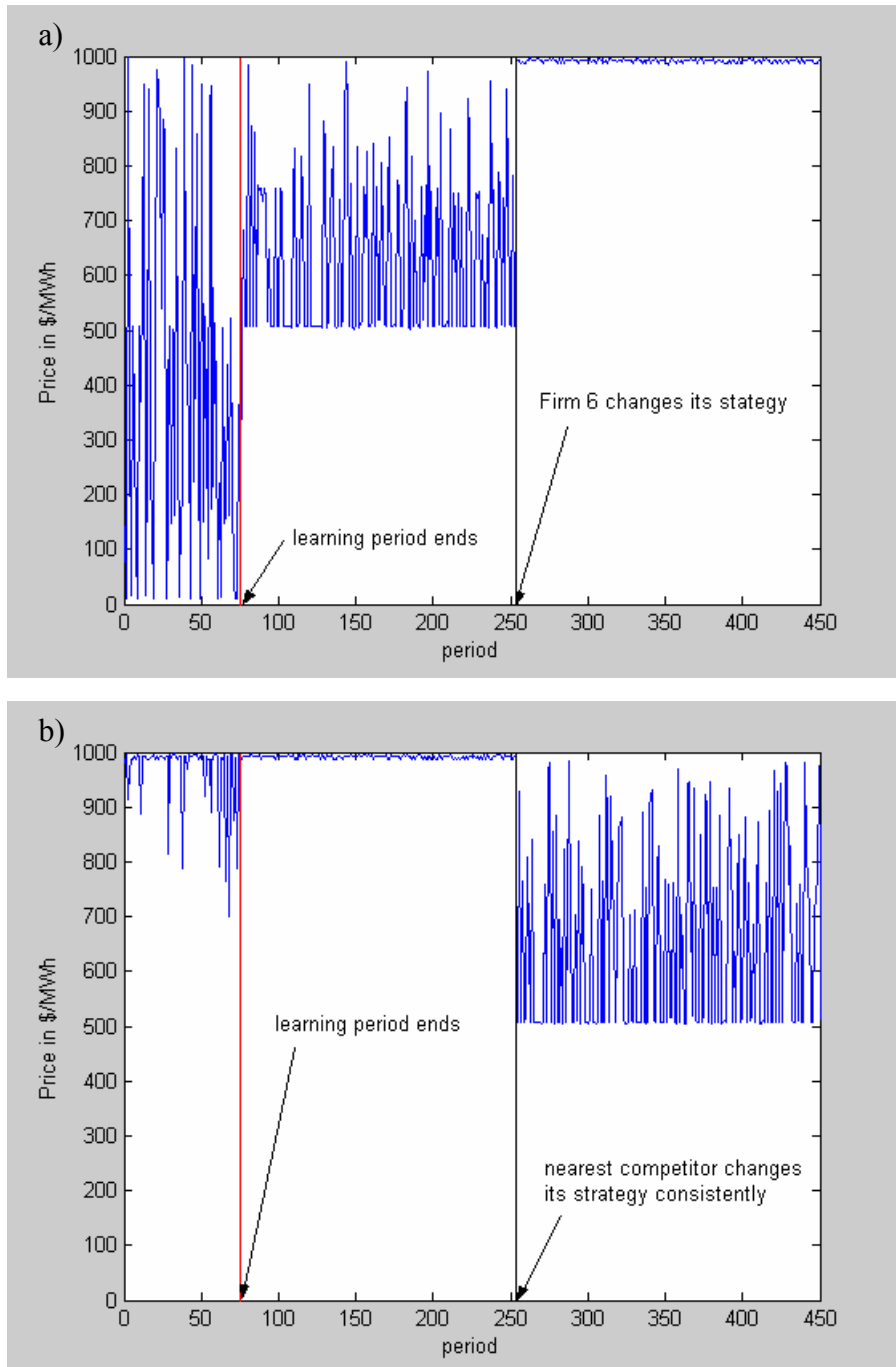


Figure 5.11 Simulated historical data for nodal prices at the Bus 23 (Firm 5) in the same cases in Fig. 8. 1., but nearest competitor (Firm 6) changes its strategy completely a) from MC to speculator and b) speculator to MC

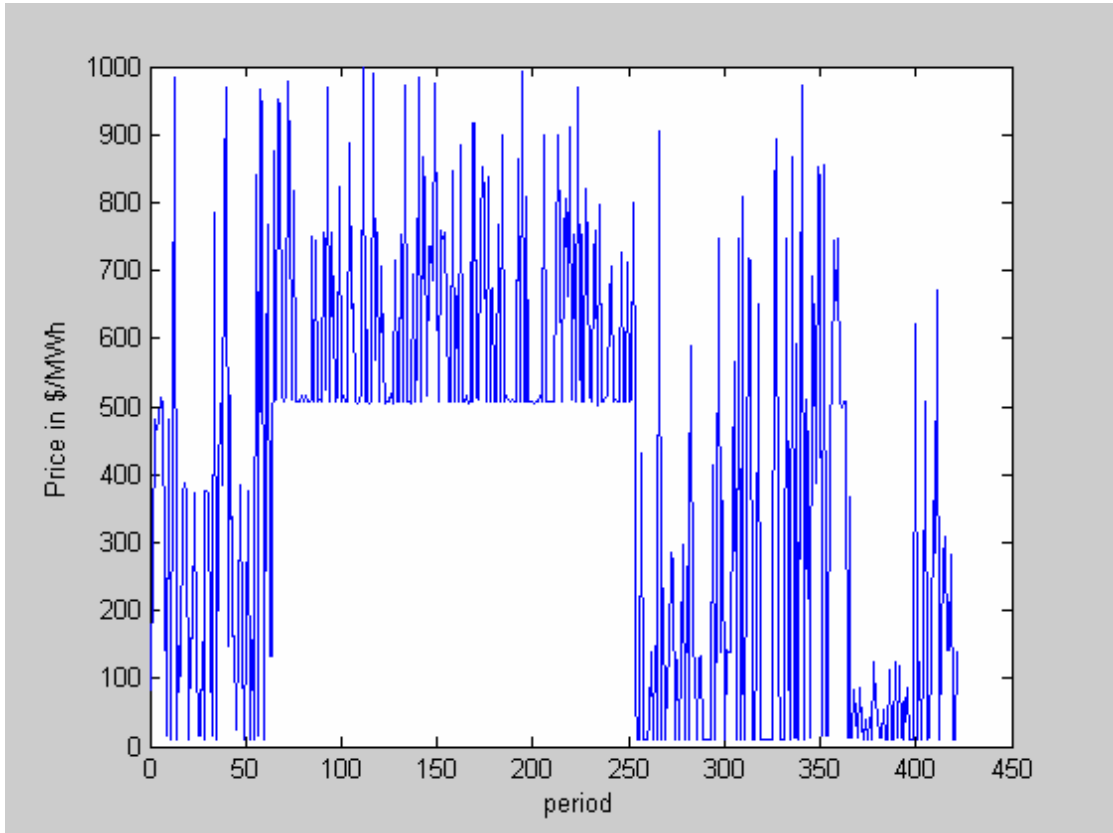


Figure 5. 12. Simulated historical data for nodal prices at the Bus 1 (Firm 1) when there is injection at Bus 28 and withdrawal at Bus 16 from the period of 253



same situation described in Figure 5. 11. The results are shown in Figure 5. 13.

#### **5.4.3. Simulation with no change in the strategies of competitors**

The competitors have differently assigned DOS; for Firm 1 – 4 were 20, 10, 25 and 15 respectively, and that for Firm 6 was 25 for a) and 85 for b). During learning periods, the nodal price data for the agent representing Firm 5 fluctuate from its marginal cost to reservation price with mean of about \$ 400/MWh and \$ 900/MWh, respectively. After learning periods, it updates the scenario set based on the error minimization process. Original matrices A contain simulated earnings from equally distributed scenario sets, and the relative errors ( $= \|Ax - b\|_2 / \|b\|_2$ ) were about 52 % and 38 % for a) and b), respectively. Note that equal distribution of strategy set was assumed before participating in the market. The matrices A were modified based on the contribution to expected earnings of each scenario. For a), the second most speculative scenario with the value of 75 for DOS was discarded and replaced with a scenario between most and second most competitive scenarios with DOS of 12.5. On the other hand, the second most competitive scenario with DOS of 25 was replaced with one of 87.5 for DOS for b). The modification of scenario set reduces error to 46 % and 27 %. With the new modified scenario set, the agent tried to find an optimal offer at given load forecast.

On a daily basis, the dimension was checked for detecting if there is a change in the market state. Figure 5. 14 shows the result of the dimension check. Since 100 data points are needed for a reliable dimension check for a dimension with a value of 2, only after 8 days the value for a dimension is reliable. From a), the dimension check

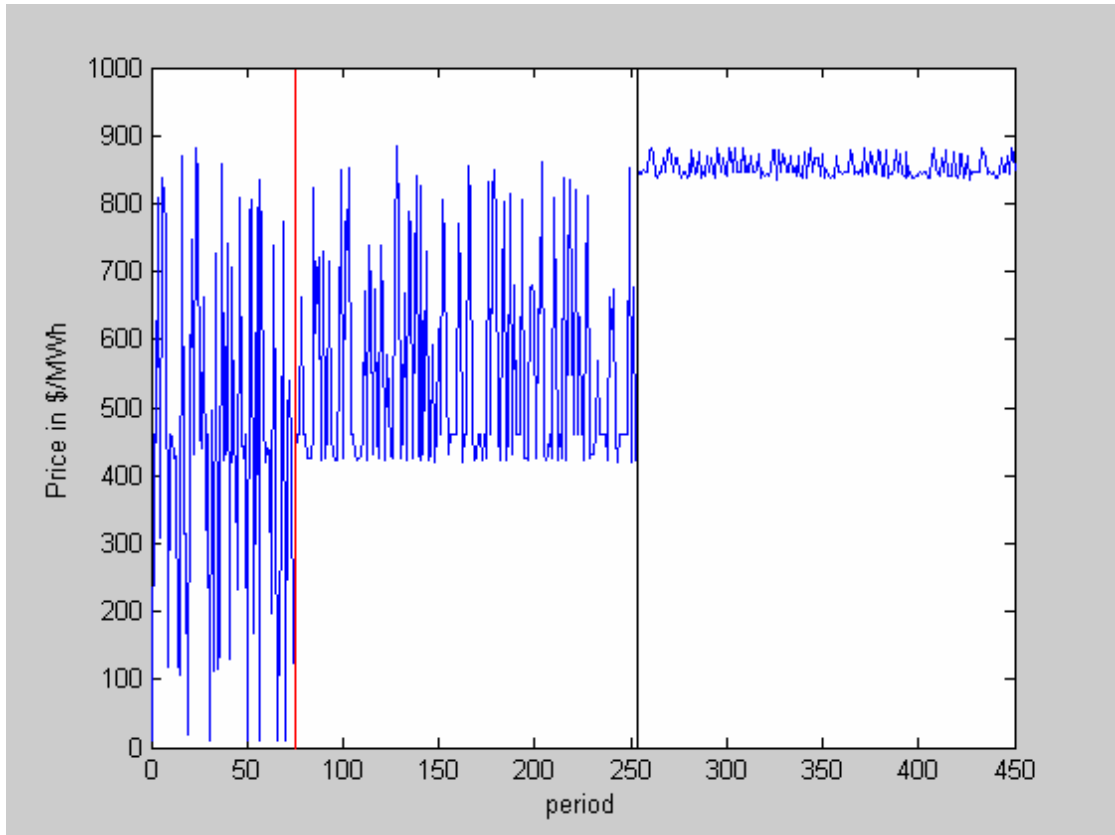


Figure 5. 13. Simulated historical data for nodal prices at the Bus 23 (Firm 5) which has no locational benefit; a competitor in Area 2 (Firm 6) changes its strategy in a more speculative way completely at the period of 253

does not detect any conceivable change in the state of market after the 8<sup>th</sup> day, which was true in fact. The false alarm on day 7<sup>th</sup> may cause unnecessary consideration on Day 8<sup>th</sup> as well as Day 7<sup>th</sup>. On both days, the agent checks the dimension and finds a change in the state. Then, the agent selects the part of data for estimate based on its data selecting algorithm discussed in chapter four. The selected data contain the information of the same state which the agent must observe from. Therefore, the performance of an agent should not be affected by the false alarm in this case. There is a possibility that malfunctioning of the tool may cause wrong selection of data causing silence after a change in the market state. In the current setup, the probability is very low since the tool should not inform a change for many days. Note that the agent evaluates dimension everyday. The dimension check shown in b) gives almost identical case except to exhibit relatively larger errors which makes the result less reliable. An agent might be uncertain if there is any change in the state. All the experimental data contain error, and correspondingly, an analysis made on such data has reliability issue when noise over signal ratio gets bigger. In the simulation for b), the change in the nodal price is relatively. In such a case, the dimension check may give unclear conclusion due to large error. Since two adjacent points in Fig. 5. 14 b) are overlapped in error range, the probability that the system is not changed is more than 10 % which is not small enough to ignore. Consequently, an agent assumes there is no change in the market state.

When the dimension check does not detect any change in the state of the market, an agent needs data for the matrix A and vector b for finding weight factor distribution, which might contain too many rows. It is not economic to carry too much data for a computation. To select proper amount of data for estimating a future state, the Liapunov exponent calculation was performed. Figure 5. 15 shows the results of

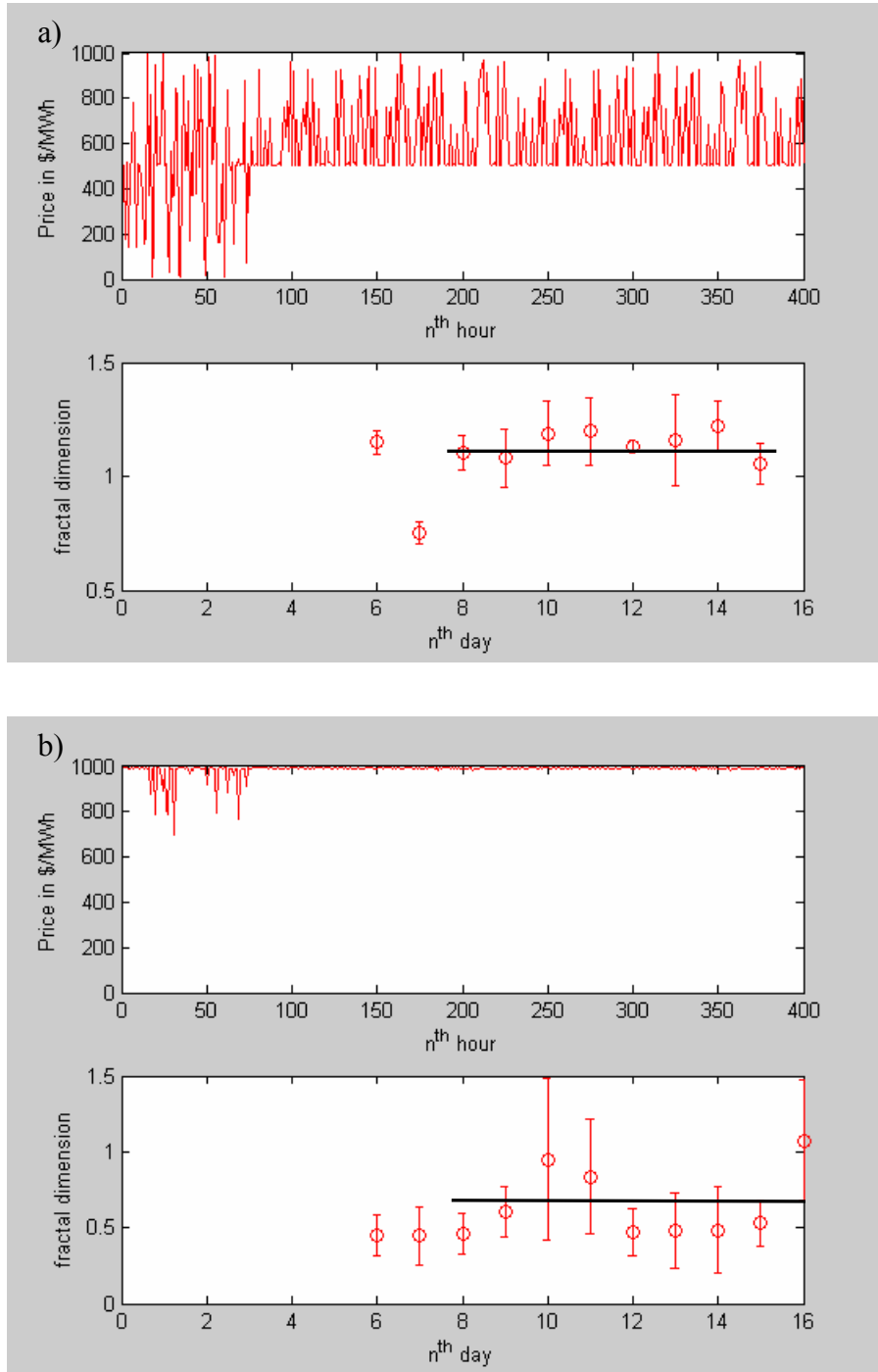


Figure 5.14. Daily dimension checks for the historical nodal price data obtained from the simulation described in Figure 5.10 a) and b), respectively.

the Liapunov exponent calculation. Both a) and b) shows no positive exponent clearly, and especially for b), the values are clearly negative. A negative exponent implies that the system settles into an equilibrium or a strange attractor. In such a case, all the data are relevant for estimating a future state, but for computational convenience, only part of the data is taken for calculating weight factor distribution. Note that default value in this study is 100 when the number of scenarios in a scenario set is 25. In both cases, an agent can check whether or not the system evolves based on a dimension check and then Liapunov exponent.

With a given weight factor distribution, an agent finds an optimal offer to maximize its profit for a given forecast. As was shown in Fig. 5. 10 a), the agent manages to keep the nodal price no less than \$ 500/MWh while the price fluctuates from \$ 10 to \$ 1,000/MWh when random offers were submitted. The similar situation occurs in Fig. 5. 10 b). Figure 5. 16 shows the simulated historical earnings for both cases from the simulation as was described in Fig. 5. 10. For b), the nearest competitor offers its quantity at a high price, and consequently the market that the agent representing Firm 5 faces must accept offers submitted by Firm 5 unless its offer is too high. Therefore, average earning from learning period are not much different from that after the period. About 30 % increase in earning was achieved. When a market is more competitive like in a), earning depends more on the offer by the agent. Average earning in the learning period was \$ 6,000/h, but that after the period was about \$ 10,000/h which was approximately 70 % increase. To show how well the market modeling is done, the expected earnings is plotted also in red line. The relative errors during learning period are 46 % and 27 % as was mentioned before, but those after the learning period are 19 % and 1 %. During the learning period, an agent searches all the space available by submitting random offers. After the period, an optimization process

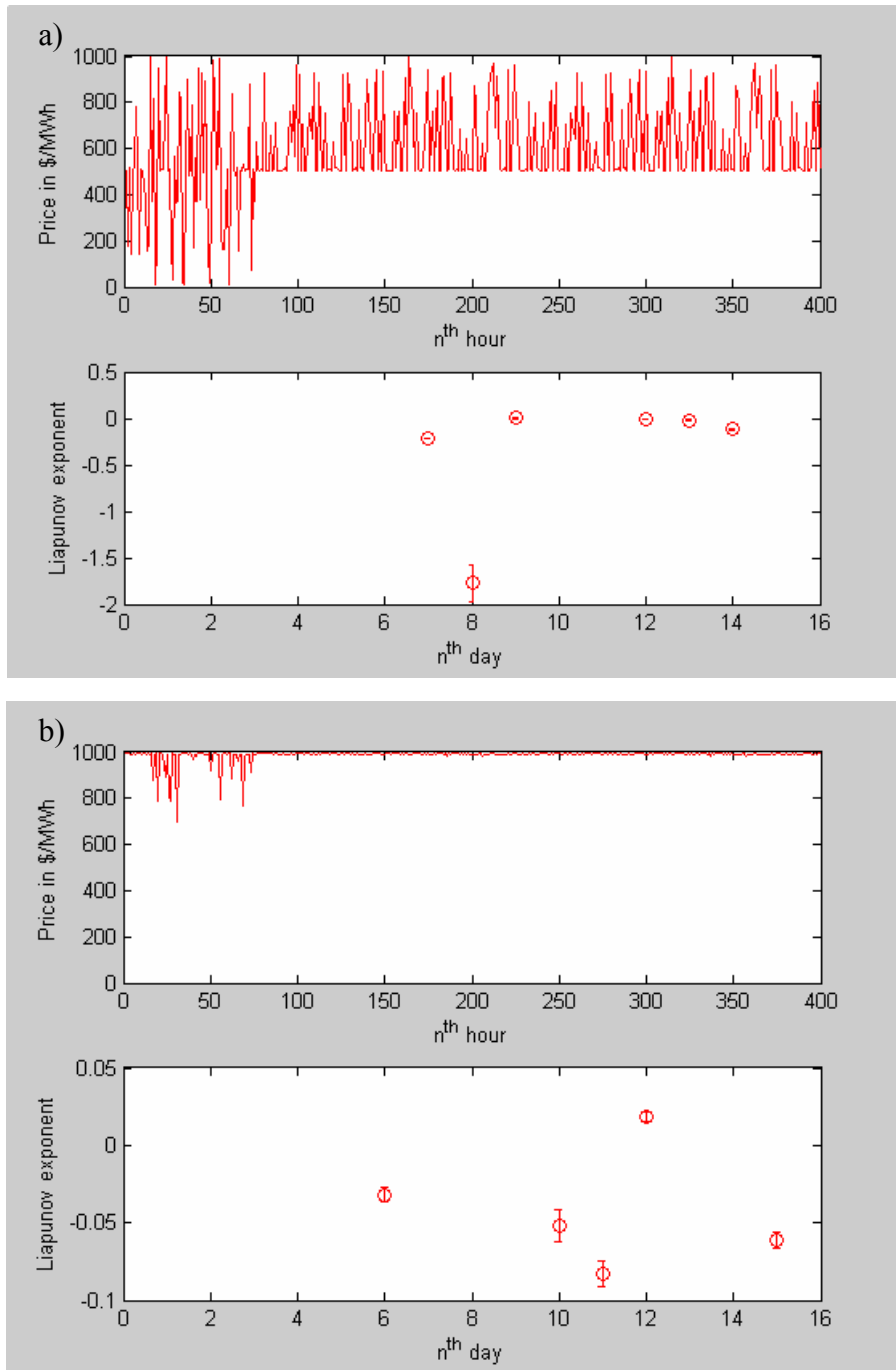


Figure 5.15 The results of Liapunov exponent calculation performed with the historical nodal price data obtained from the simulations described in Fig. 5. 10 a) and b), respectively

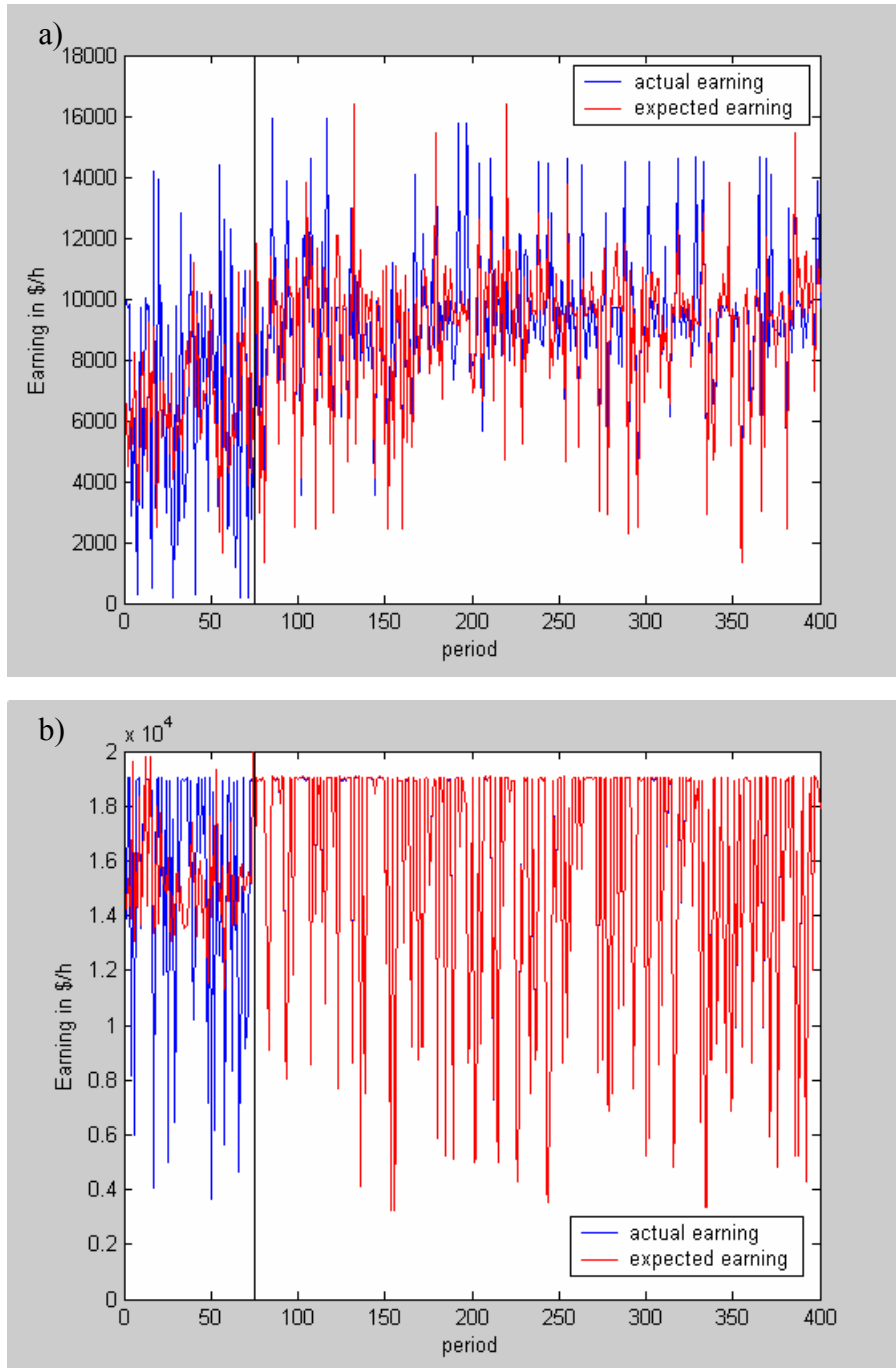


Figure 5.16 Simulated historical data for the actual and expected earning of Firm 5 from the cases described in Fig. 5.10 in blue and red line, respectively

restricts the search space into a small area, which is well defined. Therefore, the relative error should become significantly small. When the market gets less competitive, the optimizing strategy is selling more quantity to the market by offering lower price. Then, the search space is very limited, and then the error should be significantly small, which was 1 % in comparison to 19 % for a more competitive market.

#### **5.4.4. Simulation with the change in the strategies of competitors**

Before Firm 6 changes its strategy, the agent representing Firm 5 behaves approximately identical to the case described in Section 5.4.3. The relative errors were about 65 % and 33 % for a) and b), respectively. Modifying scenario set as described in Section 5.4.3 makes error reduced to 59 % and 28 %, respectively. With the new modified scenario set, the agent tried to find an optimal offer at given load forecast.

A dimension check was performed everyday in order to detect if there was a change in the market state. The results are plotted in Figure 5. 17. For a), a dimension check detects a conceivable change in the market state 4 days after Firm 6 changes its strategy. A dimension check shown in b) gives almost identical case as was before. A dimension check detects the change in the market state reliably in both cases. When the state of the market changes, it is important to find how long the change takes to settle into a new equilibrium state. The question can be answered by evaluating Liapunov exponent. In general, it takes two times of the inverse exponent for the system to reach another equilibrium. Figure 5. 18 shows the results of evaluation to the exponents. In both cases, the exponents after the change was made are very small



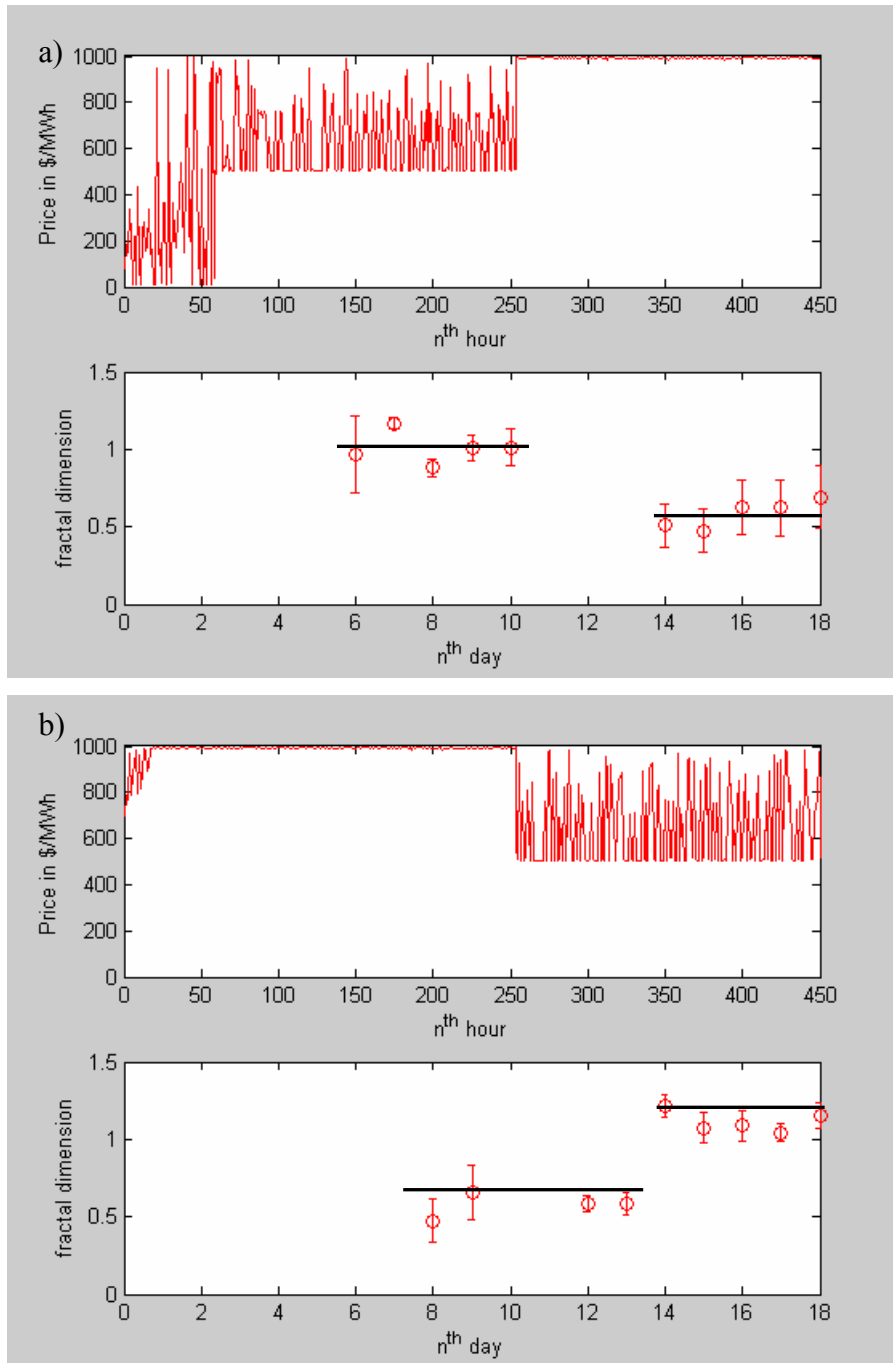


Figure 5. 17. Daily dimension check for the historical nodal price data obtained from the simulation described in Figure 5. 11

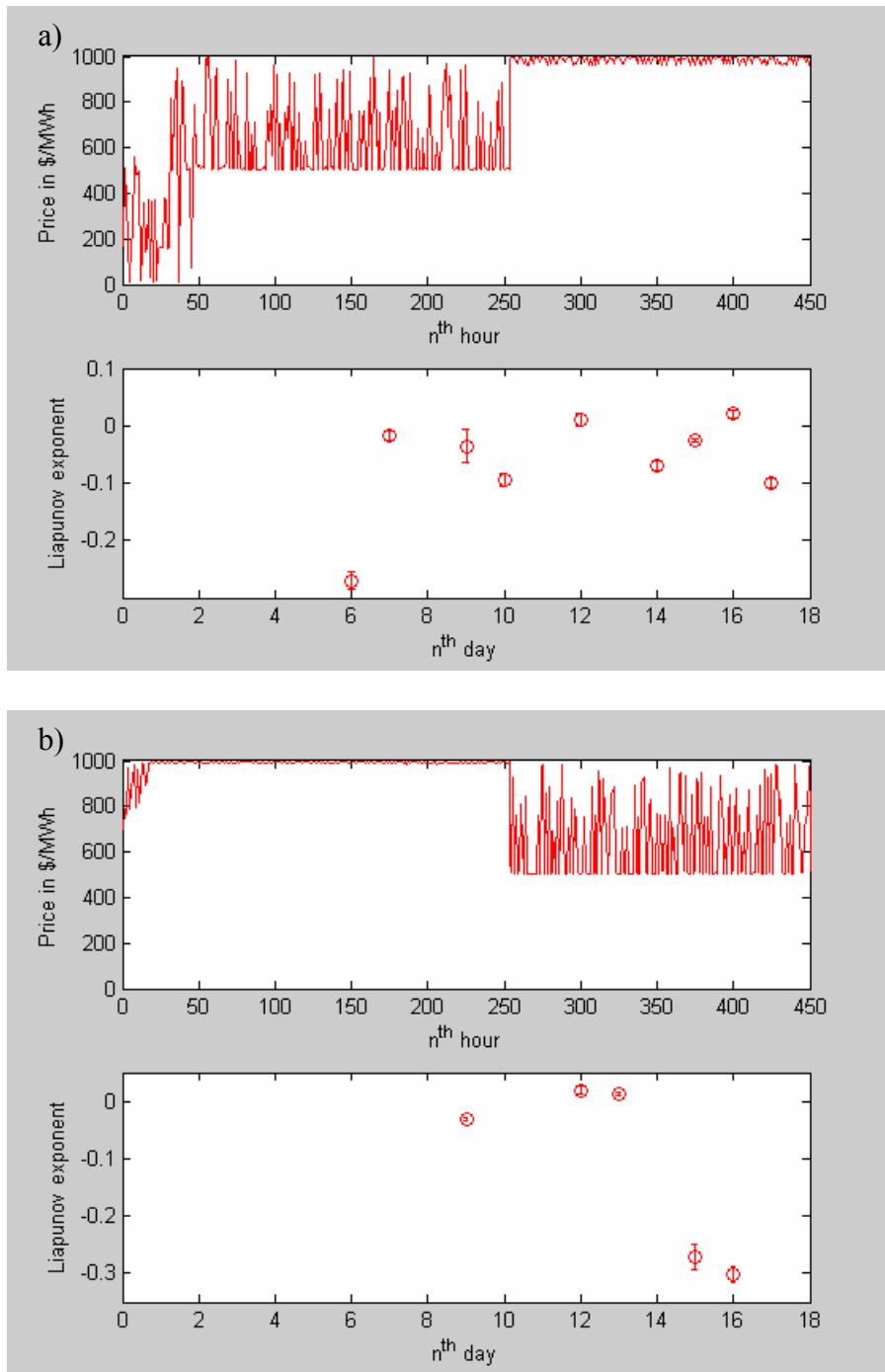


Figure 5.18 The results of Liapunov exponent calculation performed with the historical nodal price data obtained from the simulations described in Fig. 5.11 a) and b), respectively

positive numbers. For example, the values of the exponents at day 12 and 16 for a) and b) are very small and positive. In evaluating the Liapunov exponent, only a few points were randomly taken to avoid choosing biased data, and the actual value of the exponent greatly depends on the choice in the point selection. Consequently, the value of the exponent is less reliable especially when it is small. For negative or zero values of the exponent, an agent chooses only a small number of data to calculate weight factor rather than whole data for saving computational effort. When the exponent has a large positive value with small error, it implies that a system divulges very fast. A small positive value of exponent, like in these cases, implies that the dynamics is very slow, and then approximately 2 times of inverse exponent of data points are relevant for estimating a future state. Since the exponent tells how recent data are relevant to estimate a future state, it only gives an upper limit for the number of data that an agent should take. In both cases here, more than 100 and 200 data points are upper limits for a) and b), respectively. It is noteworthy that for b), the dimension was approximately 1, and the embedded dimension was 2. Correspondingly, one point in embedded space is composed of two data points, which results in 200 data points of upper limit for b). Therefore, a default value was taken for estimating weight factor distribution.

From the results of the dimension check, the performance of an agent before finding the change in the market state seems as good as that after finding. Dimension check and the Liapunov exponent give an agent a guideline to select the amount of data. Before the change of the market state, dimension check gives no change and the Liapunov exponent calculation gives a negative value, which allows an agent to take only 100 data points. Before the agent realizes the change in the state, several new data has been added into the 100 data points. Consequently, the effect of the new addition is not negligible. Without using the dimension and exponent, the agent should

carry all the data, and then the effect is small enough to be ignored since the fraction of the new data is small in comparison to the amount of data obtained from the former state. Thus, the performance could not be so good as an optimal one. For a randomly generated offer, the nodal price fluctuates a lot in a). The price during a learning period represents the nodal price in case of a random offer. It also fluctuates between \$ 700/ MWh and \$ 1,000/MWh for b) during the period. Once the agent finds a proper weight factor distribution, the price never go below \$ 500/MWh and \$ 990/MWh for against competition with MC and speculator representing Firm 6, respectively. DOS for Firm 6 was changed from 25 to 85 for a) and from 85 to 25 for b) while DOS's for other firms were unchanged.

The agent finds an optimal offer to maximize its profit for a given weight factor distribution and forecast. As was mentioned before, the agent manages to keep the nodal price no less than \$ 500/MWh and \$ 990/MWh for a) and b), respectively. Note that price fluctuates when random offers were submitted during a learning period. Figure 5. 19 shows the historical earnings for both cases from the simulation as was described in Fig. 5. 11. The results were almost identical to the cases described in the section 5.4.3 when Firm 6 behaves in the same way as was in the section. The errors after the learning period and before the change in the strategy of Firm 6 were 17 % and 1 %, respectively, and those after the change were 1 % and 21 %, respectively. A more inefficient market allows an agent to explore larger offer-earning space. From Fig. 5. 19 a), the earning recovers to an optimal one very quickly. When the agent faces a more competitive market, the search space it explores is less limited, and it should take a long time to find a new optimal strategy. As was shown in Fig. 5. 19 b), after a sudden change in the market state, the earning shows a typical initial stage of a relaxation curve. However, the relaxation was not fully developed because the agent

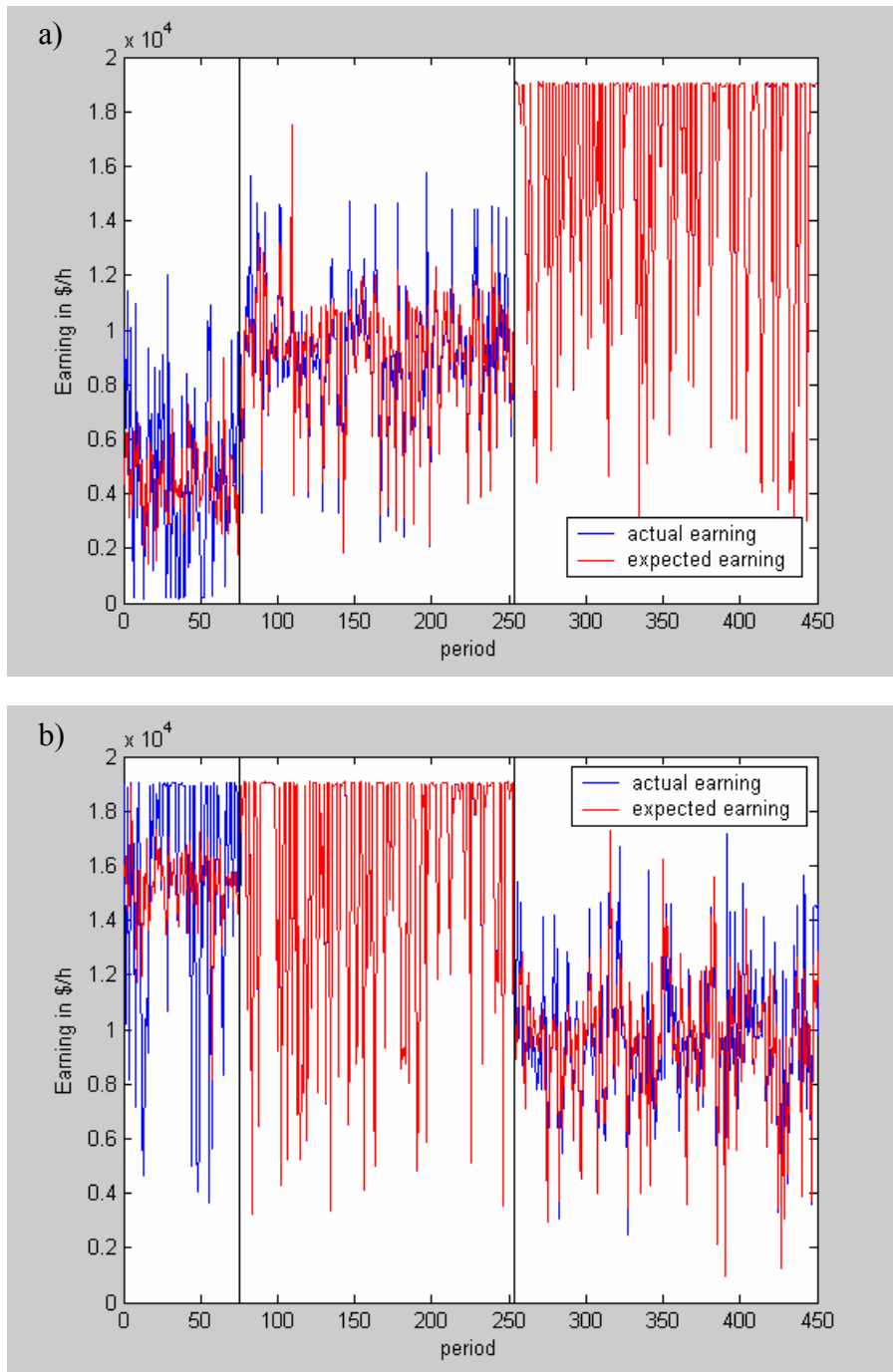


Figure 5.19 Simulated historical data for the actual and expected earning of Firm 5 from the cases described in Fig. 5.11 in blue and red lines, respectively.

adjusted its strategy quickly. It is noteworthy that the performance of the agent after the sudden change in the strategy of Firm 6 quickly recovers to the optimal one. Though Firm 6 does not change its strategy from period 1 to 253, there were many fluctuations in the nodal price as shown in Fig. 5.11 b). When the market is monitored by a snap-shot type tool such as one currently used in several ISO's, an agent should check the change of a system and adjust its strategy accordingly. The unnecessary check would cost in computation, and the adjustment would make its performance worse.

To study the strategy of the agent, the degree of speculation and the maximum offer price (MOP) were plotted from learning period, and periods before and after the sudden change of the strategy in Firm 6 as shown in Figure 5. 20. The figures in the first row in both Figs. 5. 20 a) and b) show the variables chosen for offers during the learning period. Figures in the second and third rows illustrate the variables before and after the sudden changes described in Fig. 5. 21. Second row in a) and the third row in b) correspond to the simulation against more competitive agents, while third row in a) and second row in b) do against less competitive markets. The variables from the simulations against more competitive agents seem to fluctuate more often, but it is difficult to find a difference in patterns observed both before and after the change. For getting a clearer insight, the ratio between the two variables, MOP/DOS, was calculated and plotted in Figure 5. 21. Both figures clearly show that the ratio increases as the competitor gets more and more speculative, and consequently, the market that the agent faces becomes less competitive. For a less competitive market, the agent can take advantage of the other agents by being less speculative; i) by reducing DOS and/or ii) by offering more quantity into the market, accordingly increasing MOP. In both i) and ii) cases, the ratio increases by decreasing denominator

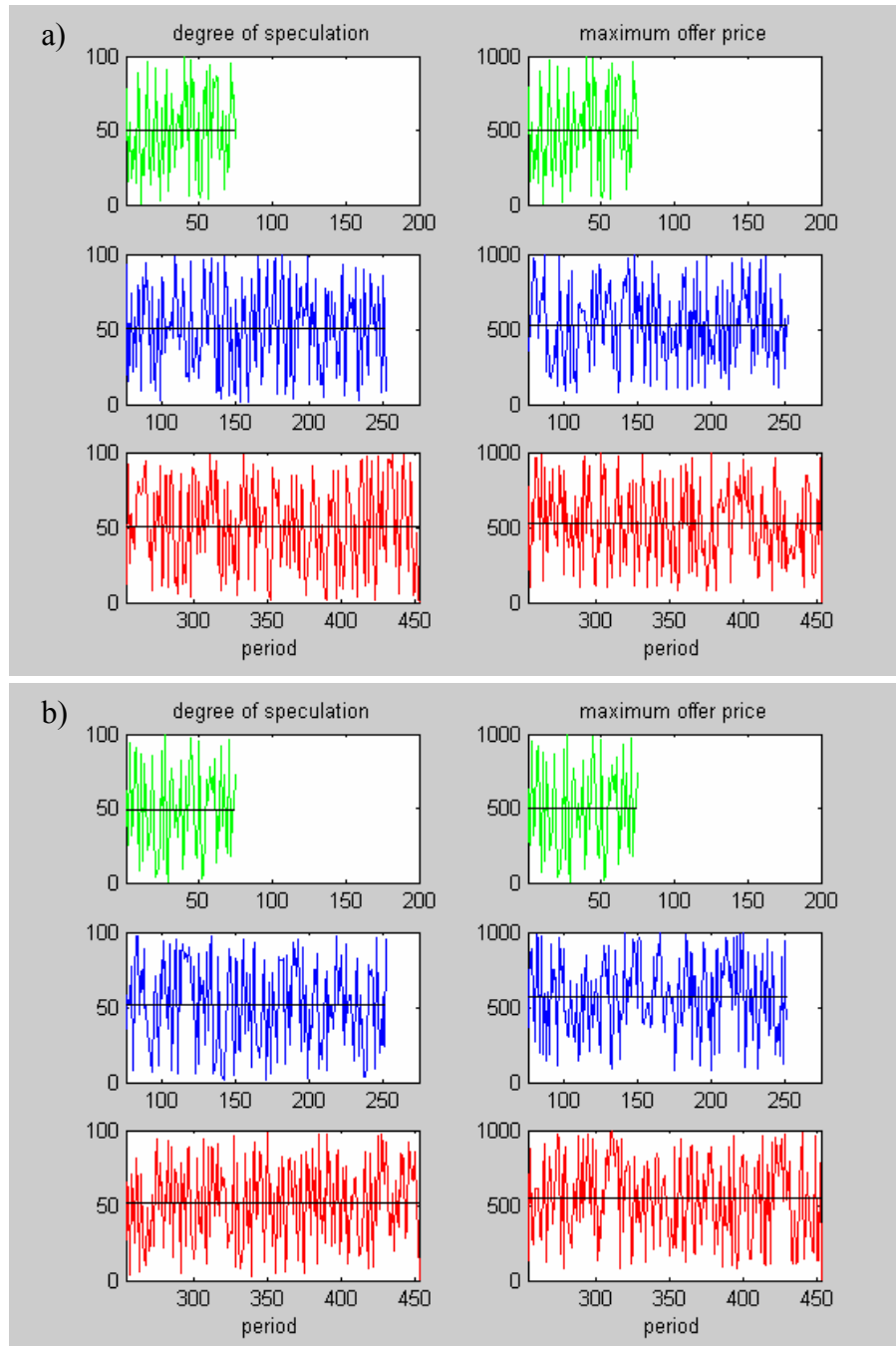


Figure 5.20 The degree of speculation and the maximum offer price changes over periods obtained from the simulation described in Fig. 5.11 a) and b), respectively; black lines indicate the mean values of the variables within the period shown in the horizontal axis.

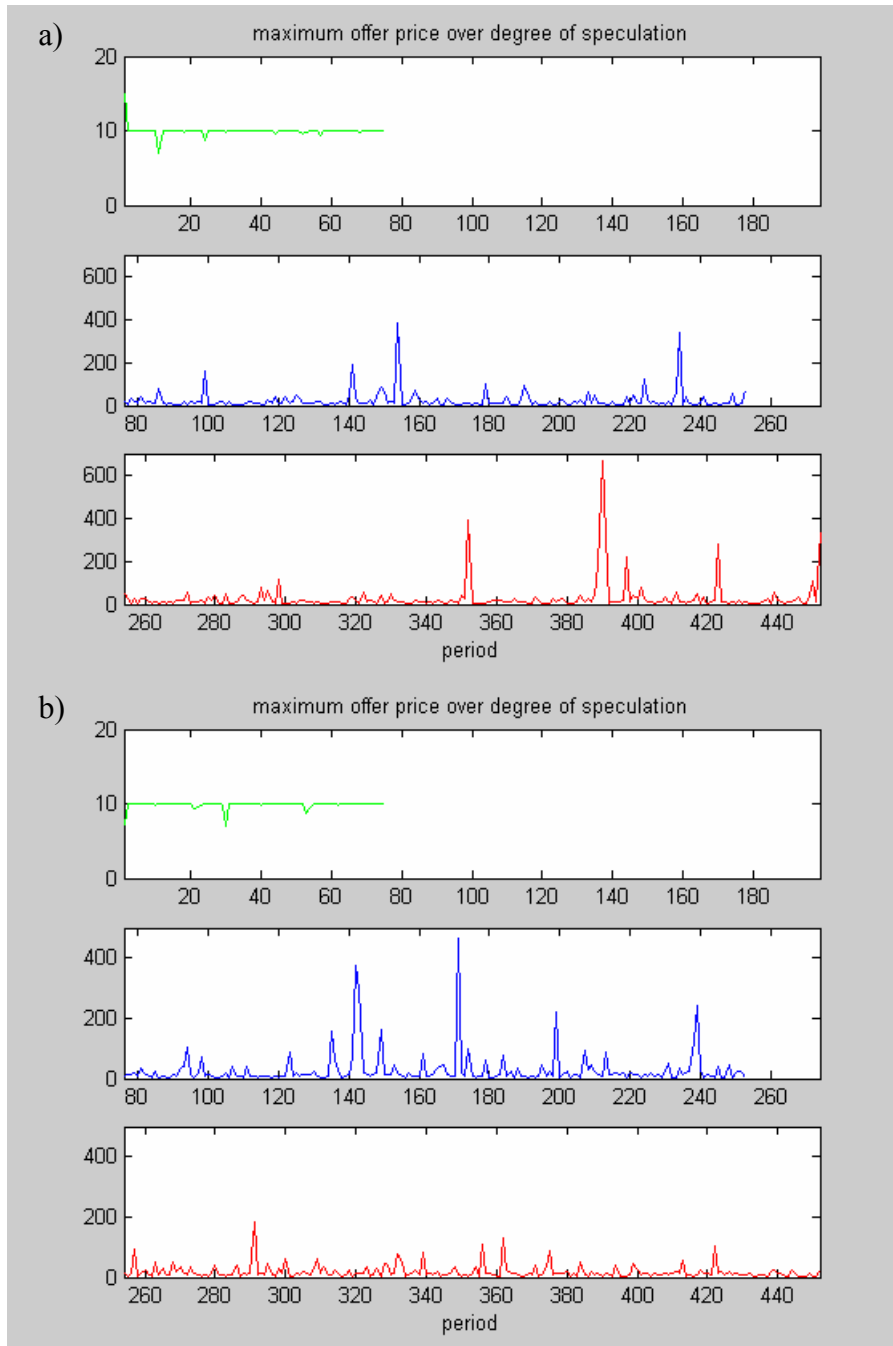


Figure 5. 21. The ratio of the maximum offer price to the degree of speculation over the periods shown in the horizontal axis; the corresponding values of both variables were shown in Fig. 5. 20



and increasing nominator from the former and latter case, respectively. Contrarily, the agent would increase its earning in a competitive market by being more speculative; i) by withholding more quantity from the market resulting in decreasing MOP and/or ii) by increasing DOS. In both cases, the ratio decreases.

#### **5.4.5. Simulation with unknown external flow**

Before an external flow exists, the price behavior is practically identical to the case described in last section. Modification on the scenario set reduces error to 58 % from 62 %. After the learning period and before the occurrence of the injection, the error is reduced to 16 %. After an external power injected into the system, the relative error increases up to 72 % of the relative error. As was shown in Fig. 5. 12, the prices after the occurrence of unknown injection fluctuate from zero to reservation price. When the prices are compared to those during learning period, the market seems even more stable due to the unknown external flow.

Figure 5. 22 a) shows the result of dimension check for finding any change in the market state. A conceivable change in the market state is detected by evaluating a dimension. As is shown in Figure 5. 22 b), the values of most Liapunov exponents are negative. Two points are positive with less than 0.1, which means that a system evolved fairly fast. With 0.1 of Liapunov exponent, only about 20 data points were relevant to predict a future state, which is less than a default of 100. In such cases, data obtained from the previous state are added to form A and b while more importance is given to the new data. Since it does not know there was an introduction of an external flow and other possible changes and it did not change its own strategy on purpose, the

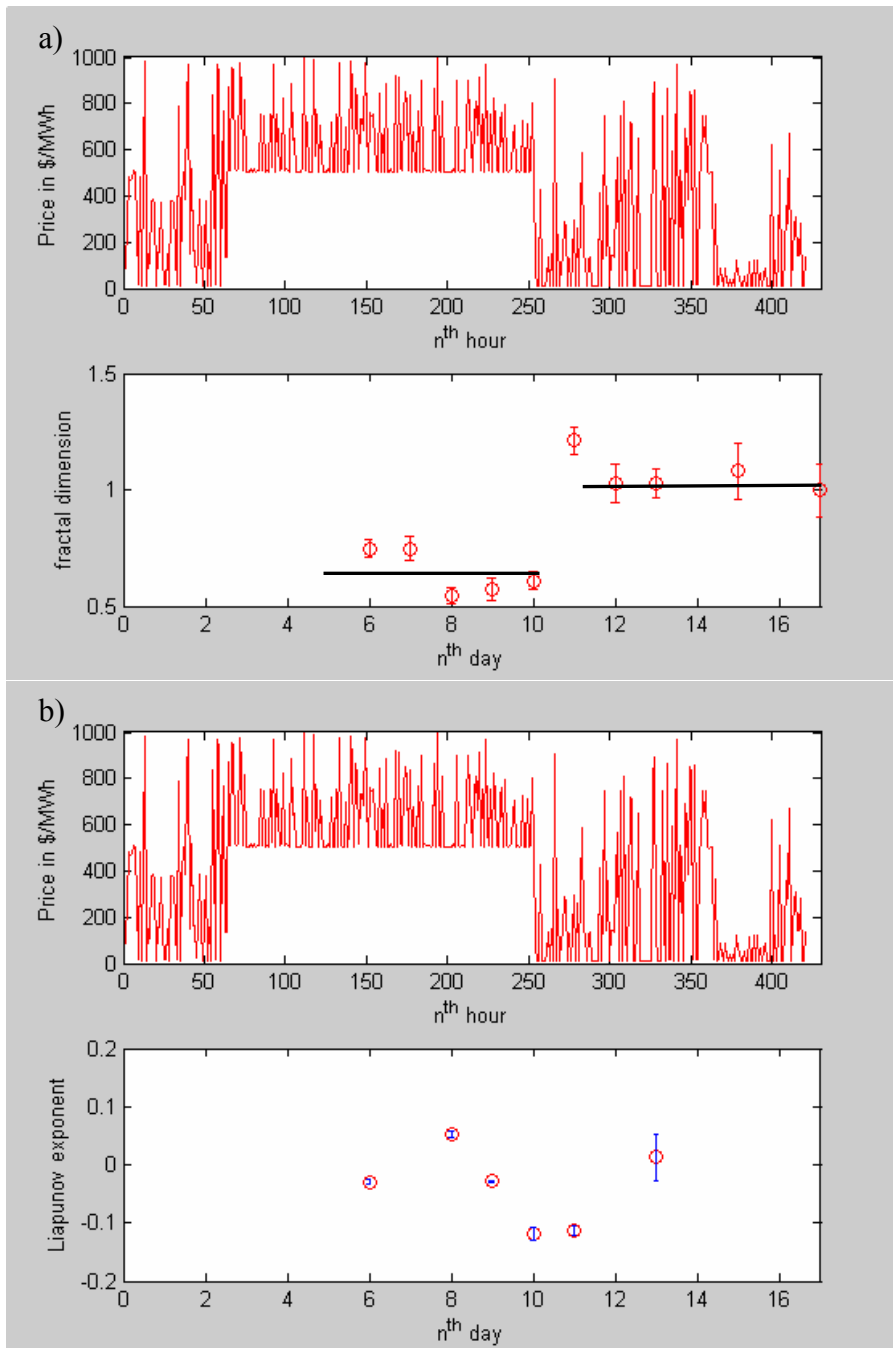


Figure 5. 22. Daily check for a) dimension and b) Liapunov exponent calculated with the simulated historical nodal price data obtained from the simulations described in Fig. 5. 12

agent assumes the change in the state is due to a change in the strategies of its competitors. Demand forecast provided by ISO includes the demand fulfilled by the external injection. Consequently, the demand contributes the value of fairshare, resulting in an overestimate for fairshare even if the demand is not fulfilled by any agents in the network. From the overestimated fairshare, the agent assumes that the market gets more competitive. Note that the information on quantity served by the competitors is not publicly available.

Consequently, the same value of the weight factor distribution does not properly map offer to earning. The agent updates the weight factor distribution and modifies the scenario set as well. As a result, the matrix A contains wrongly calculated values, and the weight factor distribution does accordingly. To compete against the “changed” competitors, the agent updates its strategy according to the way described in the last section: to decrease the ratio between MOP and DOS. The changes in the main variables and the ratio are shown in Figure 5. 23. Even if the error minimization finds the optimal weight factor distribution, the error must be significantly large according to the magnitude of the injection.

Figure 5. 24 shows the difference between the actual and expected earning. The actual earning after the change fluctuates more than that of expected earning. The reason is the actual system is spanned with a quite irrelevant scenario set. The relative errors during a learning period, before and after the injection occurs, were 58, 16 and 71 %, respectively. Significantly high values for the relative error between expected and actual earning (78 %) is a signature of the wrongly chosen scenario set. However, the same choice worked well with the error of 16 %. Therefore, it is possible for the agent to conclude that there is a change which needs updating the basis set instead of

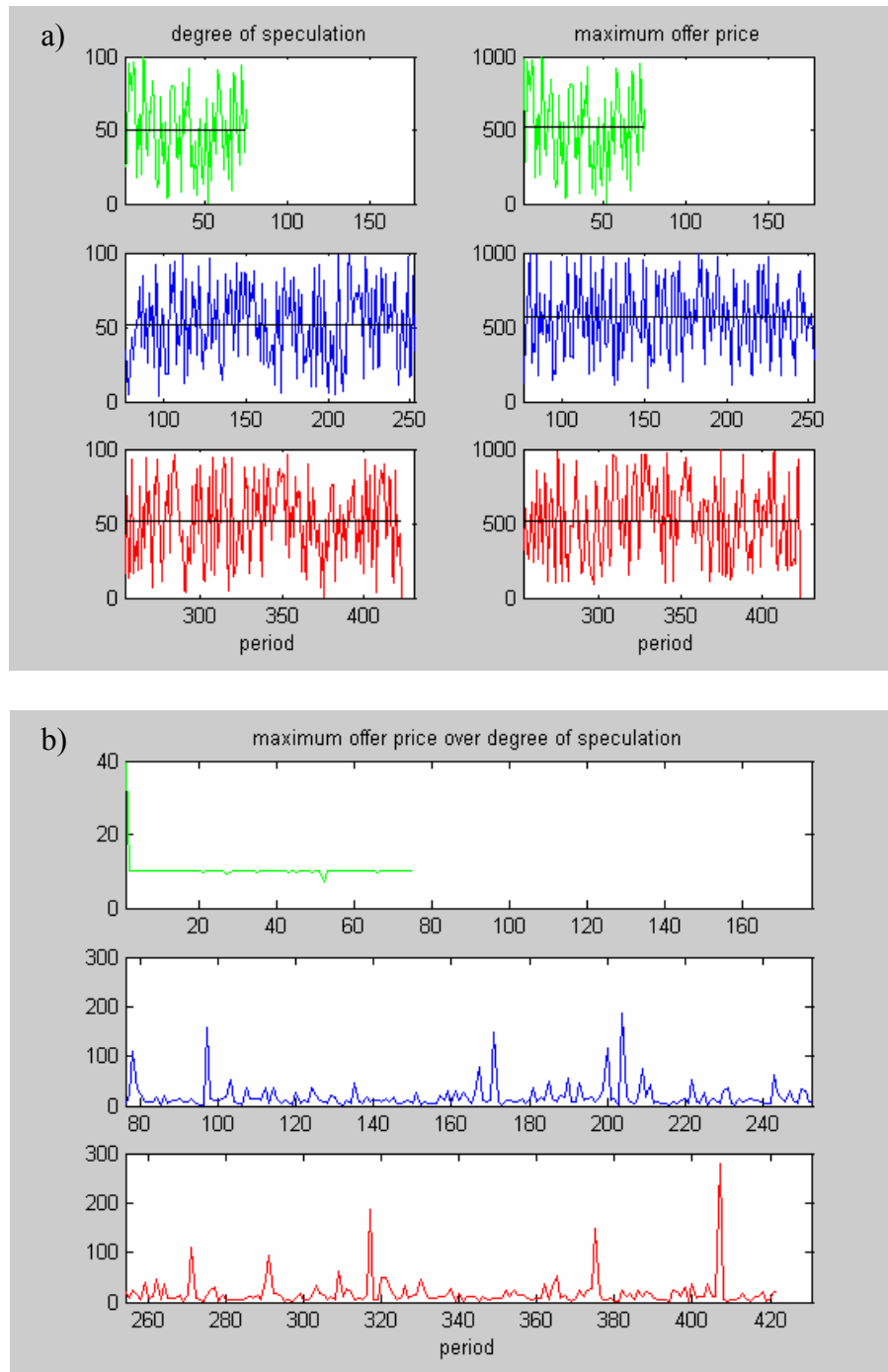


Figure 5.23. The main variables and the ratio between the variables over periods obtained from the simulation described in Fig. 5.12; the black lines in a) represent the mean values of the variables during the period

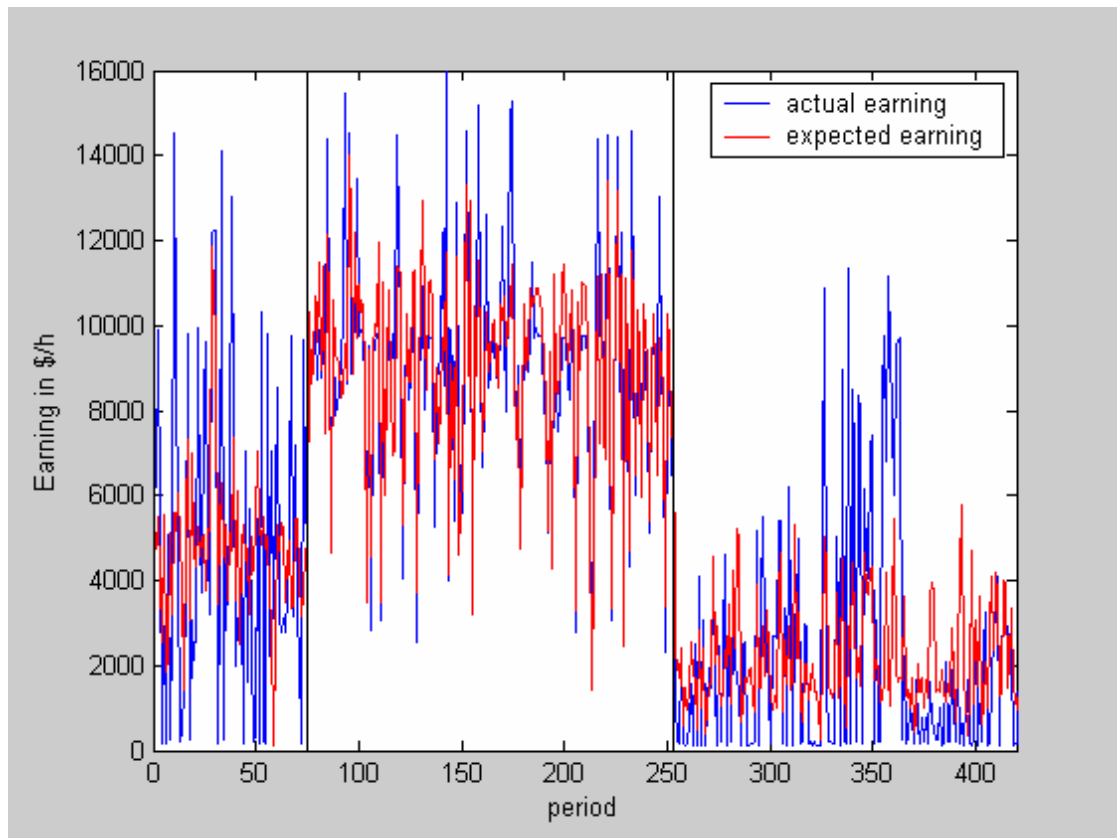


Figure 5. 24 Simulated historical data for the actual and expected earning of Firm 5 from the cases described in Fig. 5. 12 in blue and red lines, respectively.

adjusting the weight factor distribution. Once it gets the information, the agent should find the proper reason why the market state changed. As was discussed in Section 5.4.1, there are three reasons why the market state changes: change in the strategies of market participants and the other reasons like change in network. Most likely, the other reasons could be considered further to explain the change in the state of the system.

#### **5.4.6. Simulation with an agent representing a firm without locational benefit**

Similar to Section 5.4.4, the prices at the Bus 1 where an adaptive agent is located change approximately identically to the case shown in Figure 5. 11. a). Both height and frequency of the price spikes are a little lower than those in Fig. 5. 11. a). Before Firm 6 changes its strategy, the relative error was about 58 %. For a better estimate, the agent modifies the scenario set modeling its neighboring competitors located in Area 1 and 3 while leaving scenarios for Firm 5 and 6 unchanged. Modification of the scenario set described above makes error reduced to 51 %. With the new modified scenario set, the agent tried to find an optimal offer at given load forecast.

Daily dimension analysis was performed in order to check if there was a change in the market state. The results are shown in Figure 5. 25. The dimension check detects a conceivable change in the market state a couple of days after Firm 6 changes its strategy. For the market after the change, the agent needs to find how long the change takes to settle into a new equilibrium state or to divulge by evaluating the Liapunov exponent. Figure 5. 25 b) shows the results of evaluation to the exponents. No exponents before and after the change are positive with sufficiently large value, i.e.,

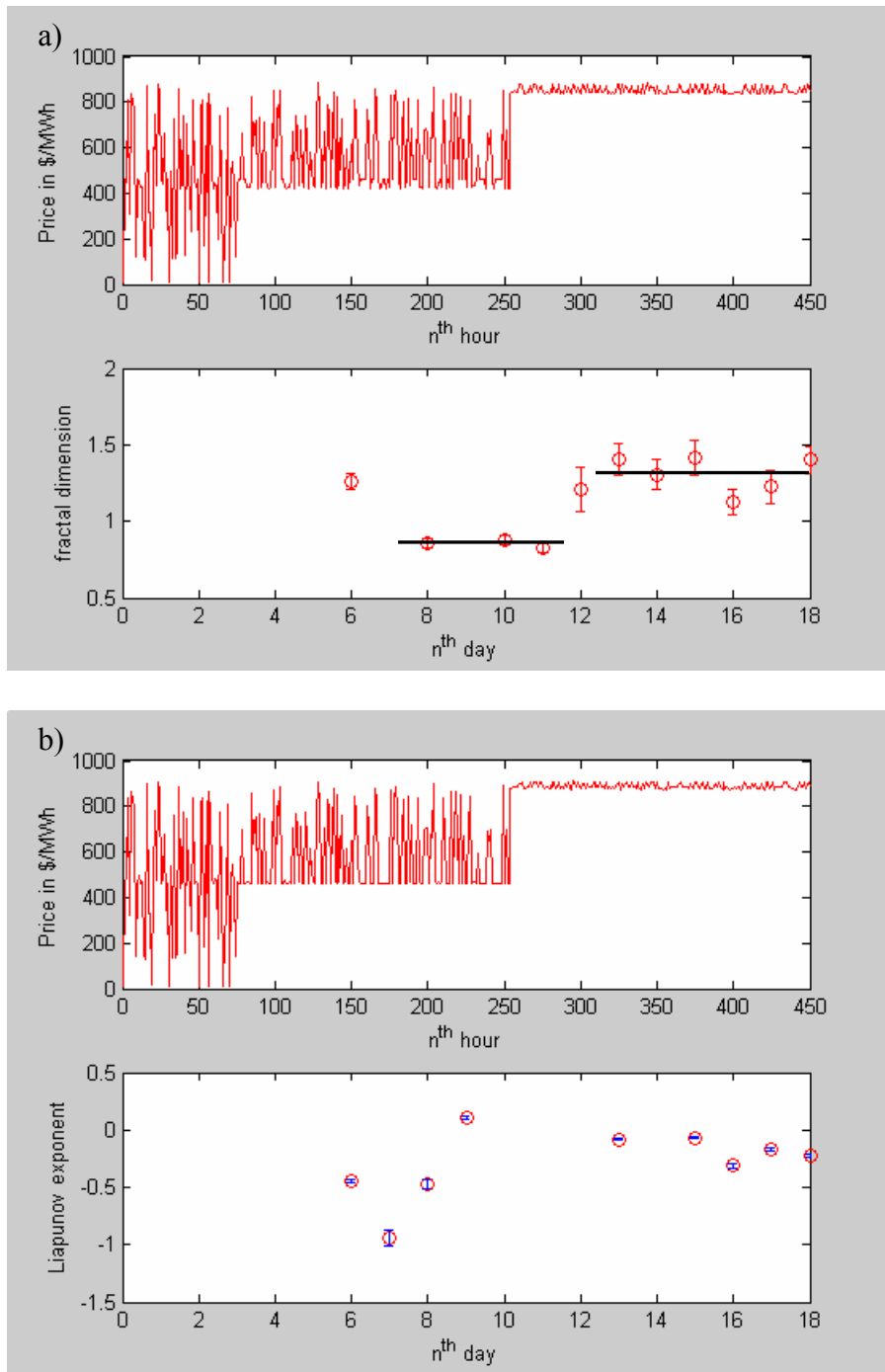


Figure 5.25. Daily check for a) dimension and b) Liapunov exponent calculated with the simulated historical nodal price data plotted in Fig. 5.13

bigger than 0.5. From both results, the agent finds that there was a consistent change in the strategies of its competitors, and the system settled into a new equilibrium. At Day 9, the Liapunov exponent shows a positive value, but the dimension check shows no change in the state. In such a case the Liapunov exponent is ignored since the dimension check is more reliable.

For showing the offer behavior of the agent, the main variables were plotted in Figure 5. 26. a). The pictures in the left hand side show the degree of speculation and those in the right hand side illustrate the maximum offer price, respectively. In the situation for second rows in the figure, competitors are less speculative, and the chance that the agent gets price spikes is much lower than that in the 3<sup>rd</sup> row. The ratio between the two variables was calculated and plotted in Figure 5. 26. b). The figures clearly show that the ratio decreases when the competitor gets more speculative, i.e., the market that the agent faces becomes less competitive accordingly. It is an interesting result since the ratio changed in the opposite direction in comparison to the case for the agent with locational benefit. When the market is less competitive, the agent can take advantage of its competitors if it can. However, the market does not become sufficiently volatile due to the change in the strategy of Firm 6. Consequently, the agent may have options; it makes the market more volatile by submitting more speculative offer, or it takes a small advantage out of the change. Optimization process finds a better way in maximizing its profit. In such a situation, the process finds that more speculative is a better way to maximize its earning. For cooperating with the Firm 6 that changed the strategy, the agent tries to help by withholding more, or being more speculative. Note that the agent may do both. The former decreases the MOP, while the latter increases DOS. Therefore, both cases result in decreasing the ratio of MOP/DOS.



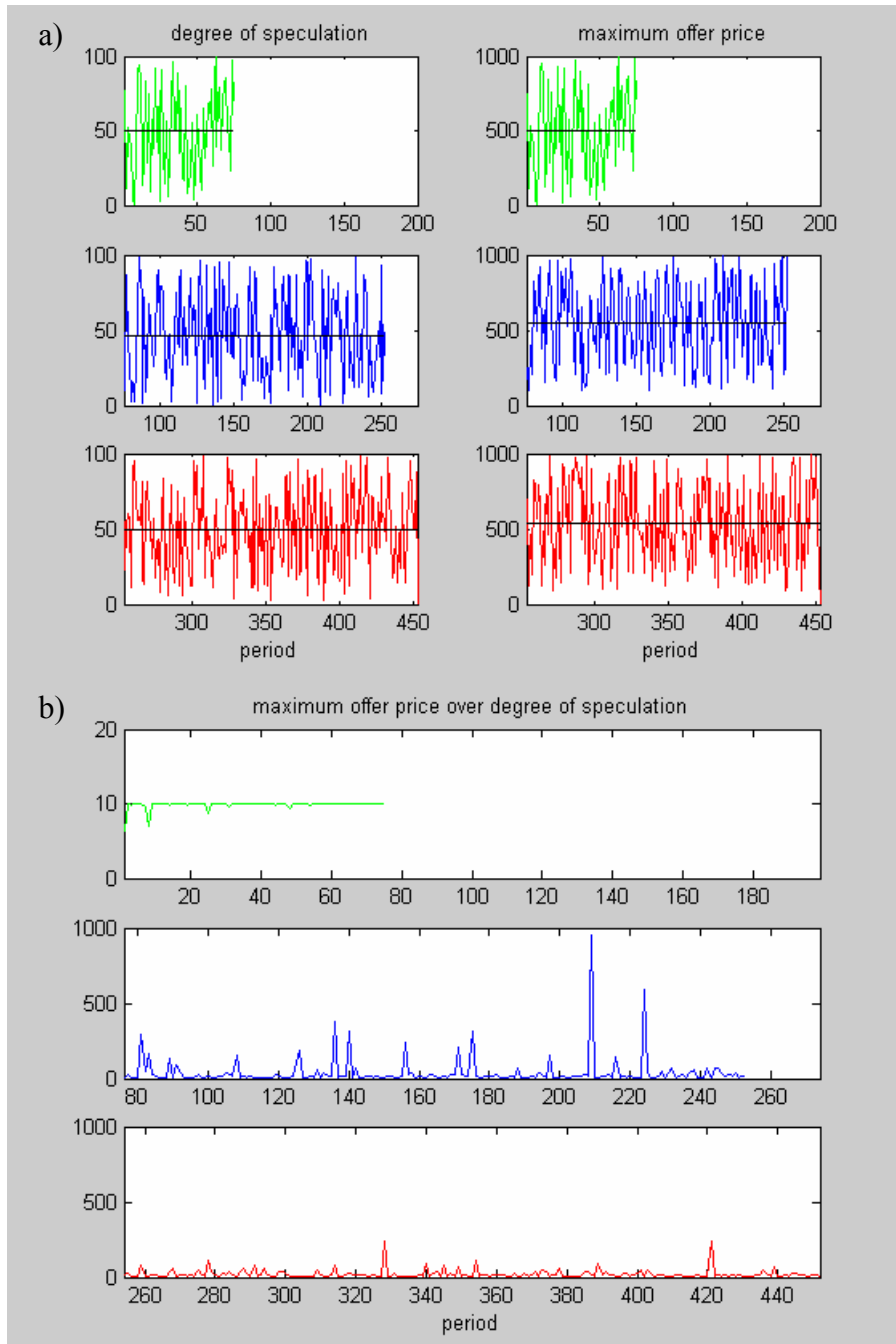


Figure 5.26. The main variables and the ratio between the variables over periods obtained from the simulation described in Fig. 5.13; the black lines in a) represents the mean values of the variables during the period

For a more competitive situation, the ratio increases in order to compete the “updated” competitors. For an agent without locational benefit, the unit that it owns may not be required to meet the demand. In such a case like competitive market and no locational benefit, speculation may increase the probability of not being dispatched. In order to avoid being de-committed, it tries to compete against its competitors. Then, it may decrease DOS or withhold less quantity, and accordingly increase MOP. Therefore, the ratio increases, which is the opposite case when the agent has locational benefit.

The agent manages to keep the nodal price about \$ 500/MWh and \$ 900/MWh for before and after the change in the strategy of Firm 6, respectively. Figure 5. 27 shows the simulated historical earnings for both cases from the simulation as was described in Fig. 5. 13. The results were almost identical to the cases described in the Section 5.4.4. The error after learning period and before the change in the strategy of Firm 6 was 19 %, and that after the change was 1 %.

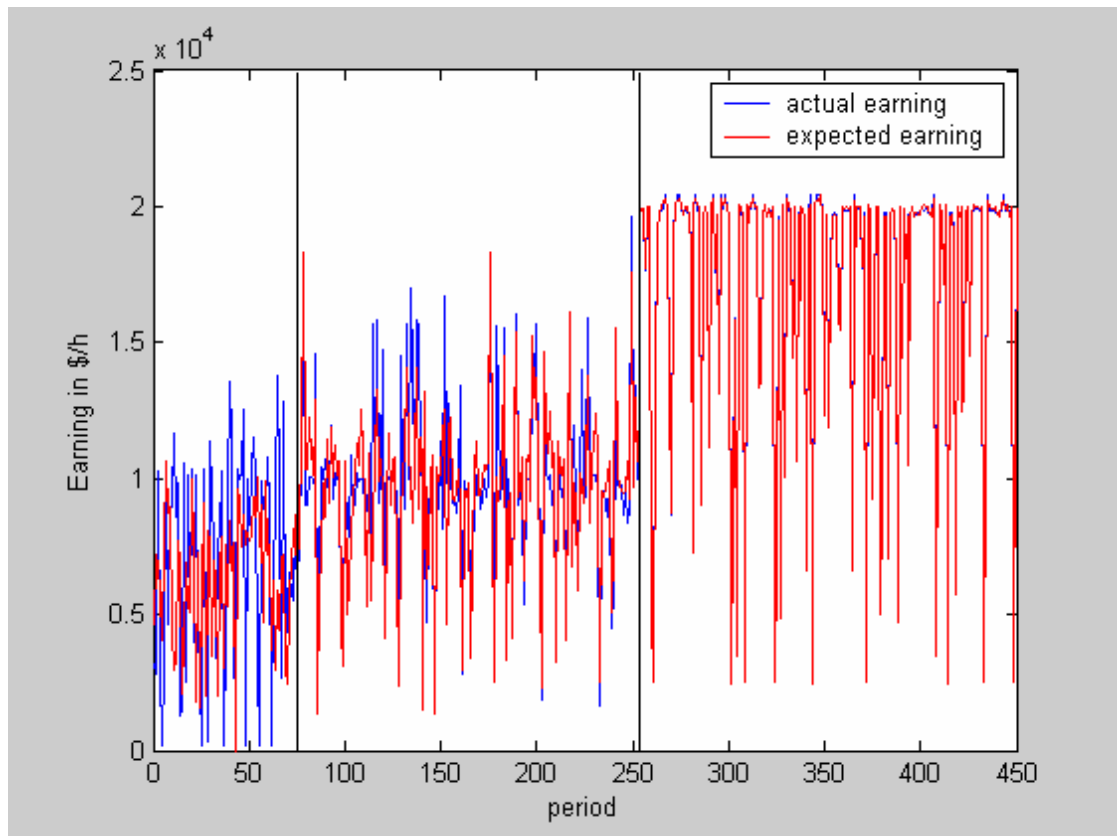


Figure 5. 27 Simulated historical data for the actual and expected earning of Firm 1 from the cases described in Fig. 5. 13 in blue and red lines, respectively.

## CHAPTER SIX

### CONCLUSIONS AND FUTURE WORK

Restructuring of electricity systems has been ongoing around the world for several decades. New auction based markets are considered more efficient, but less efficiency have been observed. Demand-side participation was claimed to make market more efficient due to the fact that only small portion of reduction in demand can reduce the number of price spikes significantly. For a better design, the implementation of such an agent must be in favor of end consumers such as less involvement and higher earning. To maximize demand-side profit with less involvement, distributors, such as NYSEG, participate in the market on behalf of end consumers, and submit an optimal bid. This dissertation has discussed the properties of demand and developed an optimal bidding function. A simulation with such demand-side agents shows a significant increase in market efficiency.

When a supply-side agent is introduced into a new unknown market, it tries to find what is happening. With available information, it can have a good knowledge on the market including network. However, the state of a market including the strategies of competitors is subject to change. The change in the market state might be either consistent or fluctuating. An optimal strategy should not change for simple fluctuations. Under the rule that no communication is allowed amongst suppliers, the agent should monitor the market state due to any consistent change based only on publicly available data such as nodal price. However, the data are affected in a way due to unknown offer strategies of competitors and network. The complicated nature of electric power markets makes a systematic study on the field difficult. This

dissertation primarily investigates finding an optimal strategy for a supply-side agent by using theoretically derived modeling and a market dynamic toolbox.

For a supply-side modeling, the objective of offer for quantity was discussed. Based on the discussion, a new model was developed and a differential equation was constructed to find an offer function. The resulting offer function theoretically derived from modeling fits existing offer data obtained from the Pennsylvania-New Jersey-Massachusetts market in 1999 successfully. Only small number of variables is needed to describe an offer curve instead of many quantity and price pairs for all the blocks submitted. Consequently, it is possible to assign the earning from each period into the number of variables.

As long as a system stays an equilibrium state, it is possible to estimate the market state with a relatively small error. In the case, time is not a variable to specify the state, i.e., it is not important when one explored the market. Therefore, all the data or any part of data observed are relevant to specify the system. For a given system in an equilibrium state, one needs some number of independent variables to describe the system, dimension. The value of dimension does not change if the system stays in the same equilibrium state or even a strange attractor. The number is closely related to the degree of freedom which the system has. Once the system evolves, one must check if the system settles into a new equilibrium or a chaotic state. In both cases, the degree of freedom changes as the system evolves, and consequently the dimension changes too. For the former case, relaxation time is an important quantity evaluating how long it will take for the system to reach another equilibrium. A similar quantity exists in the latter case such as a Liapunov exponent quantifying how long it will take for initially close states to separate far apart. The new quantities such as the dimension and a

Liapunov exponent gives an agent a way how to check the change in system as well as to decide which part of data should be used for estimating a future state. Those quantities were evaluated with the nodal price data obtained from the New York ISO web site during spring-summer 2003. The results tells that a systematic change occurred for the market state that a generator located in NYC area faced as season changed from spring to summer as demand increased consistently.

To construct a mapping function from an offer to earning, an unknown market was linearly superposed in terms of known types of competitors. The known types of agents are implemented based on the fact that the degree of speculation is the most important factor to affect earning. With the setup, an agent has an implicit way to recognize the market which it participates in. The linear superposition allowed a numerical mapping function and numerical optimization process.

Four different categories of simulations were performed for different competitors; one nearest competitor 1) did not change the strategy, 2) changed strategy consistently, and 3) external flow existed without knowledge of the agent of interest. All the simulations in the different setups with a supply-side agent showed that its performance is significantly better than that of random offer. Once a competitor changes the strategy, the dimension and a Liapunov exponent give a signal to an agent to inform the change. With help from the tools, an agent adjusts its scenario set for spanning the real world to have a better understanding on the real world. After the adjustment, an agent re-evaluated all the quantities such as scenario set and weight factor distribution. When it has no information on the network change, such as change due to an external flow, it assumes only change in competitors' strategies alters the market state. As a result, the discrepancy between the inner and the real world gets

bigger. In all the simulations, the agent found an optimal offer to maximize its profit, and it maintained the nodal price above a certain level depending on its competitors.

The supply-side agent designed in this study is a unique agent able to properly deal with transmission network, and it also performs well under stochastic demand. The strategy used by the agent under unknown situation was found to be consistent, which explains why it performs well. In the analysis of the offer behavior, the degree of speculation and the maximum offer price are key features to show how the agent reacts against the change in the market state. The ratio between them indicates the offer strategy of the agent in maximizing its profit.

Due to its computational expense, a larger system than IEEE 30-bus system was not tried in this study. Most computational burden in this study was function evaluation since it needs to run for multiple AC OPF's. However, each run can be parallelized which result in less computation time and space.

When an agent assigns a wrong reason for the change in the state of market, its performance is not good. In such a case, the error between estimated and actual earning is rather high, which is a signature of wrong reasoning. A new tool is required to detect such a signal in order to improve the performance of the agent.

Appendix A gives a way to an agent to check if a generator or subset of generators have market power. Once the agent finds out it has market power, there is a way to exercise its market power to increase its earning. If a subgroup has market power, the agent can construct a long term strategy for an investigation. In this study, such a long

term plan is not considered. However, it is reasonable for an agent to get such a plan as long as the plan might increase long-term profit.

With properly designed agents with tools mentioned above, the market behavior such as price can be forecasted. Based on the forecast, it is possible to construct a toolbox for operating and planning a power system.



## APPENDIX A

### GENERATION SENSITIVITY MATRIX FROM A NETWORK TOPOLOGY

Based on offers submitted by participating generators, a system operator finds an optimal solution to minimize whole system cost while all constraints are met such as power balance equations and voltage constraints etc. From the solution, a generation setpoint which comprised of generation and price is determined. Consider a following economic dispatch problem:

$$\begin{aligned}
 & \min_g c^T g \\
 & \text{subject to } flow_i (= F_i g) \leq capacity_i \\
 & \quad 1^T g = P_D + P_{loss}
 \end{aligned} \tag{A.1}$$

where F is part of PTDF matrix<sup>A1</sup> whose dimension is (number of lines)-by-(number of dispatched generators, n),

Lagrange relaxation technique is a well developed technology to solve such an optimization problem by forming a Lagrangian:

$$\begin{aligned}
 L &= c^T g + \mu(P_D + P_{loss} - 1^T g) + \sigma(\bar{fl} - Wg) \\
 &\rightarrow g^*, \lambda^*, \mu^* \text{ and } \sigma^*
 \end{aligned} \tag{A.2}$$

where g, λ, μ and σ stand for real power injection, locational marginal pricing (LMP, λ), shadow price of power balance equation and shadow price of binding line constraints, respectively.

---

<sup>A1</sup> Power transfer distribution factor, sometime it is called a shift factor

From the solution,  $g$  and  $\lambda$  are sensitivities of total system cost with respect to LMP and real power injection, respectively. It is possible to construct a sensitivity matrix of generation (real power injection) with respect to LMP, i.e.,

$$M \equiv \nabla_{\lambda} g = \nabla_{\lambda} (\nabla_{\lambda} Z) = \nabla_{\lambda\lambda} Z \leftrightarrow \Delta g = M\Delta\lambda \quad (\text{A.3})$$

Note that  $M$  is a Hessian matrix with a dimension of  $n$ -by- $n$ . Consequently,  $M$  is symmetric, i.e.,  $M^T = M$ . Since (A.1) is degree one homogeneous in price,  $M$  has only one structural eigenvector, corresponding eigenvalue is zero. Therefore, change in price along LMP does not alter generation.

$$\Delta g = M\Delta\lambda \Big|_{\Delta\lambda=c\lambda^*} = cM\lambda^* = 0 \quad (\text{A.4})$$

where  $c$  is non zero scalar.

One can write following Kuhn Tucker optimality conditions:

$$f = \nabla_g L = \lambda^* - \mu^* (1 - \nabla_g P_{loss}^*) - E^T \sigma = 0 \quad (\text{A.5.1})$$

$$h = \nabla_{\mu} L = 1^T g^* - P_D - P_{loss}^* = 0 \quad (\text{A.5.2})$$

$$fl = \nabla_{\sigma} L = \overline{flow} - Eg^* = 0 \quad (\text{A.5.3})$$

where  $E$  is part of  $F$  matrix for congested lines; the dimension of  $E$  matrix is  $m'$ -by- $n$ .  $E$  is comprised of row vectors of  $F$  matrix only for the lines whose constraints are binding, i.e., congested lines.

By solving equations (A.5.1), (A.5.2) and (A.5.3), generation setpoints as well as all shadow prices can be obtained. If offers in the original optimization problem (A.1) is replaced with LMP and then re-solved, the solution should be invariant due to the definition of LMP.

Suppose that the price replaced is perturbed from the exact LMP. Then all the parameters like real power injection and shadow prices ( $\mu$  and  $\sigma$ ) will be changed. However, by the property of optimization with a linear objective function and with convex constraints, the subset of active constraints does not change. Note that a linear programming, LP, with convex constraints finds solution at one of extreme points<sup>A1</sup>. Therefore, the optimality condition is only perturbed around the original points:

$$\begin{aligned} \Delta f &= \Delta\lambda + \mu^* (\nabla_{gg} P_{loss}^*) \Delta g - \Delta\mu (1 - \nabla_g P_{loss}^*) - E^T \Delta\sigma = 0 \\ \rightarrow 1 - \nabla_g P_{loss}^* &= \frac{1}{\Delta\mu} [\Delta\lambda + \mu^* (\nabla_{gg} P_{loss}^* \Delta g)] - \frac{1}{\Delta\mu} E^T \Delta\sigma \end{aligned} \quad (\text{A.6.1})$$

$$\Delta h = (1 - \nabla_g P_{loss}^*)^T \Delta g = 0 \quad (\text{A.6.2})$$

$$\Delta fl = E(g^* + \Delta g) - E g^* = E \Delta g = 0 \quad (\text{A.6.3})$$

Combining equations (A.6.1) and (A.6.2) gives,

$$(1 - \nabla_g P_{loss}^*)^T \Delta g = \frac{1}{\Delta\mu} [\Delta\lambda + \mu^* (\nabla_{gg} P_{loss}^*) \Delta g]^T \Delta g - \frac{1}{\Delta\mu} \Delta\sigma^T E \Delta g = 0 \quad (\text{A.7})$$

Since the second term in equation (A.7) vanishes by using equation (A.6.3) and  $\Delta\mu$  is a scalar, equation (A.7) gives a following expression for M matrix by using the definition of M matrix as given in equation (A.3):

$$\Delta\lambda^T [I + \mu^* (\nabla_{gg} P_{loss}^*) M]^T M \Delta\lambda = 0 \quad (\text{A.8})$$

Note that equation (A.8) needs to be satisfied for all  $\Delta\lambda$ . Consequently, one can write a following equation:

---

<sup>A1</sup> The corners or vertices of the feasible region

$$\left[ B^{-1} + \mu^* M \right]^T B^T M = A^T B^T M = 0 \leftrightarrow M(BA) = 0 \quad (\text{A.9})$$

where  $A \equiv B^{-1} + \mu^* M$  and  $B \equiv \nabla_{gg} P_{loss}^*$

Note that B matrix is symmetric since B is a Hessian matrix of loss, and consequently so are  $B^{-1}$  and A. From the definition of A matrix, one can find the inner product of A and LMP:

$$A\lambda^* = \left[ B^{-1} + \mu^* M \right] \lambda^* = B^{-1} \lambda^* + \mu^* M \lambda^* = B^{-1} \lambda^* \quad (\text{A.10})$$

Congestion makes the power system restricted in a certain way such that only certain patterns of perturbation in generation are allowed. Therefore, in this study, uncongested case and congested case will be discussed separately.

### Uncongested network

If there is no binding line constraint, the system is similar to networkless except loss. In the case, LMP is the sum of the system marginal cost of generation and delivery cost. Since no line constraint is binding, delivery cost is not high. Therefore, each price has similar value with each other. From the last expression in equation (A.9), one can find following relations for each column of the resulting matrix (BA):

$$M(ba)_j = 0 \quad \text{for } j = 1, \dots, n \quad (\text{A.11})$$

where ba is a column vector of BA matrix.

As was discussed earlier, M matrix has only one structural eigenvector which is parallel to LMP for an uncongested case. Consequently, all the columns of BA matrix must be parallel to the structural eigenvector which is also parallel to LMP. Therefore, all the columns of BA matrix are parallel to LMP, i.e.:

$$BA = \begin{bmatrix} \alpha_1 \lambda^* & \cdots & \alpha_n \lambda^* \end{bmatrix} = \lambda^{*n \times 1} \alpha^{1 \times n} \quad (\text{A.12})$$

where  $\alpha$  is a row vector whose elements are all proportionality constants of each column vector of BA matrix.

Since B is given and invertible matrix, one can rewrite equation (A.12) in a following way:

$$A = B^{-1} \lambda^{*n \times 1} \alpha^{1 \times n} = \delta^{n \times 1} \alpha^{1 \times n} \quad (\text{A.13})$$

where  $\delta = B^{-1} \lambda^*$ . Since A is symmetric,  $A_{ij} = A_{ji}$ , i.e.:

$$A_{ij} = \delta_i \alpha_j = A_{ji} = \delta_j \alpha_i \rightarrow \alpha_i = \left( \frac{\alpha_k}{\delta_k} \right) \delta_i \quad (\text{A.14})$$

Therefore,

$$A = \begin{bmatrix} \alpha_1 \delta & \cdots & \alpha_n \delta \end{bmatrix} = \left( \frac{\alpha_k}{\delta_k} \right) \delta \delta^T \quad (\text{A.15})$$

By using equation (A.10), one finds:

$$\begin{aligned} A \lambda^* &= \left( \frac{\alpha_k}{\delta_k} \right) \delta \delta^T \lambda^* = \left[ \left( \frac{\alpha_k}{\delta_k} \right) \delta^T \lambda^* \right] \delta = B^{-1} \lambda^* = \delta \\ \rightarrow \left( \frac{\alpha_k}{\delta_k} \right) &= \frac{1}{\delta^T \lambda^*} = \frac{1}{\lambda^{*T} B^{-1} \lambda^*} \end{aligned} \quad (\text{A.16})$$

From equations (A.15) and (A.16), A and M matrix can be found:

$$A = \frac{B^{-1} \lambda^* \lambda^{*T} B^{-1}}{\lambda^{*T} B^{-1} \lambda^*} \quad (\text{A.17})$$

$$M = \frac{B^{-1}}{\mu^*} \left( \frac{\lambda^* \lambda^{*T} B^{-1}}{\lambda^{*T} B^{-1} \lambda^*} - I \right) \quad (\text{A.18})$$

### Congested network

From equation (A.6.3), one finds

$$E \Delta g = EM \Delta \lambda = 0 \rightarrow EM = 0 \quad (\text{A.19})$$

Note that left hand side of arrow holds for all perturbation of LMP. Since LMP stays on the null space of M matrix, the null space of M is composed of LMP and row vectors of E matrix. From equation (A.9),  $A^T B^T M = ABM = 0$  since A and B are symmetric matrices. Consequently, each row vector of AB matrix lies on the null space of M matrix, i.e., each row vector of AB matrix is linear combination of  $e_j$  ( $j = 1, \dots, m'$ ) and  $\lambda^{*T}$  where  $e$  is a row vector of E matrix. Therefore, AB matrix can be expressed in terms of E and LMP in a following way:

$$\begin{aligned} AB &= \begin{pmatrix} \alpha_1^1 e_1 + \dots + \alpha_{m-1}^1 e_{m-1} + \alpha_m^1 \lambda^{*T} \\ \alpha_1^2 e_1 + \dots + \alpha_{m-1}^2 e_{m-1} + \alpha_m^2 \lambda^{*T} \\ \vdots \\ \alpha_1^n e_1 + \dots + \alpha_{m-1}^n e_{m-1} + \alpha_m^n \lambda^{*T} \end{pmatrix} = \begin{pmatrix} \alpha_1^1 & \dots & \alpha_m^1 \\ \alpha_1^2 & \dots & \alpha_m^2 \\ \vdots & \ddots & \vdots \\ \alpha_1^n & \dots & \alpha_m^n \end{pmatrix} \begin{pmatrix} e_1^{1 \times n} \\ \vdots \\ e_{m-1}^{1 \times n} \\ \lambda^{*T} \end{pmatrix} \\ &= \begin{bmatrix} \alpha_1^{m \times m} \\ \alpha_2^{(n-m) \times m} \end{bmatrix} \begin{pmatrix} E \\ \lambda^{*T} \end{pmatrix} = \begin{bmatrix} \alpha_1^{m \times m} \\ \alpha_2^{(n-m) \times m} \end{bmatrix} L \end{aligned} \quad (\text{A.20})$$

where  $\alpha$ 's stand for proportionality factors,  $m$  equals to  $m' + 1$ , and  $L$  represents an  $E$  matrix with one additional row of LMP.

By multiplying  $B^{-1}$  on both sides, one will get:

$$A = \begin{bmatrix} \alpha_1^{m \times m} \\ \alpha_2^{(n-m) \times m} \end{bmatrix} L B^{-1} = \begin{bmatrix} \alpha_1^{m \times m} \\ \alpha_2^{(n-m) \times m} \end{bmatrix} \begin{bmatrix} G_1^{m \times m} & G_2^{m \times (n-m)} \end{bmatrix} = \begin{pmatrix} \alpha_1 G_1 & \alpha_1 G_2 \\ \alpha_2 G_1 & \alpha_2 G_2 \end{pmatrix} \quad (\text{A.21})$$

where  $G$  is defined  $LB^{-1}$ .

Since  $A$  is symmetric, one can get:

$$(\alpha_1 G_1)^T = G_1^T \alpha_1^T = \alpha_1 G_1 \rightarrow \alpha_1^T = G_1^{-T} \alpha_1 G_1 \quad (\text{A.22.1})$$

$$(\alpha_1 G_2)^T = G_2^T \alpha_1^T = \alpha_2 G_1 \rightarrow \alpha_2 = G_2^T \alpha_1^T G_1^{-1} = G_2^T G_1^{-T} \alpha_1 \quad (\text{A.22.2})$$

Combining equations (A.21) and (A.22.2) gives:

$$A = \begin{pmatrix} \alpha_1 \\ G_2^T G_1^{-T} \alpha_1 \end{pmatrix} \begin{pmatrix} G_1 & G_2 \end{pmatrix} = G^T G_1^{-T} \alpha_1 G \quad (\text{A.23})$$

Note that  $G$  is known, then only unknown in equation (A.23) is  $\alpha_1$ .

By using equation (A.10), one finds:

$$A \lambda^* = G^T G_1^{-T} \alpha_1 G \lambda^* = B^{-1} \lambda^* \rightarrow I \lambda^* = B G^T G_1^{-T} \alpha_1 G \lambda^* \quad (\text{A.24})$$

Note that:

$$G\lambda^* = \begin{pmatrix} G_1 & G_2 \end{pmatrix} \begin{bmatrix} \lambda_1^{*m \times 1} \\ \lambda_2^{*(n-m) \times 1} \end{bmatrix} = G_1\lambda_1^* + G_2\lambda_2^* \quad (\text{A.25})$$

Let C be  $BG^T G_1^{-T}$ , then:

$$C = BG^T G_1^{-T} = \begin{bmatrix} B_1^{m \times n} \\ B_2^{(n-m) \times n} \end{bmatrix} G^T G_1^{-T} = \begin{bmatrix} C_1^{m \times m} \\ C_2^{(n-m) \times m} \end{bmatrix} \quad (\text{A.26})$$

Combining equations (A.24) and (A.26) gives:

$$\begin{pmatrix} \lambda_1^* \\ \lambda_2^* \end{pmatrix} = C\alpha_1 G\lambda^* = \begin{pmatrix} C_1\alpha_1 G\lambda^* \\ C_2\alpha_1 G\lambda^* \end{pmatrix} \rightarrow \lambda_2^* = C_2 C_1^{-1} \lambda_1^* \quad (\text{A.27})$$

Equation (A.27) shows that only m prices among n are independent and rest can be calculated from the m price by using network parameters.

One can also find price explicitly in a following way:

$$\lambda^* = \begin{pmatrix} \lambda_1^* \\ \lambda_2^* \end{pmatrix} = \begin{pmatrix} \lambda_1^* \\ C_2 C_1^{-1} \lambda_1^* \end{pmatrix} = CC_1^{-1} \lambda_1^* \quad (\text{A.28})$$

By substituting expressions for C's as given in equation (A.26), LMP is:

$$\begin{aligned} \lambda^* &= (BG^T G_1^{-T}) (B_1 G G_1^{-T})^{-1} \lambda_1^* = BG^T (B_1 G^T)^{-1} \lambda_1^* \\ &= B(LB^{-1})^T [B_1 (LB^{-1})^T]^{-1} \lambda_1^* = L^T (B_1 B^{-1} L^T)^{-1} \lambda_1^* \end{aligned} \quad (\text{A.29})$$

Equations (A.27) and (A.29) can be combined to lead to:

$$C_1\alpha_1 G\lambda^* = C_1\alpha_1 G [BG^T (B_1 G^T)^{-1} \lambda_1^*] = I\lambda_1^* \quad (\text{A.30})$$

Equation (A.30) is valid for all  $\lambda_1^*$ , which results in:



$$\alpha_1 = C_1^{-1} (B_1 G^T) (GBG^T)^{-1} = (B_1 G^T G_1^{-T})^{-1} (B_1 G^T) (GBG^T)^{-1} = G_1^T (GBG^T)^{-1} \quad (\text{A.31})$$

A and M matrix can be found by combining equations (A.23) and (A.31) in a following way:

$$\begin{aligned} A &= G^T G_1^{-T} \alpha_1 G = G^T (GBG^T)^{-1} G = (LB^{-1})^T \left[ (LB^{-1}) B (LB^{-1})^T \right]^{-1} (LB^{-1}) \\ &= B^{-1} L^T (LB^{-1} L^T)^{-1} LB^{-1} \end{aligned} \quad (\text{A.32})$$

$$M = \frac{B^{-1}}{\mu^*} \left[ L^T (LB^{-1} L^T)^{-1} LB^{-1} - I \right] \quad \text{where } L = \begin{pmatrix} E \\ \lambda^{*T} \end{pmatrix} \quad (\text{A.33})$$

M matrix can be calculated by using equations (A.18) and (A.33) with publicly available and predictable data such as LMP, B and PTDF matrix.

Market power is very closely related to M matrix since change in revenue according to change in price can be calculated in a following way:

$$\begin{aligned} \Delta r_i &= \Delta(\lambda_i g_i) = \lambda_i^* \Delta g_i + g_i^* \Delta \lambda_i = \lambda_i^* \left( \sum_j M_{ij} \Delta \lambda_j \right) + g_i^* \Delta \lambda_i \\ &= [Diag(\lambda_i^*) M \Delta \lambda]_i + [Diag(g_i^*) \Delta \lambda]_i \end{aligned} \quad (\text{A.34})$$

$$\Delta r = [Diag(\lambda_i^*) M + Diag(g_i^*)] \Delta \lambda \quad (\text{A.35})$$

If an agent owns multiple generators, then by using equation (A.35) it can find if it has market power as a group and furthermore can have a guideline of the way to exercise market power before submitting its offers.

## APPENDIX B

### ERROR MINIMIZATION WITH 2-NORM

A good weight factor distribution gives an estimate to the market providing which norm should be chosen. In this study, 2 norm is chosen. QR-factorization is a very stable way to solve LLS, where Q is an orthogonal matrix<sup>A2</sup> and R is upper triangular matrix<sup>A3</sup>.

$$\begin{aligned}
 \min \|A \cdot x - b\|_2 &= \min \|(Q \cdot R) \cdot x - I \cdot b\|_2 = \min \|(Q \cdot R) \cdot x - Q \cdot Q^T \cdot b\|_2 \\
 &= \min \|Q \cdot (R \cdot x - Q^T \cdot b)\|_2 = \min \|Q\|_2 \|R \cdot x - Q^T \cdot b\|_2 \\
 &= \min \|Q\|_2 \|R\|_2 \|x - R^{-1}(Q^T \cdot b)\|_2 \\
 &\leftrightarrow \min \|x - R^{-1} \cdot (Q^T \cdot b)\|_2
 \end{aligned} \tag{A.36}$$

When only n number of components exists in the set, non-zero elements in R matrix are n<sup>2</sup> and multiplying Q<sup>T</sup>b costs only m-by-n since the multiplication is only between matrix and vector. Beside the computational efficiency, orthogonal matrix Q could be well defined even for an ill-defined matrix.

Another approach is LU-factorization. When matrix A is m-by-n matrix with m greater than n, L is m-by-n and U is n-by-n matrix. While the diagonal element in L is ones, all the ill-defined property enters into U, i.e. there are r zeros in the diagonal of U matrix if r columns are a linear combination of (n - r) columns. Since r columns are dependent, there is only (n - r) information available which means that r variables in x vector cannot be uniquely defined. Note that one can arbitrarily assign values for

---

<sup>A2</sup> a matrix containing column vectors orthogonal with each other, i.e.,  $Q \cdot Q^T = Q^T \cdot Q = I$  where T stands for transpose and I is an identity matrix

<sup>A3</sup> a matrix that all the elements under the diagonal are zeros

undetermined variables without increasing error. From the properties of U matrix being an upper triangular matrix, the corresponding elements to the zero diagonal element in U matrix can be set to zero arbitrarily. Then the r columns in U matrix are meaningless to determine elements in x since the columns are multiplied with zeros. A reduced U matrix that is the U matrix where those r columns were deleted is well defined. Consequently, the LLS problem for the reduced U matrix and vectors x and  $b'$  ( $= L^{-1}(P^T b)$ ) yields a 2-norm minimizing weight factor distribution vector x.

$$\begin{aligned}
 \min \|A \cdot x - b\|_2 &= \min \|(L \cdot U) \cdot x - b\|_2 \\
 \leftrightarrow \min \|U \cdot x - L^{-1} \cdot b\|_2 & \tag{A.37} \\
 \leftrightarrow \min \|U_1 \cdot x_1 - (L^{-1} \cdot b)_1\|_2 &
 \end{aligned}$$

Figure A-1 illustrates the procedure described in equation (A.37) schematically. It should be noted that the above argument is only valid for a stationary system.

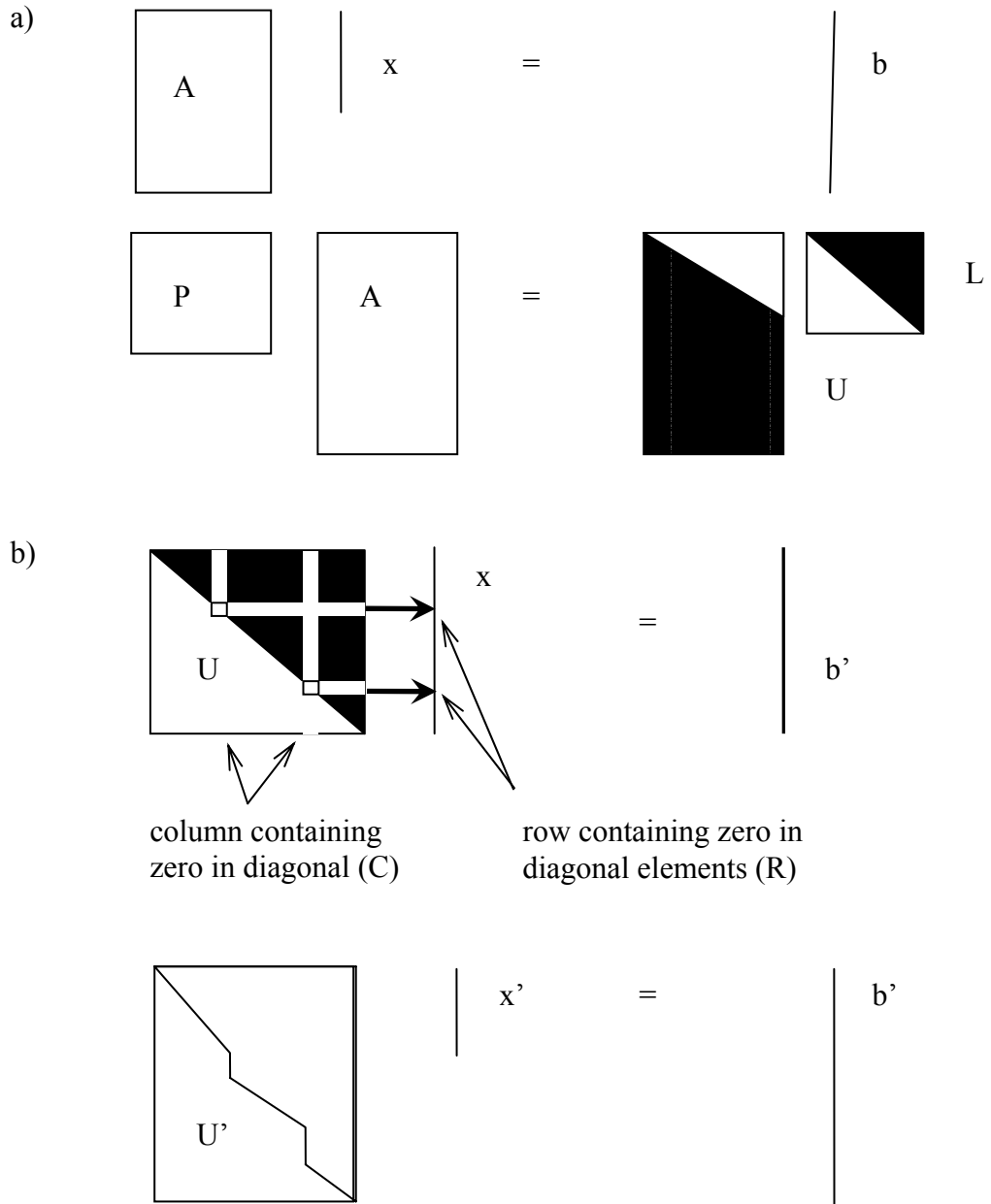


Figure A-1. A schematic diagram for explaining how to determine a weight factor distribution,  $x$ , a) by using traditional LU-factorization and b) by using LU-factorization where  $b' = L^{-1}(P^T b)$ . The thick arrows show where zeros could be assigned in the vector  $x$ , and eliminating  $R$  rows from  $U$  and the assigned elements from  $x$  yields  $U'$  and  $x'$ , respectively.

## APPENDIX C<sup>A4</sup>

### TRUST REGION METHOD

#### Trust Region Method for Unconstrained Minimization Problems

Trust region methods are widely and successfully used for unconstrained optimization process due to its strong convergence and fewer numbers of iterations. However, the cost of the linear algebra for the methods is higher. Consequently, trust region methods are effective on highly nonlinear problems of which function has high cost to evaluate. This method is recently proven to work successfully in solving problems to the large-scale setting.

When a function  $f$  is twice continuously differentiable, Taylor series expansion of  $f$  gives

$$f(x_k + s) = f(x_k) + \nabla f_k^T s + \frac{1}{2} s^T \nabla^2 f_k s + o(\|s\|^2) \quad (\text{A.38})$$

where  $o(x)$  stands for the quantity approaches zeros faster than  $x$  when  $x$  goes to zero. Consequently,  $\nabla f_k^T s + \frac{1}{2} s^T \nabla^2 f_k s$  equals to the change in  $f$ ,  $f(x_k + s) - f(x_k)$ , approximately around  $x_k \in \mathbb{R}^n$ . The trust region subproblem can be defined at  $x_k$ ;

$$\min \left\{ \nabla f_k^T s + \frac{1}{2} s^T \nabla^2 f_k s : \|s\|_2 \leq \Delta_k \right\} \quad (\text{A.39})$$

Note that equation (A.39) is a little bit different from general trust region subproblem in that 2-norm is used because 2-norm may allow an efficient global

---

<sup>A4</sup> Most part of Appendix II were taken from the textbook [T. F. Colman and A. Verma, "The Solution of Large-Scale Optimization Problems", Cornell University, Ithaca, NY 2003) 54-61]

solution. Equation (A.39) defines a trial step for sufficiently small  $\Delta_k$  and  $f(x_k + s_k) < f(x_k)$ . It is noteworthy that the subproblem is well defined regardless of  $\nabla^2 f_k$  enough not to assume that  $\nabla^2 f_k$  is positive definite<sup>A5</sup>. There are three different cases for  $\nabla^2 f_k$ . For a positive definite  $\nabla^2 f_k$ , the solution to the subproblem is the Newton step,  $-(\nabla^2 f_k)^{-1} \nabla f_k$  for a large value of  $\Delta_k$ . When the smallest eigenvalue of  $\nabla^2 f_k$  is negative, the solution  $s_k$  satisfies  $\|s_k\| = \Delta_k$ <sup>A6</sup>. If the smallest eigenvalue is zero, a (not unique) solution exists on the surface of n-ellipsoid. A general procedure of trust region method is following; solve equation (A.39) for trial step  $s_k$ , and calculate  $f(x_k + s_k)$ ,  $\nabla f_k^T s_k + 1/2 s_k^T \nabla^2 f_k s_k$  and  $[f(x_k + s_k) - f(x_k)] / [\nabla f_k^T s_k + 1/2 s_k^T \nabla^2 f_k s_k]$ , and then adjust the size of n-ellipsoid,  $\Delta_k$ ; for a large ratio,  $[f(x_k + s_k) - f(x_k)] / [\nabla f_k^T s_k + 1/2 s_k^T \nabla^2 f_k s_k]$ , decrease the size, and for a small ratio, increase the size, and otherwise, maintain the size. Repeat these procedures until stopping criteria is met. The constants to define the size of ratio and to decide how much increase or decrease are predetermined and do not change with the period k. The main advantage of the trust region method (less number of function evaluation) comes from updating algorithm: update  $x_{k+1} = x_k + s_k$  only for positive ratio<sup>A7</sup> (whenever moving by  $s_k$  decreases the value of f). Generally speaking, the ratio tells how well the solution to equation (A.39) predicts the real change in f; the higher value the ratio is, the better the performance is.

---

<sup>A5</sup> positive definite matrix means a matrix of which eigenvalues are all positive

<sup>A6</sup> if  $\|s_k\| < \Delta_k$ ,  $s_k$  is an unconstrained local minimizer of an indefinite quadratic function which is impossible

<sup>A7</sup> for non-positive ratio,  $f(x_k + s_k) \geq f(x_k)$  since  $\nabla f_k^T s_k + \frac{1}{2} s_k^T \nabla^2 f_k s_k$  is negative; note that  $s_k$  is the solution of the subproblem (equation (A.39)). Since equation (A.39) is minimization problem and zero is a trivial solution for equation (A.39) satisfying the constraint,  $\|s_k\| \leq \Delta_k$  when  $s_k = 0$ ,  $\nabla f_k^T s_k + \frac{1}{2} s_k^T \nabla^2 f_k s_k$  must be negative

Suppose there are  $s_*$  and  $\lambda_*$  satisfying following equations:

$$(H + \lambda I)s = -g \quad (\text{A.40})$$

$$(H + \lambda I) \text{ is positive semi-definite} \quad (\text{A.41})$$

$$\|s\|_2 \leq \Delta \quad (\text{A.42})$$

$$(\|s\|_2 - \Delta)\lambda = 0 \quad (\text{A.43})$$

From equations (A.40) and (A.41),  $s_*$  is the unconstrained minimizer of the quadratic function  $g^T s + \frac{1}{2} s^T (H + \lambda_* I) s$ . Consequently, one can find a following inequality:

$$g^T s_* + \frac{1}{2} s_*^T H s_* \leq g^T s + \frac{1}{2} s^T H s + \frac{\lambda_*}{2} (\|s\|_2^2 - \|s_*\|_2^2) \quad (\text{A.44})$$

For all feasible  $s$ ,  $\lambda_* (\|s\|_2^2 - \|s_*\|_2^2) / 2$  is non-positive<sup>A8</sup>, i.e.,  $s_*$  is the global solution to the subproblem. Since  $s_*$  is the global solution, applying equation (A.40) in equation (A.44) allows:

$$\begin{aligned} & g^T (s - s_*) + \frac{1}{2} s^T H s - \frac{1}{2} s_*^T H s_* + \frac{\lambda_*}{2} (\|s\|_2^2 - \|s_*\|_2^2) \\ &= g^T (s - s_*) + \frac{1}{2} s^T H s - \frac{1}{2} s^T H s_* + \frac{1}{2} s^T H s_* - \frac{1}{2} s_*^T H s_* \\ & \quad + \frac{\lambda_*}{2} (s^T s - s^T s_* + s_*^T s - s_*^T s_*) + \frac{\lambda_*}{2} (s^T s_* - s_*^T s) \geq 0 \end{aligned} \quad (\text{A.45})$$

Since  $s^T H s_*$  and  $s_*^T s_*$  is a scalar, they equal to their transpose ( $(s^T H s_*)^T = s_*^T H^T s = s_*^T H s$ <sup>A9</sup> and  $(s_*^T s_*)^T = s_*^T s_*$ ). By the same argument,  $[(s^T - s_*^T) H s_*]^T = s_*^T H^T (s - s_*) = s_*^T H (s - s_*)$ . Consequently, one obtains:

---

<sup>A8</sup> from equation (A.43),  $\lambda_* = 0$  or  $\|s_*\|_2 = \Delta$ , and  $\|s\|_2 \leq \Delta$  for all feasible  $s$  from equation (A.42), consequently,  $\frac{\lambda_*}{2} (\|s\|_2^2 - \|s_*\|_2^2)$  is non-positive

<sup>A9</sup>  $H$  is a Hessian matrix which is symmetric, i.e.,  $H^T = H$

$$\begin{aligned}
& g^T (s - s_*) + \frac{1}{2} s^T H s - \frac{1}{2} s^T H s_* + \frac{1}{2} s_*^T H s - \frac{1}{2} s_*^T H s_* + \frac{\lambda_*}{2} (s^T + s_*^T) (s - s_*) \\
& = \left[ g^T + \frac{1}{2} s^T H + \frac{1}{2} s_*^T H + \frac{\lambda_*}{2} (s + s_*)^T \right] (s - s_*) \geq 0
\end{aligned} \tag{A.46}$$

From equation (A.40), the expression for the transpose of  $g$  is obtained;  $g^T = -[(H + \lambda I)s_*]^T = -s_*^T (H^T + \lambda_*^T I^T) = -s_*^T (H + \lambda_* I)$ . Therefore, an inequality is derived from equation (A.46) in a following way:

$$\begin{aligned}
& \left[ g^T + \frac{1}{2} s^T H + \frac{1}{2} s_*^T H + \frac{\lambda_*}{2} (s + s_*)^T \right] (s - s_*) \\
& = \left[ -s_*^T (H + \lambda_* I) + \frac{1}{2} (s^T + s_*^T) H + \frac{\lambda_*}{2} (s + s_*)^T \right] (s - s_*) \\
& = \frac{1}{2} (s - s_*)^T (H + \lambda_* I) (s - s_*) \geq 0
\end{aligned} \tag{A.47}$$

Equation (A.47) implies that the matrix  $H + \lambda_* I$  is positive semi-definite.<sup>A10</sup>

Suppose  $H = V \Lambda V^T$  where the columns of  $V$  are orthonormal eigenvectors of  $H$ <sup>A11</sup>.

Then, equation (A.40) and substitution of  $\bar{s} = V^T s$  allow:

---

<sup>A10</sup> from [D. Sorenson, "Trust Region Methods for Unconstrained Optimization", SIAM J. Numer. Anal., 19 (1982) 409 – 426]

<sup>A11</sup> for a symmetric matrix  $H$ ,  $Hv = \lambda v \leftrightarrow \bar{v}^T H v = \lambda \bar{v}^T v = \lambda \sum_{i=1}^n |v_i|^2 \leftrightarrow \lambda = \bar{\lambda}$  ( $\lambda$  is real), then there is a set of orthonormal eigenvectors of  $H$ , i.e.,  $q_i$  for  $i = 1 \sim n$  such that  $Aq_i = \lambda_i q_i, q_i^T q_j = \delta_{ij}$ ; in a matrix form, there is an orthogonal  $V$  such that  $V^{-1} H V = V^T H V = \Lambda \leftrightarrow H = V \Lambda V^T$  where  $\Lambda$  is a diagonal matrix of which diagonal elements are the eigenvalues of the matrix  $H$



$$\begin{aligned} (H + \lambda I)s &= (H + \lambda I)V^T \bar{s} = V(\Lambda + \lambda I)V^T V\bar{s} = V(\Lambda + \lambda I)\bar{s} = -g \\ \leftrightarrow \alpha &\equiv (\Lambda + \lambda I)\bar{s} = -V^T g \end{aligned} \quad (\text{A.48})$$

Since  $H + \lambda I$  is a positive semi-definite matrix by equation (A.41), all the  $\lambda$  must be bigger than or equal to the smallest eigenvalue of  $H$ ,  $\lambda_1$ . Consequently, all vectors satisfying equations (A.40) and (A.41) are expressed in a following way:

$$s = \sum_{\{i:\lambda_i+\lambda>0\}} \left( \frac{\alpha_i}{\lambda_i + \lambda} \right) v_i + \sum_{\{j:\lambda_j+\lambda=0\}} \beta_j v_j \quad (\text{A.49})$$

By assuming the form for  $s$  is given in equation (A.49), setting  $\|s\| = \Delta$  gives an algorithm to find a trial step<sup>A12</sup>. There are different cases depending on the smallest eigenvalue of  $H$  ( $\lambda_1$ ) for obtaining expression for  $s$ . For positive  $\lambda_1$ , if the Newton step is inside the  $n$ -ellipsoid,  $\|H^{-1}g\| \leq \Delta$ , the optimal solution is the Newton step,  $s_* = -H^{-1}g$  and  $\lambda_* = 0$ , otherwise,  $s(\lambda) = \sum_{i=1}^n \left( \frac{\alpha_i}{\lambda_i + \lambda} \right) v_i$  for non-negative  $\lambda$ <sup>A13</sup>. For

non-positive  $\lambda_1$ , there are two different cases depending on  $\alpha$  (when denominator in equation (A.49) equals to zero),  $\alpha_i$  is zero or it is not. If  $\alpha_i$  is zero, then set  $s(\lambda) = \sum_{i=1}^n \left( \frac{\alpha_i}{\lambda_i + \lambda} \right) v_i$  leading to one solution to  $\|s\| = \Delta$ <sup>A14</sup>. If  $\alpha_i$  is not zero, the

expression for  $s(\lambda)$  does not hold since it diverges at  $\lambda = -\lambda_1$ . To make use of general

---

<sup>A12</sup> note that if  $\|s\| \neq \Delta$ ,  $\lambda = 0$  by equation (A.33) and  $\|s\| < \Delta$  by equation (A.32) which gives a trivial solution

<sup>A13</sup> note that  $\|s(\lambda)\|$  approaches zero as  $\lambda$  diverges

<sup>A14</sup>  $\lim_{\lambda \rightarrow -\lambda^+} \|s(\lambda)\| = \lim_{\lambda \rightarrow -\lambda^+} \left\| \sum_{i=1}^n \left( \frac{\alpha_i}{\lambda_i + \lambda} \right) v_i \right\| \rightarrow \infty$ ,  $\lim_{\lambda \rightarrow \infty} \|s(\lambda)\| = \lim_{\lambda \rightarrow \infty} \left\| \sum_{i=1}^n \left( \frac{\alpha_i}{\lambda_i + \lambda} \right) v_i \right\| \rightarrow 0$  and

the convexity of  $\|s(\lambda)\|$  imply that  $\|s(\lambda)\|$  intersects  $\Delta$  in exactly one place for  $\lambda > -\lambda_1$

form of  $s$ , equation (A.49),  $s_1(\lambda)$  is defined as  $s_1(\lambda) = \sum_{\{i:\lambda_i+\lambda>0\}} \left( \frac{\alpha_i}{\lambda_i+\lambda} \right) v_i$ , and then if

$\|s_1(-\lambda_1)\| = \left\| \sum_{\{i:\lambda_i>\lambda_1\}} \left( \frac{\alpha_i}{\lambda_i-\lambda_1} \right) v_i \right\| \geq \Delta$ , there exist  $\lambda$  satisfying  $\|s\| = \Delta$  then

$s(\lambda) = s_1(\lambda) = \sum_{\{i:\lambda_i+\lambda>0\}} \left( \frac{\alpha_i}{\lambda_i+\lambda} \right) v_i$ , otherwise,  $s(\lambda) = \sum_{\{i:\lambda_i>\lambda_1\}} \left( \frac{\alpha_i}{\lambda_i-\lambda_1} \right) v_i + \sum_{\{j:\lambda_j+\lambda=0\}} \beta_j v_j$

with a proper choice<sup>A15</sup> of  $\beta$  to satisfy  $\|s\| = \Delta$ .

### Minimization Problems with Box Constraints<sup>A16</sup>

As was mentioned in chapter two, an offer equation has two short term variables bounded with box constraints. Trust region method is described for unconstrained problems here. When constraints have been added to a problem, finding a solution gets more difficult. There was an approach to solve such nonlinear problems by using interior trust region method, which gives strong convergence.

The problem considered here is following:

$$\min_{x \in R^n} f(x) \text{ subject to } l \leq x \leq u \quad (\text{A.50})$$

---

<sup>A15</sup>  $\sum_i \beta_i^2 = \Delta^2 - \left\| \sum_{\{i:\lambda_i>\lambda_1\}} \left( \frac{\alpha_i}{\lambda_i-\lambda_1} \right) v_i \right\|^2$  – from orthogonality – and  $\lambda_* = -\lambda_1$

<sup>A16</sup> Most part taken from [T. F. Coleman and Y. Li, “An Interior Trust Region Approach for Nonlinear Minimization Subject to Bounds”, SIAM J. Optimization, 6 (1998) 418 – 445]

where  $l$  and  $u$  are lower and upper limits for  $x$ , and the objective function  $f$  is the negative value of earning.

Among feasible set,  $\text{int}(F)$  is defined as  $\text{int}(F) \equiv \{x : l < x < u\}$  which is whole feasible region excluding the boundary. Let define a vector  $v(x) \in \mathbb{R}^n$  and a diagonal matrix  $\text{Diag}(x)$  for each component  $1 \leq i \leq n$ ;

$$v_i \equiv \begin{cases} x_i - u_i & \text{if } g_i < 0 \text{ and } u_i < \infty \\ x_i - l_i & \text{if } g_i \geq 0 \text{ and } l_i > -\infty \\ -1 & \text{if } g_i < 0 \text{ and } u_i = \infty \\ 1 & \text{if } g_i \geq 0 \text{ and } l_i = -\infty \end{cases} \quad (\text{A.51})$$

$$\text{Diag}(x) \equiv \text{diag} \left( |v(x)|^{-\frac{1}{2}} \right)$$

where  $g$  is the first derivative of  $f(x)$ .

By using the definitions, the first-order necessary conditions<sup>A17</sup> for a local minimizer  $x^*$  can be expressed in a following way:

$$\begin{cases} g_{*i} = 0 & \text{if } l_i < x_{*i} < u_i \\ g_{*i} \leq 0 & \text{if } x_{*i} = u_i \Leftrightarrow \text{Diag}(x)^{-2} g(x) = 0 \\ g_{*i} \geq 0 & \text{if } x_{*i} = l_i \end{cases} \quad (\text{A.52})$$

By the definition of  $\text{Diag}(x)$ , the points where  $v_i$  equals to zero must be avoided. It can be easily done by letting  $x$  to be in  $\text{int}(F)$ . If  $x$  is in  $\text{int}(F)$ , one can find a Newton step satisfying equation (A.52):

$$\left[ \text{Diag}_{g_k}^{-2} \nabla^2 f(x_k) + \text{diag}(g_k) J_k^v \right] d_k = -\text{Diag}_{g_k}^{-2} g_k \quad (\text{A.53})$$

---

<sup>A17</sup> for an continuously differentiable function  $f$  on an open set,  $\text{Diag} \subseteq \mathbb{R}^n$ , a local minimizer  $x^*$  satisfies  $\nabla f(x_*) = 0$

where  $J^v$  is the Jacobian matrix of  $|v(x)|$ .

Let the  $i^{\text{th}}$  row of  $J^v$  set to be zero, and then all the points are differentiable if all the elements of the vector  $g_k$  since  $v_i$  is not zero for  $x$  inside  $\text{int}(F)$ . Consequently, for the problems with finite constraints,  $J^v = \text{diag}[\text{sign}(g)]$ . Coleman et al<sup>A18</sup> developed a quadratic model:

$$\psi_k(s) \equiv g_k^T s + \frac{1}{2} s^T T_k s \quad (\text{A.54})$$

where  $T_k \equiv H_k + \text{Diag}_k \text{diag}(g_k) J_k^v \text{Diag}_k$

The trust region subproblem with constraints is;

$$\min_{s \in R^n} \{ \psi_k(s) : \|\text{Diag}_k s\| \leq \Delta_k \} \quad (\text{A.55})$$

By substituting variables in equation (A.54), one can modify equation (A.55);

$$\begin{aligned} \psi_k(s) &\equiv g_k^T s + \frac{1}{2} s^T T_k s \\ &= (g_k^T \text{Diag}_k^{-1}) (\text{Diag}_k s) + \frac{1}{2} (s^T \text{Diag}_k) (\text{Diag}_k^{-1} T_k \text{Diag}_k^{-1}) (\text{Diag}_k s) \\ &= (\text{Diag}_k^{-1} g_k)^T (\text{Diag}_k s) + \frac{1}{2} (\text{Diag}_k s)^T (\text{Diag}_k^{-1} T_k \text{Diag}_k^{-1}) (\text{Diag}_k s) \\ &= \hat{g}_k^T \hat{s} + \frac{1}{2} \hat{s}^T \hat{T}_k \hat{s} \equiv \hat{\psi}_k(\hat{s}) \end{aligned} \quad (\text{A.56})$$

$$\hat{g}_k = \text{Diag}_k^{-1} g_k = \text{diag}\left(|v_k|^{\frac{1}{2}}\right) g_k, \quad \hat{s} = \text{Diag}_k s \quad (\text{A.57})$$

where

$$\hat{T}_k = \text{Diag}_k^{-1} T_k \text{Diag}_k^{-1} = \text{diag}\left(|v_k|^{\frac{1}{2}}\right) H_k \text{diag}\left(|v_k|^{\frac{1}{2}}\right) + \text{diag}(g_k) J_k^v$$

---

<sup>A18</sup> T. F. Coleman and Y. Li, "On the Convergence of Reflective Newton Methods for Large-Scale Nonlinear Minimization Subject to Bounds", Math. Programming, 67(1994) 189 - 224

Consequently, one can write a trust region subproblem in a following way, which is the same form as that for unconstrained problem:

$$\min_{\hat{s} \in R^n} \{ \hat{\psi}_k(\hat{s}) : \|\hat{s}\| \leq \Delta_k \} \quad (\text{A.58})$$

A solution to equation (A.58) gives a trial step for the trust region method. Let  $d_k$  be a trial step obtained from the solution to equation (A.58). Since the control variable  $x$  is constrained,  $x$  needs to be in the boundary; there is bound for a step-size

$$\alpha_k \equiv \min \left\{ \max \left[ \frac{l_i - x_{ki}}{d_{ki}}, \frac{u_i - x_{ki}}{d_{ki}} \right] : 1 \leq i \leq n \right\} \quad (\text{A.59})$$

The minimum value of  $\psi_k(s)$  along the direction  $d_k$  within the trust region is

$$\psi_k^*(d_k) = \psi_k(\tau_k^* d_k) \equiv \min \{ \psi_k(\tau d_k) : \|\tau \text{Diag}_k d_k\| \leq \Delta_k \text{ and } x_k + \tau d_k \in F \} \quad (\text{A.60})$$

In order to guarantee strict feasibility ( $x \in \text{int}(F)$ ), a new step obtained from  $d_k$  with step back  $\theta_k$ <sup>A19</sup> is defined:

$$\alpha_k^*(d_k) \equiv \theta_k \tau_k^* d_k \quad (\text{A.61})$$

Similar to unconstrained problem, trial step is taken only under following circumstance in order to make sure that enough value of function  $f$  is reduced if the step taken:

---

<sup>A19</sup> if a trial vector leads to a point on the boundary of constraints, step back makes the step take partial movement along the trial step, i.e.,

$\theta_k \in [\theta_l, 1)$ ,  $\theta_k - 1 = O(\|d_k\|)$  and  $\theta_k = 1$  for  $x_k + \tau_k^* d_k \in \text{int}(F)$

$$\rho_k^f = \frac{f(x_k + s_k) - f(x_k) + \frac{1}{2} s_k^T \text{Diag}_k \text{diag}(g_k) J_k^v \text{Diag}_k s_k}{\psi_k(s_k)} > \mu \quad (\text{A.62})$$

where  $\mu$  is a positive constant.

For significant reduction of  $\psi_k(s)$ , Coleman et al<sup>A20</sup> proposed to use a step along the scaled steepest descent direction and to take the step only when the value of  $\psi_k(s)$  is significantly decreased:

$$\rho_k^c = \frac{\psi_k(s_k)}{\psi_k^*[-\text{Diag}_k^{-2} g_k]} > \beta \quad (\text{A.63})$$

where  $\beta$  is a positive constant

Only a trial step satisfying equations (A.62) and (A.63) will be taken, i.e., double-trust region method. The algorithm is following; Assign positive constants quantities defined in unconstrained problems and  $\mu > 0, \beta < \eta < 1$  and  $x_0 \in \text{int}(F)$ . At  $k^{\text{th}}$  step, Compute  $f(x_k), g_k, H_k$  and  $\text{Diag}_k \text{diag}(g_k) J_k^v \text{Diag}_k$  to define  $\psi_k(s) = g_k^T s + \frac{1}{2} s^T T_k s$ , and then find a solution to equation (A.55) ( $p_k$ ). With the solution calculate following quantities:

$$\begin{aligned} s_k &= \alpha_k^* [p_k], \rho_k^c = \frac{\psi_k(s_k)}{\psi_k^*[-\text{Diag}_k^{-2} g_k]}, \rho_k^f \\ &= \frac{f(x_k + s_k) - f(x_k) + \frac{1}{2} s_k^T \text{Diag}_k \text{diag}(g_k) J_k^v \text{Diag}_k s_k}{\psi_k(s_k)} \end{aligned} \quad (\text{A.64})$$

---

<sup>A20</sup> T. F. Coleman and Y. Li, "An Interior Trust Region Approach for Nonlinear Minimization Subject to Bounds", SIAM J. Optimization, 6 (1998) 418 - 445

Only for a step satisfying equations (A.62) and (A.63) is taken;  $x_{k+1} = x_k + s_k$ .  
 Finally choose the size ( $\Delta_{k+1}$ ) of the n-ellipsoidal trust region in a following way for  
 $0 < \gamma_1 < 1 < \gamma_2$ :

$$\Delta_{k+1} \in \begin{cases} (0, \gamma_1 \Delta_k] & \text{if } \rho_k^f \leq \mu \text{ or } \rho_k^c \leq \beta \\ [\gamma_1 \Delta_k, \Delta_k] & \text{if } \rho_k^f \in (\mu, \eta) \\ [\Delta_k, \gamma_2 \Delta_k] & \text{if } \rho_k^f \geq \eta \text{ and } \rho_k^c \geq \eta \\ [\gamma_1 \Delta_k, \Delta_k] & \text{if } \rho_k^f \geq \eta \text{ and } \beta < \rho_k^c < \eta \\ (0, \gamma_1 \Delta_k] & \text{if } \rho_k^f \geq \eta \text{ and } \rho_k^c \geq \beta \end{cases} \quad (\text{A.65})$$

Then repeat these procedures until stopping criteria is met.

## APPENDIX D

### CHAOS AND NONLINEAR DYNAMICS

#### Lorenz equation

Lorenz introduced an equation (so called Lorenz equation<sup>A21</sup>) of which solution settles down to a complicated set in phase space as shown in Figure A-2. The complex geometric shape with fine structure at arbitrarily small scale is referred to as fractals. When a small part of the shape is magnified, it shows reminiscent feature of the whole. The Cantor set is one of most famous examples showing self-similarity. Figure A-3 illustrates the way how to construct the Cantor set. When a small part of the Cantor set is taken and magnified, the part reproduces the whole regardless of the place where the part is originally located. The Cantor set is made from a line, closed interval of [0, 1]. It is interesting to perform any measurement on the set: usually a physical measurement on 1 dimensional space is length. To calculate the length of Cantor set, it is more convenient to calculate the sum of length of the parts taken and then to subtract the sum from the length of the original interval, unity. The sum of the length of left over parts is

$$\frac{1}{3} + \frac{2}{9} + \frac{4}{27} + \frac{8}{81} + \dots = \frac{1}{3} \left[ 1 + \frac{2}{3} + \left(\frac{2}{3}\right)^2 + \left(\frac{2}{3}\right)^3 + \dots \right] = \frac{1}{3} \frac{1}{1 - \frac{2}{3}} = 1.$$

---


$$\begin{aligned} \left(\frac{\partial x}{\partial t}\right)_{y,z} &= \sigma(y - x) \\ \text{A21} \quad \left(\frac{\partial y}{\partial t}\right)_{z,x} &= rx - y - xz, \text{ where } \sigma, r \text{ and } b \text{ are all positive parameters from Ref. [31]} \\ \left(\frac{\partial z}{\partial t}\right)_{x,y} &= xy - bz \end{aligned}$$



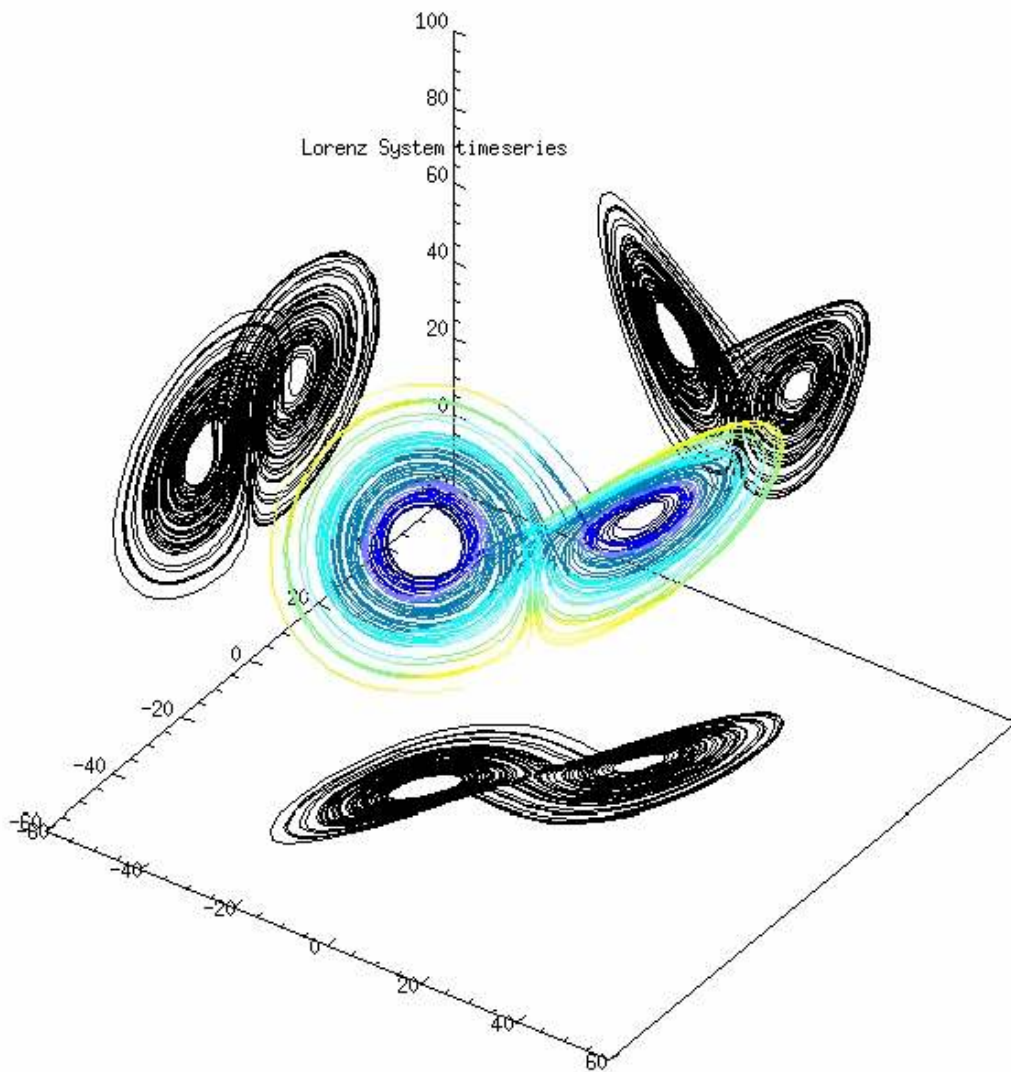


Figure A-2. Solution of the Lorenz equation (in color) and xy, yz and zx two-dimensional projections which show artifact crosses

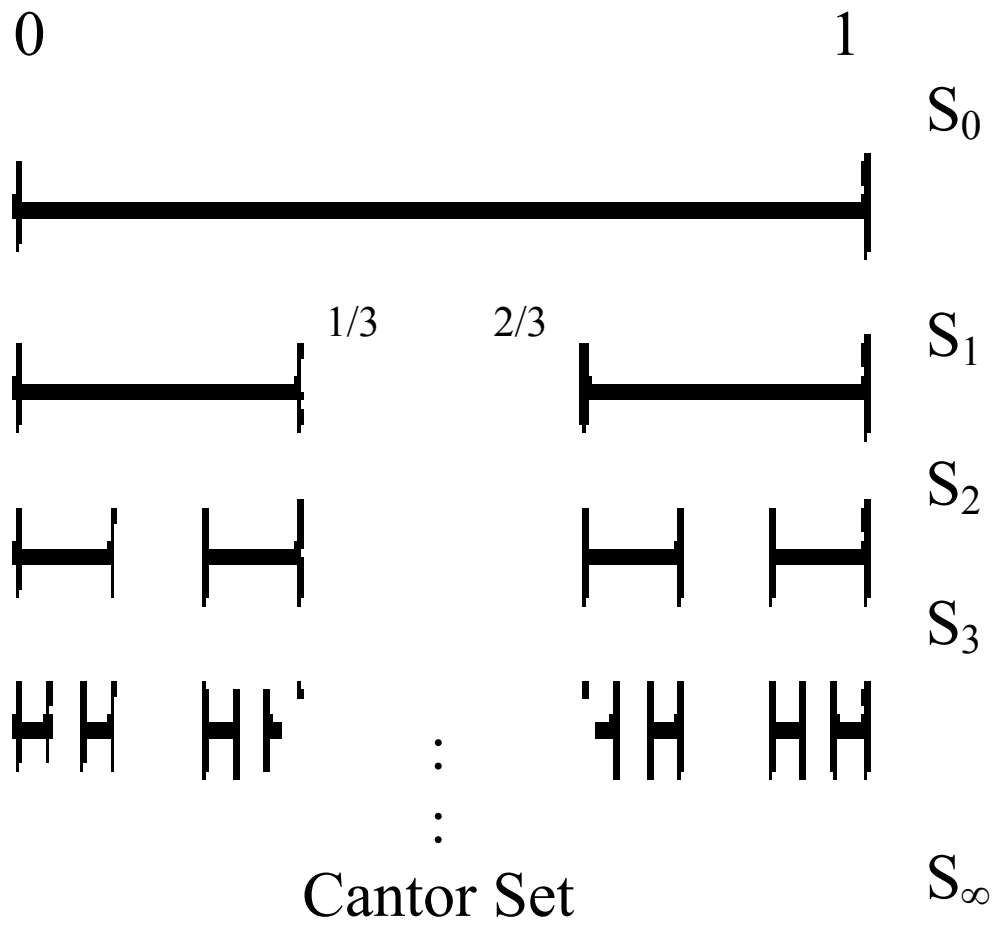


Figure A-3. Start with the closed interval  $S_0, [0, 1]$ , and remove the open middle third resulting in closed interval  $S_1$ . The same procedure is kept performed to produce  $S_2, S_3$  and so on. The limiting set  $S_\infty$  is the Cantor Set

Consequently, the length of the Cantor set is zero which might imply a line with no length. One may find a contradiction since the set was supposed to be a line. The problem in measuring anything in fractals is not confined to 1 dimension. To see the problem in higher dimension, consider the von Koch curve (Figure A-4). The length of the von Koch curve can be calculated since the length increases  $4/3$  in every step. As the number of step diverges, the length diverges also;  $(4/3)^n \rightarrow \infty$  as  $n \rightarrow \infty$ , but the curve does not cover the whole surface. Therefore, the von Koch curve is infinitely long curve confined to limited area. Note that the curve is not 2 dimensional object. This puzzle could be understood when the dimension of the Cantor set is not 1 and that of the von Koch curve is not 2. It is noteworthy that the dimensions are 0.63 and 1.26, respectively which are non-integer. Since the Cantor set contains infinitely many points but not many enough to form 1 dimension, the length is zero. To describe fractals correctly, dimension need to be defined in a following way; the minimum number of coordinates needed to describe every points in the set. This definition provides an enumeration of characteristics related to fractals (similarity dimension). Suppose that a self-similar set is composed of  $m$  copies of itself scaled down by a factor of  $r$ . Then the similarity dimension is defined in a following way:

$$d = \frac{\log m}{\log r} \quad (\text{A.66})$$

Equation (A.66) is convenient to define dimension of fractals with self-similarity. However, self-similarity is difficult to define for objects in real life. To deal with fractals with not evident self-similarity, generalized definition is needed like box dimension as was proposed by Falconer<sup>A22</sup>. Let  $S$  be a subset of  $d$ -dimensional space,

---

<sup>A22</sup> K. Falconer, "Fractal Geometry: Mathematical Foundations and Applications", Wiley, Chichester, England (1990)

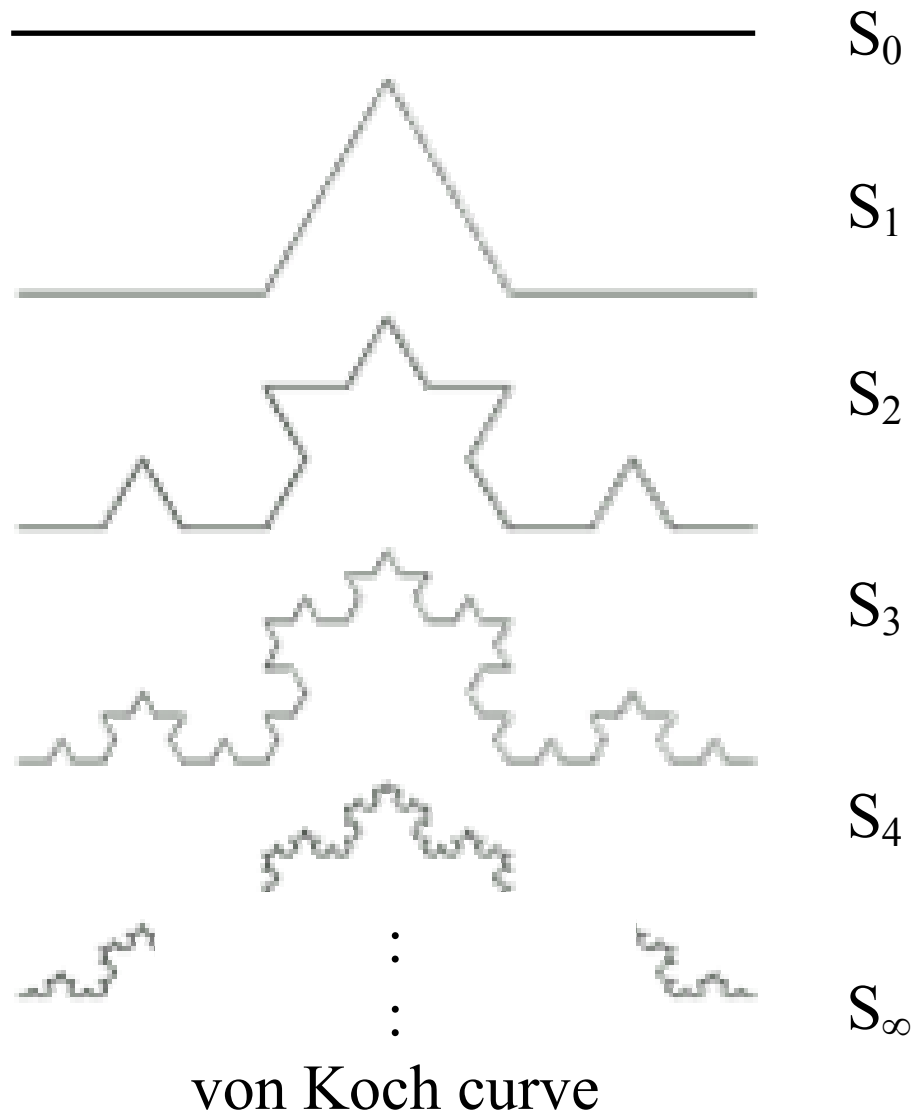


Figure A-4. Start with a line segment  $S_0$ ,  $[0, 1]$ , and delete the middle third and replace with the other two sides of an equilateral triangle,  $S_1$ . Then repeat the same step to generate  $S_2$ ,  $S_3$  and so on. The limiting set  $S_\infty$  is the von Koch curve

and  $N(\varepsilon)$  be the minimum number of  $d$ -dimensional cubes of side  $\varepsilon$  needed to cover  $S$ . As  $\varepsilon$  decreases, more  $d$ -dimensional cubes are required. The box dimension is defined in a following way:

$$d = \lim_{\varepsilon \rightarrow 0} \frac{\log N(\varepsilon)}{\log(1/\varepsilon)} \quad (\text{A67})$$

To see how it can be used for quantifying fractals in a real life, consider the length of the coast of Norway shown in Fig. A-5. There can be many ways to define the length of the coast, but it is impossible to measure when all the small interfaces between water and sand grain is considered. A good way is shown in Figure A-5: count the number of 2-dimensional box to cover whole coast as a function of the length of one side of the square. As was shown in the 2<sup>nd</sup> graph of Figure A-5, the coast of Norway shows a linear relationship with dimension of 1.52.

The dimensions discussed before are convenient to define static fractals, but not applicable to the chaotic system settling down to a strange attractor<sup>A23</sup> in phase space. Practical way for describing a dynamic system, a pointwise dimension is introduced. For a fixed point  $x$ , define  $N_x(\varepsilon)$  to be the number of points inside a ball of radius  $\varepsilon$  around  $x$ . Most of points in the ball come from later parts that just happen to pass close to  $x$ , and they are unrelated to the immediate portion of the trajectory through  $x$ .  $N_x(\varepsilon) \propto \varepsilon^d$  where  $d$  stands for the pointwise dimension at  $x$ .

$$d = \lim_{\varepsilon \rightarrow 0} \frac{\log N_x(\varepsilon)}{\log \varepsilon} \quad (\text{A.68})$$

---

<sup>A23</sup> an attractor that exhibits sensitive dependence on initial condition

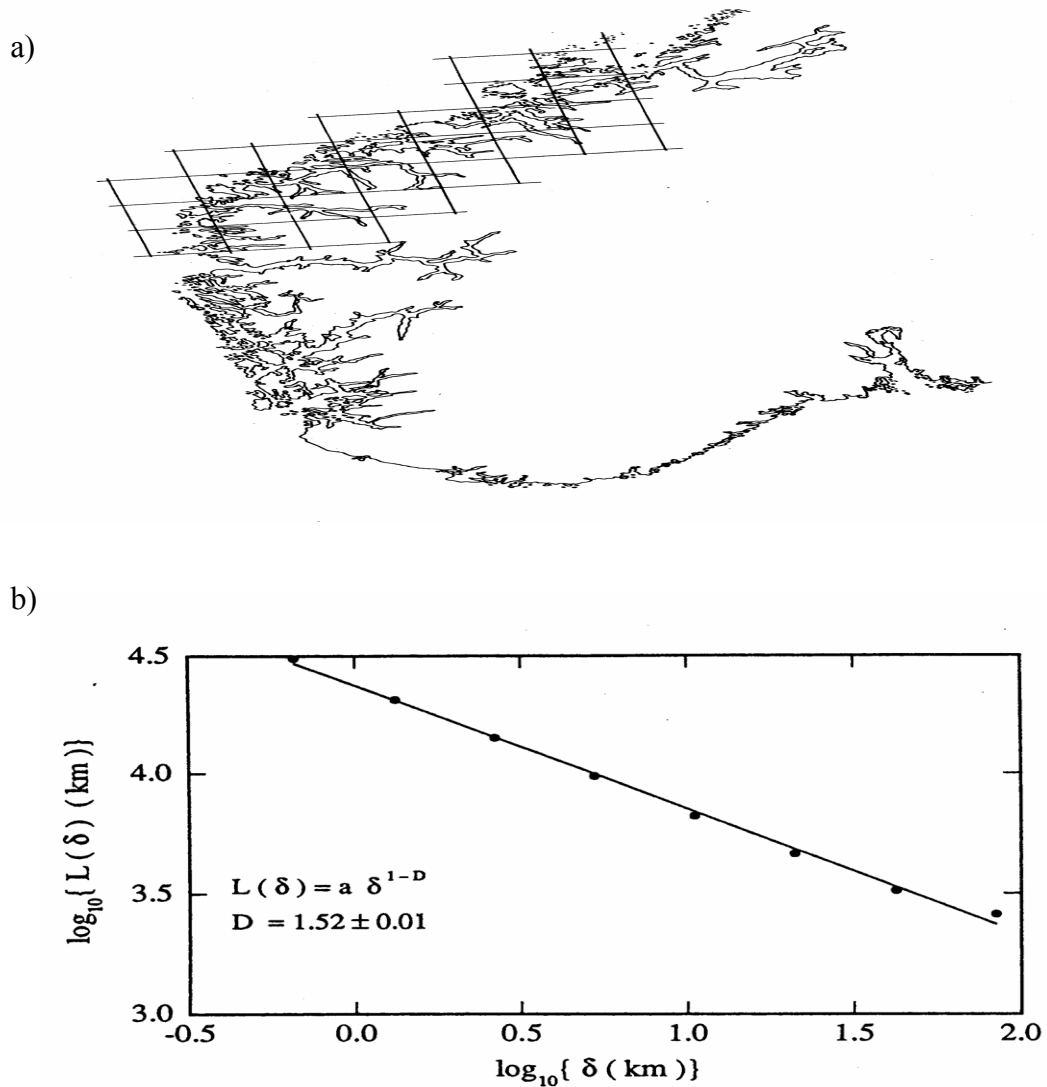


Figure A-5. a) The coast of the southern part of Norway. The square grid indicated has a spacing of  $\delta \sim 50$  km (taken from the Figure 2. 1 of [J. Feder, "Fractals", Plenum Press, New York and London (1998)]) and b) The measured length of the coastline shown in Figure A-5, as a function of the size  $\delta$  of the  $\delta \times \delta$  squares used to cover the coastline on the map. The straight line in this log-log plot corresponds to the relation  $L(\delta) = a\delta^{1-D}$ ;  $L$ ,  $\delta$  and  $D$  correspond to  $N$ ,  $\varepsilon$  and  $d$  in equation (A.67)

The pointwise dimension may not be a global quantity since it can depend on  $x$ . Furthermore, there are many practical applications where the geometric object has to be reconstructed from a finite sample of data points with errors. In such cases, correlation dimension is most widely used. As a system evolves for a long time, one can obtain a set of many points  $\{x_i, i = 1, \dots, n\}$  on a phase space. Grassberger and Procaccia proposed a way to evaluate dimensions like correlation dimension<sup>A24</sup>. For an overall dimension, the  $x$ -dependent  $N_x(\varepsilon)$  can be averaged in a following way;

$$C(\varepsilon) \equiv \frac{2}{N(N-1)} \sum_{i=1}^N \sum_{j=i+1}^N u(\varepsilon - \|x_i - x_j\|) \quad (\text{A.69})$$

where  $u$  stands for a unit step function.

The correlation dimension can be derived from an empirical relationship between correlation sum,  $C(\varepsilon)$ , and  $\varepsilon$ ;  $C(\varepsilon) \propto \varepsilon^d$  where  $d$  is the correlation dimension. Consequently, one can calculate the correlation dimension in the following way:

$$d = \frac{d \log[C(\varepsilon)]}{d \log \varepsilon} \quad (\text{A.70})$$

The correlation dimension involves an invariant measure supported on a fractal, not just fractal itself, i.e., it takes into account of the density of points on the attractor resulting in differing from the box dimension by weighing all occupied box equally regardless of the number of points. If equation (A.70) were valid for whole range of  $\varepsilon$ , there should be a straight line in  $\log C(\varepsilon)$  vs.  $\log \varepsilon$  - slope  $d$ . In most practical cases, the power law holds only over an intermediate range. The curve saturates at large

---

<sup>A24</sup> Grassberger, P., and Procaccia, I. "Measuring the strangeness of strange attractors", *Physica D* 9 (1983) 189

values of  $\varepsilon$  because the balls with radius of  $\varepsilon$  surround the whole attractor and therefore  $N_x(\varepsilon)$  cannot grow any further. On the other hand, the balls with extremely small radius of  $\varepsilon$  contains  $x$  only. Therefore, the power law holds only in the intermediate scaling region. Typical  $\log C(\varepsilon)$  vs.  $\log \varepsilon$  plot is shown in Figure A-6. Data only in the region need to be chosen for an evaluation for the correlation dimension.



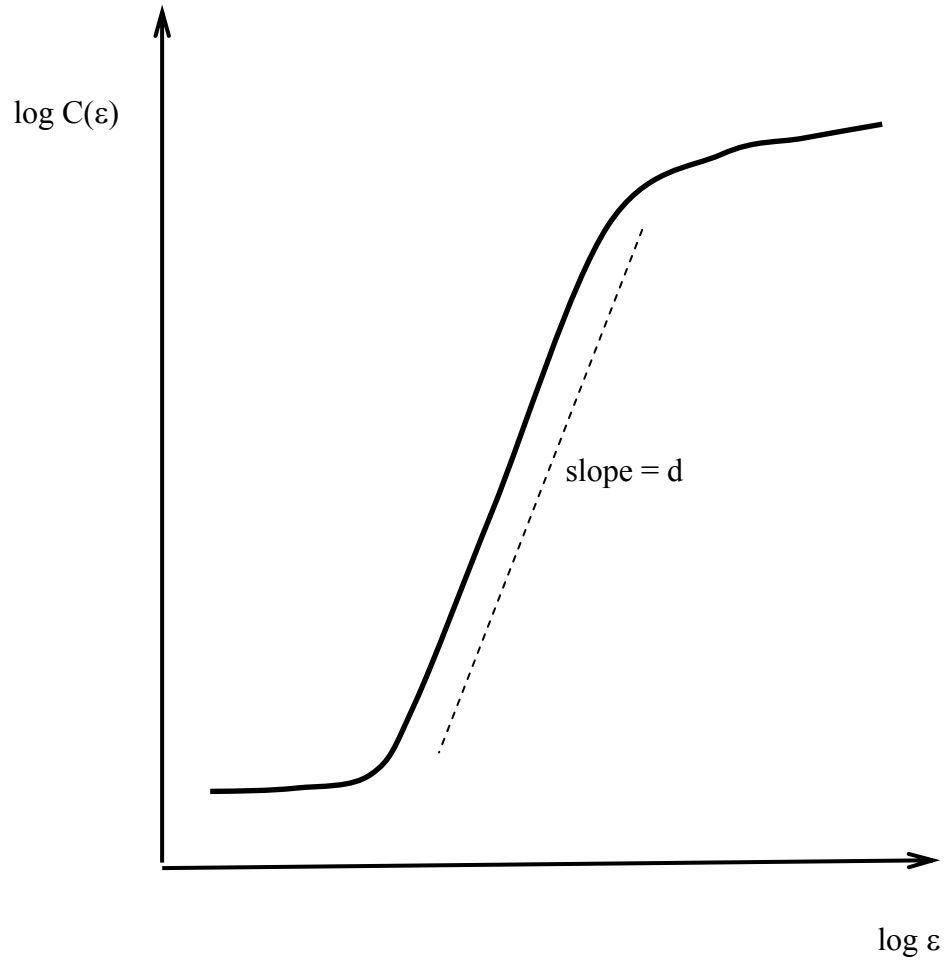


Figure A-6 Log-log plot to estimate the correlation dimension of a fractal. Typically, the plot shows two bends both at lower values of  $\varepsilon$  and at higher values of  $\varepsilon$

## APPENDIX E

### STOCK MARKET AND CHAOS

One of early examples is Hurst exponent in Ref. [33] for measuring heights of river. Hurst was an English hydrologist, who worked in the early 20<sup>th</sup> century on the Nile River Dam project. When designing a dam, the yearly changes in the water level are of particular concern in order to adapt the dam's storage capacity according to the natural environment. Studying an Egyptian 847-year record of the Nile River's overflows, Hurst observed that flood occurrences could be characterized as persistent, i.e. heavier floods were accompanied by above average flood occurrences, while below average occurrences were followed by minor floods. In the process of this finding, he developed the rescaled range (R/S) analysis. Suppose there exists a time series,  $t$ , with  $u$  observations:

$$X_{t,N} = \sum_{u=1}^t (e_u - M_N) \quad (\text{A.71})$$

where  $X_{t,N}$ ,  $e_u$  and  $M_N$  stand for cumulative deviation over  $N$  periods, influx in year  $u$  and average  $e_u$  over  $N$  periods, respectively.

The range becomes the difference between the maximum and minimum levels attained in equation (A.71):

$$R = \max(X_{t,N}) - \min(X_{t,N}) \quad (\text{A.72})$$

where  $R$  stands for range of  $X$ .

Then Hurst found a following relation

$$R/S \propto N^H \quad (\text{A.73})$$

where  $S$  and  $H$  represent the standard deviation of the original observation and Hurst exponent, respectively. The Hurst exponent has an inverse dependence with the fractal dimension. Hurst's idea of R/S analysis was recently used in analyzing stock markets.

Peters tried to get a fractal dimension of some stock markets in US, UK, Japan and German by using historical S&P 500 data, and found they were between 2 and 3 (see Ref. [32] for detail). He claimed the method might be useful to estimate likelihood that two consecutive events are likely to occur, and tried to show the stock markets did not follow a random process. For above stock markets, dimensions were evaluated, and then independent variables were identified. Note that a dimension is the minimum number of variables to describe all the points in the fractal of interest. However, for this technique, it is usually not possible to evaluate the Liapunov exponent and the dimension of a fractal without pretreatment since the measured data contain a large error. Thus, it is necessary to eliminate or reduce the effect of error. First, based on assumption that the distribution of errors was known, it adds the known type of error to the measurement. Then, measured data are "filtered out" in order to reduce error. This error reduction process gives rise to major criticism<sup>A25</sup>, and makes analysis on a stock market arbitrary.

---

<sup>A25</sup> if added error does not follow the original error distribution and it has a bigger contribution to the values for the quantity to be estimated than original signal, "filtering out" process may wash off the original signal and leftover value represents only the arbitrary added error

## REFERENCES

- [1]. R. A. Bettis and C. K. Prahalad, “The Dominant Logic: Retrospective and Extension”, *Strategic Manage. J.*, Vol. 16, No. 1 (1995) 5-14
- [2]. A. E. Rot and I. Erev, “Learning in Extensive-form Games: Experimental Data and Simple Dynamic Models in the Intermediate Term”, *Games Econom. Behav.*, Vol. 8, No. 1, (1995) 164-212
- [3]. I. Erev and A. E. Rot, “Predicting How People Play Games: Reinforcement Learning in Experimental Games with Unique, Mixed Strategy Equilibria”, *Amer. Econom. Rev.*, Vol. 88, No. 4 (1998) 848-881
- [4]. C. Richter and G. Sheblè, “Genetic Algorithm Evolution of Utility Bidding Strategies for the Competitive Marketplace”, *IEEE Trans. Power Syst.*, Vol. 13, No. 1. (1998) 256 – 261
- [5]. C. Richter, G. Sheblé and D. Ashlock, “Comprehensive Bidding Strategies with Genetic Programming/Finite State Automata”, *IEEE Trans. On Power Syst.*, Vol. 14, No. 4 (1999) 1207 – 1212
- [6]. C. Ritcher and G. Sheblè, “A Profit-Based Unit Commitment GA for the Competitive Environment”, *IEEE Trans. On Power Syst.*, Vol. 15, No. 2 (2000) 715 – 721

- [7]. Z. Michalewicz, "Genetic Algorithms + Data Structures = Evolution Programs", 2<sup>nd</sup> Ed., Berlin, Germany, Springer-Verlag (1992)
- [8]. D. W. Bunn and F. S. Oliveira, "Agent-based simulation-an application to the new electricity trading arrangements of England and Wales", IEEE Trans. Evol. Comp., Vol. 5 (2001 ) 493 – 503
- [9]. D. W. Bunn, "Forecasting loads and prices in competitive power markets", Proc. IEEE Vol. 88, (2000) 163 – 169
- [10]. D. W. Bunn, "Evaluation of market power using agent based simulation", Power Eng. Soc. General Meeting, Vol. 1, (2003) 506 - 508
- [11]. H.-N. Oh, "Simulation Methods for Modeling Offer Behavior and Spot Prices in Restructured Markets for Electricity", dissertation, Cornell University (2003)
- [12]. H. Oh, R. J. Thomas, B. Leiseutre and T. D. Mount, "A method for classifying offer strategies observed in an electricity market", J. Decision Support System, (2005) (in press)
- [13]. J. Crank, "The Mathematics of Diffusion", Second Edition, Clarendon Press, Oxford (1975) 38 – 40
- [14]. D. Bernoulli, "Specimen Theoriae Novae Demensura Sortis", (1738) Proceedings of the St. Petersburg Imperial Academy of Science, 5 – translated into English (1954)

- [15]. C. J. Grayson, "Decisions under Uncertainty: Drilling Decisions by Oil and Gas Operators", Technical Report, Division of Research, Harvard Business School, Boston (1960)
  
- [16]. R. A. Swalin, "Thermodynamics of Solids", 2<sup>nd</sup> Ed., New York John Wiley & Sons (1972)
  
- [17]. H. W. Kuhn and A. W. Tucker, "Nonlinear Programming", in Jerzy Neyman, Proceedings of the Second Berkeley Symposium, University of California Press, Berkeley (1951) 481 - 492
  
- [18]. C. Kittel, "Thermal Physics", 2<sup>nd</sup> Ed., (1980) W H Freeman & Company, San Francisco (1980)
  
- [19]. T. D. Mount, "Strategic Behavior in Spot Markets for Electricity When Load is Stochastic", presented as a selected paper at the Hawaii International Conference on System Science, Maui. (2000)
  
- [20]. R. Baldick and W. Hogan, "Capacity Constrained Supply Function Equilibrium Models of Electricity Markets: Stability, Non-Decreasing Constraints, and Function Space Iterations", POWER working paper on <http://www.ucei.berkeley.edu/ucei/pubs-pwp.html> (2001)

- [21]. R. Rajaraman and F. Alvarado, "Optimal Bidding Strategy in Electricity Markets Under Uncertain Energy and Reserve Prices", Power System Engineering Research Center (PSERC) on [http://www.pserc.wisc.edu/cgi-pserc/getbig/publicatio/reports/2003report/alvarado\\_bidding\\_report\\_0411.pdf](http://www.pserc.wisc.edu/cgi-pserc/getbig/publicatio/reports/2003report/alvarado_bidding_report_0411.pdf) (2003)
- [22]. S. de la Torre, J. M. Arroyo, A. J. Conejo and J. Contreras, "Price Maker Self-Scheduling in a Pool-Based Electricity Market: A Mixed-Integer LP Approach", IEEE Transactions on Power Syst., Vol. 17, No. 4, (2002)
- [23]. J. Contreras, O. Candiles, J. Fuente and T. Gómez, "A Coweb Bidding Model for Competitive Electricity Markets", IEEE Trans. On Power Syst., Vol/ 17, No. 1 (2002) 148-153
- [24]. T. L. Fine, "Feedforward Neural Network Methodology", Springer-Verlag, New York (1999)
- [25]. Smith, "Neural Networks for Statistical Modeling", Boston International Thomson Computer Press (1996)
- [26]. S. Geman., E. Bienenstock. and R. Doursat, "Neural Networks and the Bias/Variance Dilemma", Neural Computation, 4 (1992) 1-58.
- [27]. California Independent System Operator, "ISO Market Monitoring & Information Protocol", on <http://www.caiso.com/docs/2002/02/12/2002021215391318952.pdf> (2002)

- [28.] C. A. Berry, B. F. Hobbs, W. A. Meroney, R. P. O'Neill and W. R. Steward, "Analyzing Strategic Bidding Behavior in Transmission Networks", *Game Theory Application in Electricity Markets*, 99TP-136-0, IEEE PES Winter Meeting (1999) 7-32
  
- [29.] J. D. Weber and T. J. Overbye, "A Two-Level Optimization Problem for Analysis of Market Bidding Strategies", *Power Engineering Society Summer Meeting*, IEEE, Vol. 2, (1999) 682 – 687
  
- [30.] S. H. Strogatz, "Nonlinear Dynamics and Chaos", Westview, Cambridge (2000)
  
- [31.] E. N. Lorenz, "Deterministic Nonperiodic Flow", *J. Atmos. Sci.*, 20 (1963) 130
  
- [32.] Peters, E. "Chaos and Order in the Capital Markets A New View of Cycles, Prices, and Market Volatility", New York, John Wiley & Sons, Inc (1991)
  
- [33.] H. E. Hurst, "Long-Term Storage of Reservoirs", *Transactions of the American Society of Civil Engineers* (1951) 116
  
- [34.] A. Wolf, J. B. Swift, H. L. Swinney and J. A. Vastano, "Determining Lyapunov Exponents from a Time Series", *Physica* 16D (1985) 285-317
  
- [35.] Kantz, H. and Schreiber, T. "Nonlinear Time Series Analysis", Cambridge, Cambridge Univ. Press (1999)



- [36]. S. Collins and C. J. De Luca, "Upright, Correlated Random Walk: A Statistical-Biomechanics Approach to the Human Postural Control System", *CHAOS*, 5 (1995) 57
- [37]. H. Kantz, "A Robust Method to Estimate the Maximal Lyapunov Exponent of a Time Series", *Phys. Lett. A.*, 185 (1994) 77
- [38]. R. S. Sutton, "Reinforcement Learning: an Introduction" MIT Press, Cambridge Mass. (1998); electronic version can be found at [http://encompass.library.cornell.edu/cgi-bin/checkIP.cgi?access=gateway\\_standard%26url=http://encompass.library.cornell.edu/cgi-bin/scripts/ebooks.cgi?bookid=1094](http://encompass.library.cornell.edu/cgi-bin/checkIP.cgi?access=gateway_standard%26url=http://encompass.library.cornell.edu/cgi-bin/scripts/ebooks.cgi?bookid=1094)